

**THE CHEMISTRY OF GROUP SIX METAL CARBONYLS
WITH N-DONOR LIGANDS**

BY

CORMAC HEGARTY B.Sc.

THESIS SUBMITTED FOR THE DEGREE

OF

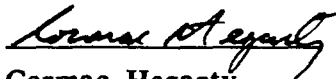
MASTER OF SCIENCE

DUBLIN CITY UNIVERSITY, DUBLIN

SEPTEMBER 1989

DECLARATION

I hereby declare that the contents of this thesis, except where otherwise stated, are based entirely on my own work which was carried out at the Dublin City University, Dublin.


Cormac Hegarty

TO MY PARENTS

ACKNOWLEDGEMENT

I wish to thank the following people for their help and encouragement during the course of this work

My Supervisor Dr Conor Long, for his advice, encouragement, and friendship

My fellow post-graduate students for their friendship and help, especially Nigel McSweeney, my laboratory partner, and Paula Shearan for proof-reading this Thesis

All the Academic and Technical staff in the School of Chemical Sciences, Dublin City University, for their friendship and help With special thanks to Dr Chris Breen (now with Sheffield City Polytechnic) for his help with the thermogravimetric analysis of $W(CO)_6(2,2'-dipyridylamine)$

Dr John Kelly, Trinity College Dublin, for the use of the laser flash photolysis apparatus

Special thanks to Delia Finnegan for typing this thesis and helping me meet the deadline

		<u>Page No.</u>
<u>CHAPTER ONE</u>	INTRODUCTION	
1.a.	Introduction	1
1b	References	14
<u>CHAPTER TWO</u>	KINETIC STUDY OF TUNGSTEN HEXACARBONYL	
2.a.I.	A laser flash Photolysis study of $W(CO)_6$ in cyclohexane containing 2- and 4-picoline.	18
2.a.II	Results and Discussion.	20
2.b.I	Kinetic Study of the Solvent Displacement from $W(CO)_5(R-OH)$ (R = Et- and Bu-) by 2- and 4-picoline.	26
2.b.II	Results and Discussion.	29
2.c.I	Kinetic Study of the formation of $W(CO)_4L$ (L = 2,2' Bipyridine and 3,6-Bis(2-pyridyl)-1,4-dihydro-1,2,4,5-tetrazene) from $W(CO)_6$	38
2.c II	Results and Discussion.	40
2.d	Conclusion.	50
2.e	Experimental.	53
2.e.I	Apparatus	53
2.e.II	Materials	54
2.f	References.	56

CHAPTER 3**SYNTHESIS OF GROUP SIX METAL
HEXACARBONYL COMPLEXES
WITH N-DONOR LIGANDS****Page No**

3 a	Introduction	58
3 b I	Ultraviolet/visible spectroscopy of $W(CO)_5(L)$ (L = pyridine and substituted pyridine) complexes.	61
3.b.II	Infrared spectroscopy of $W(CO)_5(L)$ (L = pyridine and substituted pyridine) complexes.	63
3.b.III	Proton nuclear magnetic resonance spectroscopy of $W(CO)_5(L)$ (L = substituted pyridine) complexes.	68
3.c	The crystal and molecular structure of $W(CO)_5$ (2,2'-dipyridylamine).	71
3.d	Thermogravimetric analysis of $W(CO)_5(2,2'$ -dipyridylamine)	75
3 e.I	The Preparation of $M(CO)_4$ -3,6-bis(2-pyridyl)-1,4- dihydro-1,2,4,5-tetrazene	77
3.e.II	Ultraviolet/visible Spectroscopy of $M(CO)_4$ - 3,6-bis(2-pyridyl)-1,4- dihydro-1,2,4,5-tetrazene.	78
3 e.III	Infrared Spectroscopy of $M(CO)_4$ 3,6-bis(2-pyridyl)- 1,4-dihydro-1,2,4,5-tetrazene (M = Cr, Mo, or W) Complexes.	81
3.e.IV	Proton Nuclear Magnetic Resonance Spectroscopy of the 3,6-bis (2-pyridyl)-1,4-dihydro-1,2,4,5-tetrazene Derivatives of $M(CO)_6$ (M = Cr, Mo, or W).	83
3.f	The Crystal and Molecular Structure of $W(CO)_4$ - (3,6-bis(2-pyridyl)-1,4-dihydro-1,2,4,5-tetrazene.	84

3.g	The Preparation of $W(CO)_5$ 2-aminomethylpyridine and $W(CO)_5$ Bispicoylamine.	87
3.h.I	The Solvatochromic Behaviour of Some Group Six Metal Carbonyl Complexes with N-Donor Ligands	88
3 h.II	Solvatochromism of $W(CO)_5$ (Pyridine and Substituted Pyridine) Complexes	90
3.h.III	Solvatochromism of the $M(CO)_4(3,6\text{-bis}(2\text{-pyridyl})1,4\text{-dihydro-1,2,4,5-tetrazene}$ ($M = Cr, Mo, \text{ or } W$) and $W(CO)_4(6\text{-styryl-2,2' bipyridine})$ complexes	98
3.i	Conclusion	103
3.j	Experimental	104
3.j.I	Photochemical Reactor	104
3.j.II	The preparation of $W(CO)_5(L)$ complexes ($L =$ pyridine or substituted pyridine)	104
3 j.III	The preparation of $W(CO)_5(L)$ complexes ($L =$ 2-amino-methylpyridine or bispicoylamine)	105
3 j.IV	The preparation of $M(CO)_4(SL)$ complexes ($M = Cr, Mo, \text{ or } W$; $SL =$ 3,6 bis(2-pyridyl)1,4-dihydro-1,2,4,5-tetrazene	106
3.j.V	Materials	107
3.j.VI	Apparatus	107
3.k	References	108

LIST OF FIGURES**Page No.**

Figure 1.1	Schematic representation of σ and π bonding in metal carbonyl complexes	3
Figure 1.2	The molecular orbital diagram for the group six metal hexacarbonyls	4
Figure 1.3	A comparison of the ultraviolet spectra of the group six hexacarbonyls in perfluoromethylcyclohexane	7
Figure 1.4	The ultraviolet spectrum of $W(CO)_6$ in cyclohexane	9
Figure 1.5	The photochemical behaviour of $M(CO)_5$ in a mixed matrix containing X and Y	12
Figure 2.1	A typical transient absorption of $W(CO)_5(\text{cyclohexane})$ in the presence of $1.15 \times 10^{-1} \text{ mol}$ 2-picoline	21
Figure 2.2	Plot of k_{obs} against 2- and 4-picoline concentration	24
Figure 2.3	Arrhenius plot for the reaction of $W(CO)_5(\text{cyclohexane})$ with 4-picoline	25
Figure 2.4	Plot of k_{obs} against concentration of 4-picoline at different temperatures	31
Figure 2.5	Plot of k_{obs} against concentration of 2-picoline at different temperatures	32
Figure 2.6	Absorption spectral sequence of a solution of $W(CO)_5(R-OH)$ at 50°C at 20 minute intervals	37
Figure 2.7	Absorption spectral sequence recorded following $\sim 2\text{-s}$ uv irradiation of a solution of $5 \times 10^{-4} W(CO)_6$ in toluene containing $3 \times 10^{-3} \text{M}$ 2,2'-bipyridine at 20°C	41

		<u>Page No.</u>
Figure 2.8	First order plot for the rate of formation of $W(CO)_4(2,2'$ -bipyridine)	42
Figure 2.9	Absorption spectral sequence recorded following ~ 2 -s u v irradiation of a solution of 5×10^{-4} mol $W(CO)_6$ in toluene at $20^\circ C$ with 3 minute intervals	44
Figure 2.10	Absorption spectral sequence recorded following ~ 2 -s u v irradiation of a solution of $5 \times 10^{-4} M$ $W(CO)_6$ in toluene containing $4 \times 10^{-3} M$ SL at $20^\circ C$ with 3 minute intervals	47
Figure 2.11	Absorption spectral sequence recorded following ~ 2 -s u v irradiation of a solution of $5 \times 10^{-4} M$ $W(CO)_6$ in toluene containing $4 \times 10^{-3} M$ SL at $20^\circ C$ with 20 second intervals	48
Figure 2.12	The laser flash photolysis apparatus	55
Figure 3.1	d-orbital energy diagram for $M(CO)_5(L)$ complexes	59
Figure 3.2	Ultraviolet/visible spectrum of the $W(CO)_5$ - (4-phenylpyridine) complex recorded in CCl_4 and thf	62
Figure 3.3	Infrared spectrum of $W(CO)_5(2,2'$ -dipyridylamine) before and after heating	66
Figure 3.4	The 1H nmr spectra of the $W(CO)_5(4$ -phenylpyridine) complex	69
Figure 3.5	The molecular structure of 4-phenylpyridine	70
Figure 3.6	The crystal structure of $W(CO)_5(2,2'$ -dipyridylamine)	72

Figure 3.7	The thermogravimetric analysis of the $W(CO)_5(2,2$ - dipyridylamine) complex	76
Figure 3.8	The molecular structure of 3,6-bis(2-pyridyl)-1,4- dihydro-1,2,4,5-tetrazene	77
Figure 3.9	The crystal structure of $W(CO)_4(SL)$	85
Figure 3.10	The molecular structure of bispicoylamine	87
Figure 3.11	The uv/vis spectrum of $W(CO)_5(4$ -phenylpyridine) recorded in (a) CCl_4 , (b) cyclohexane, and (c) thf	91
Figure 3.12	The uv/vis spectrum of $W(CO)_4(SL)$ recorded in (a) toluene, (b) thf, and (c) acetonitrile	99

LIST OF TABLES

		<u>Page No.</u>
Table 1.1	The M-C and C-O bond strengths in $M(CO)_6$ (M = Cr, Mo, or W)	6
Table 2.1	Kinetic data for the displacement of cyclohexane from $W(CO)_5(\text{cyclohexane})$ by 2- and 4-picoline	23
Table 2.2	Kinetic data for the displacement of ethanol from $W(CO)_5(\text{Et-OH})$ by 2- and 4-picoline	30
Table 2.3	Second order rate constants (k) for the 2- and 4-picoline systems at varying temperatures	34
Table 2.4	Activation parameters for the $W(CO)_5(\text{R-OH})$ reactions with 2- and 4-picoline	35
Table 2.5	First order rate constants obtained from the reaction of $W(CO)_5(L)$ to form $W(CO)_4(L)$ and CO	43
Table 3.1	Ultraviolet/visible spectral data for the $M(CO)_5(L)$ complexes	61
Table 3.2	The carbonyl stretching absorptions of $W(CO)_5$ (pyridine and substituted pyridine) complexes	64
Table 3.3	The carbonyl stretching absorptions of $W(CO)_5$ (2,2'-dipyridylamine) recorded at different time intervals after being heated to 110°C	67
Table 3.4	The chemical shift of protons in $W(CO)_5$ (4-phenylpyridine) and free 4-phenylpyridine	70
Table 3.5	Table of bond lengths and angles of the $W(CO)_5$ (2,2'-dipyridylamine) complex	74

Table 3.6	Ultraviolet spectral data for the $M(CO)_4(SL)$ ($M = Cr, Mo, \text{ or } W$) complexes	79
Table 3.7	The carbonyl stretching absorptions of $M(CO)_4(SL)$, ($M = Cr, Mo, \text{ or } W$) complexes	82
Table 3.8	Table of bond lengths and angles of the $W(CO)_4(SL)$ complex	86
Table 3.9	The MLCT absorption maxima (nm) for $W(CO)_5(L)$ complexes	92
Table 3.10	Energy positions (ϵ_{MLCT} (kJmol^{-1}) of the MLCT absorption maxima for $W(CO)_5(L)$ complexes	93
Table 3.11	Relevant solvent parameters	95
Table 3.12	The MLCT absorption maxima (nm) for the group 6 metal-tetracarbonyl complexes	100
Table 3.13	Energy positions (ϵ_{MLCT} (kJmol^{-1}) of the MLCT absorption maxima for the group 6 metal tetracarbonyl complexes	101
Table 3.14	Elemental analysis of the $W(CO)_5(L)$ complexes prepared	105
Table 3.15	Elemental analysis of the $M(CO)_4(SL)$ complexes	106

ABSTRACT

The behaviour of the photochemically produced tungsten pentacarbonyl is investigated by laser flash photolysis and conventional ultraviolet/visible spectrophotometric methods. Rate constants for their reactions with 2- and 4-picoline and other pyridine derivatives are reported along with their proposed mechanisms.

$W(CO)_5(L)$ complexes (L = pyridine, 2- or 4-phenylpyridine, or 2,2'-dipyridylamine) are synthesised along with 3,6-bis(2-pyridyl)-1,4-dihydro-1,2,4,5-tetrazene derivatives of $M(CO)_6$ (M = Cr, Mo, or W). These complexes are characterised by infrared, ultraviolet/visible, proton nuclear magnetic resonance spectroscopy, and by X-ray diffraction analysis. Attempts to synthesise the $W(CO)_5(L)$ complexes (L = 2-aminomethylpyridine or bispicolamine) were also reported. The solvatochromic behaviour of these penta and tetra-carbonyl complexes was also investigated.

CHAPTER I

INTRODUCTION

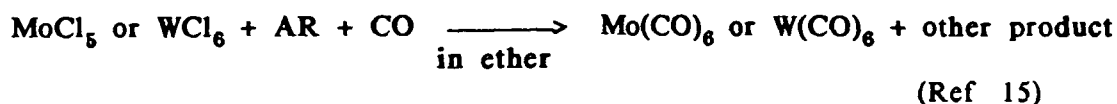
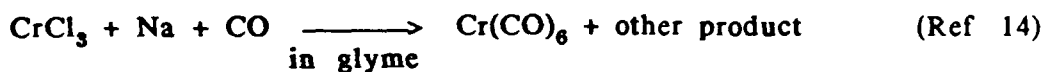
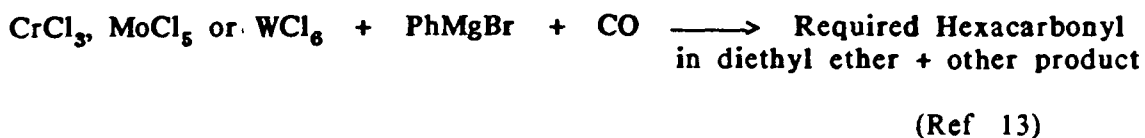
1.A INTRODUCTION

For the past few decades, the hexacarbonyls of group six metals have been the subject of several experimental and theoretical papers. Information about the nature of ligand substitution is useful in systematic organometallic synthesis and in the design of homogenous catalytic processes^{1a}. A good introduction into the chemistry of these metal hexacarbonyls can be found in "Comprehensive Organometallic Chemistry"^{1b}.

The first metal complex containing carbon monoxide as a ligand was synthesised by Schutzenberger in the latter end of the 19th century². He produced dicarbonyl chloroplatinate ($\text{PtCl}_2(\text{CO})_2$) by passing chlorine and carbon monoxide through a glass tube containing hot platinum black. The discovery that carbon monoxide could act as a ligand opened what is probably one of the most important areas of inorganic and organometallic chemistry.

It was not until twenty years later that the first binary metal carbonyl complex was reported by Mond et al³. A year later, in 1891, the discovery of iron pentacarbonyl was announced by two groups, working independently⁴. It was with iron pentacarbonyl that Mond first recognised the great photosensitivity of metal carbonyl complexes^{4a}.

The first group six hexacarbonyl $\text{Mo}(\text{CO})_6$, was not reported until 1910 by Mond and co-workers⁵. $\text{Mo}(\text{CO})_6$ was synthesised by reacting pyrophoric molybdenum, obtained from the oxychloride by hydrogen reduction, with carbon monoxide at 250 atm and 200°C⁵. More recently, group six metal hexacarbonyls can be synthesised by a Grignard method⁶, (Scheme 1.1), however, a more preferred method now used and giving higher yields is reductive carbonylation⁷, (Scheme 1.1)



Scheme 1.1

Since group six metal hexacarbonyls are available from a number of commercial sources, few workers in the field currently synthesise it

The nature of the bond between metal atoms and carbonyl ligands presented considerable problems for early workers. Originally there was debate as to whether the carbonyl group was bound to the metal by a metal to carbon or metal to oxygen bond. More recently, X-ray diffraction analysis of Fe(CO)_5 confirmed that the bonding was to the carbon atom of the carbonyl group⁸

The development of infrared spectroscopy allowed a fuller understanding of the bonding and structure of metal carbonyl complexes. The high extinction coefficients of most carbonyl stretching absorption permits an unambiguous assignment of these absorptions in the infrared spectrum. The carbonyl stretching bonds of metal complexes generally occur at lower energies than that of free carbon monoxide at 2155cm^{-1} . This has been explained by proposing that the metal can back donate electron density into the π^* -orbitals on the carbonyl ligands. It is widely believed that the bonding between the metal and carbon monoxide is a combination of σ and π bonding⁹. Delocalisation of the π -d electrons from the central metal into the π^* carbonyl orbital gives rise to π -back bonding, and overlap of the σ symmetry orbitals of the metal and carbonyl yields

a strong σ donor interaction for the carbonyl. The σ bond tends to increase the electron density on the metal, while the π -back bonding tends to reduce it (Figure 1.1)

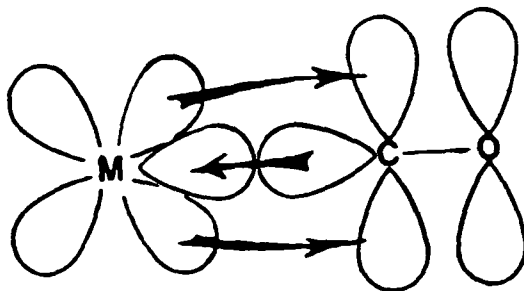


Figure 1.1 - Schematic representation of σ and π bonding in metal carbonyl complexes

The population of the carbonyl π^* -orbital reduces the effective bond order between the carbon and the oxygen, and this explains the drop in carbonyl stretching frequency compared to free carbon monoxide. However, the actual extent of electron transfer and consequent contribution of the forward (σ) and back (π) bonding is still the subject of debate¹⁶

The molecular structure of the group six hexacarbonyls is an excellent approximation to octahedral symmetry as determined by X-ray diffraction¹⁰, electron diffraction¹¹, and infrared spectroscopy¹². The molecular orbital diagram for group six metal hexacarbonyls has been developed by considering the interaction of the $nd, (n+1)s$ and $(n+1)p$ orbitals on the metal with the $2s$ and $2p$ orbitals on the carbon¹⁷. A more complete version was later presented by the same authors¹⁸. Figure 1.2 shows the resulting molecular orbital diagram

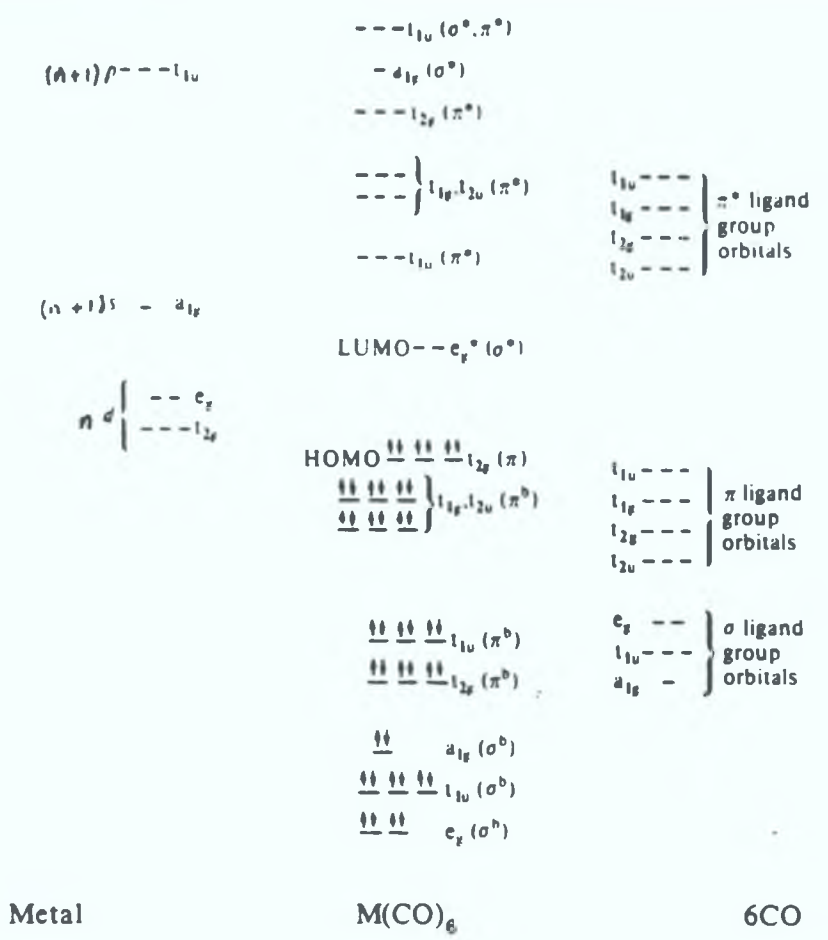


Figure 1.2 The Molecular Orbital Diagram for the Group Six Metal Hexacarbonyls

The σ -bonding system comprises the linear combination of the $nd(e_g)$, $(n+1)s (a_{1g})$ and $(n+1)p (t_{1u})$ orbitals with orbitals of suitable symmetry on the carbonyl ligands. As in Figure 1.2, this results in the formation of 6 bonding (σ^b) and 6 anti-bonding (σ^*) σ -molecular orbitals.

The π -molecular orbitals result from the combination of the metal $nd(t_{2g})$ orbitals with the t_{2g} combinations of both π - and π^* orbitals on the ligands. This results in three degenerate strongly bonding π - molecular orbitals, three orbitals which might be either bonding, non-bonding, or slightly anti-bonding depending on the relative stabilities of the contributing orbitals. The $(n+1)p$ orbitals of the metal may also interact with the orbitals of t_{1u} symmetry on the ligands however, and

are primarily involved in the σ -bonding. This would result in three bonding orbitals, mainly centred on the ligands, and six anti-bonding orbitals, three centred on the ligands and three on the metal.

The earliest studies of $M(\text{CO})_6$ ($M = \text{Cr}, \text{Mo}, \text{or W}$) utilized IR spectroscopy to examine the carbonyl stretching vibrations.¹² As stated earlier, the population of the carbonyl π^* orbital reduces the effective bond order between the carbon and the oxygen, and this explains the drop in carbonyl stretching frequency compared to free carbon monoxide. Force constants for the bonds can be calculated from the carbonyl stretching frequencies¹² and Cotton and Kraihanzel have presented a force field model (CKFF) for the derivation of such parameters.^{12(a)(b)} In the CKFF model, the carbonyl vibrations may be treated as if they were completely decoupled from the rest of the molecule. A value of 1649 mdyne/ \AA for the force constant for the C-O bond in $\text{Cr}(\text{CO})_6$ was obtained^{12(c)} and since the force constant of free CO is 184 mdyne/ \AA , a decrease in the C-O bond strength was indicated. The CKFF model does not allow for the anharmonicity of the fundamental vibrations, and has been criticised by Jones *et al*.¹⁹

More sophisticated calculations of the force constants were made by correcting for anharmonicity and/or using a general quadratic force field that does not assume that the carbonyl vibrations are decoupled.¹⁹ A value of 1724 mdyne/ \AA was obtained for the force constant for the C-O bond in $\text{Cr}(\text{CO})_6$. Values for the force constants of both the M-C and C-O bonds for $M(\text{CO})_6$ ($M = \text{Cr}, \text{Mo}, \text{or W}$) are presented in Table 11 along with bond energies for the M-C bond.

Compound	M-C bond energy ¹ (kJ mol ⁻¹)	F _{M-C} (mdyne/Å) general quadratic harmonic ²	F _{C-O} (mdyne/Å) general quadratic harmonic ²
Cr(CO) ₆	107	2.08	17.24
Mo(CO) ₆	151	1.96	17.33
W(CO) ₆	174	2.36	17.22

1. F.A. Cotton, A.K. Fischer, and G. Wilkinson., J. Am. Chem. Soc., 1959, **81**, 800.
2. L.H.Jones, R.S. McDowell, and M. Goldblatt., Inorg. Chem., 1969, **8**, 2349.

Table 1.1 The M-C and C-O Bond Strengths in M(CO)₆ (M = Cr, Mo, or W).

As can be seen, there is little correlation between the M-C force constant and the M-C bond energy. Both methods however, agree that the W-CO bond is significantly stronger than the Mo-CO or Cr-CO bond. The CKFF model however, has been used to predict both the positions and relative intensities of the carbonyl absorptions in many metal carbonyl complexes²⁰, and also the probable structure of the group six metal pentacarbonyls^{12d}.

The electronic spectra of M(CO)₆ (M = Cr, Mo, or W) have been examined in some detail^{1a}. All three complexes are colourless and their principal absorptions occur below 300nm (Figure 13). The nature of these absorptions has been studied by vapour phase¹⁸ and low temperature ultraviolet spectroscopy^{17,21} and also by X-ray photoelectron spectroscopy²². More recently, a study of the circular dichroism of these complexes has been presented²³ and there is general agreement as to the nature of the absorptions.

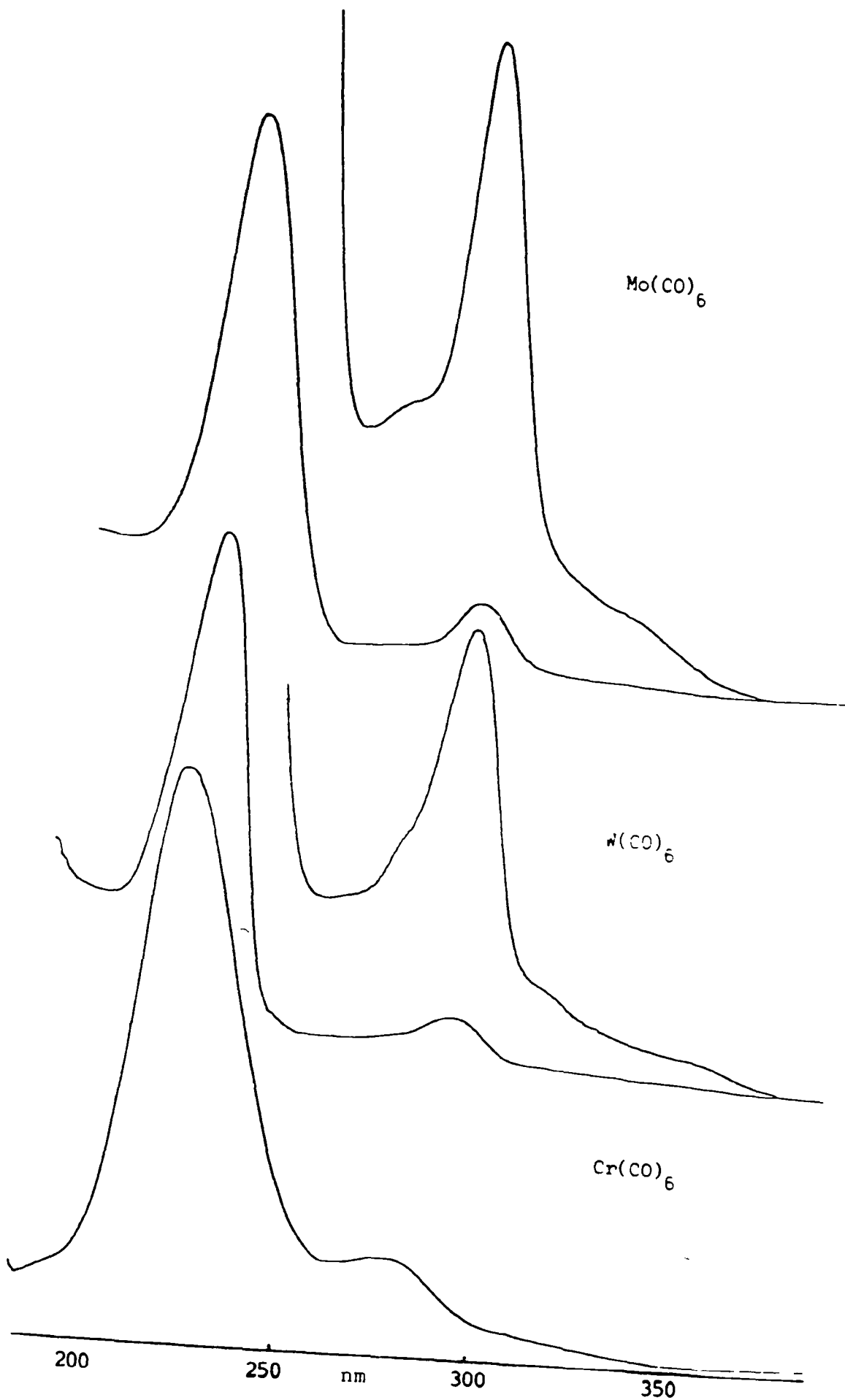
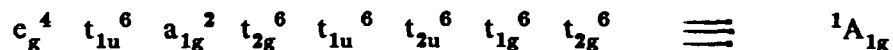


Figure 1.3 A comparison of the ultraviolet spectra of the Group VI hexacarbonyls in perfluoromethylcyclohexane.

As seen in Figure 13, there are 36 electrons available from the carbonyl ligands, plus a further six electrons from the metal. Thus the ground state for the $M(\text{CO})_6$ ($M = \text{Cr}, \text{Mo}, \text{or W}$) complexes is



The excited state of lowest energy results from the symmetry forbidden ${}^1A_{1g} \longrightarrow {}^1T_{1g}$ and ${}^1A_{1g} \longrightarrow {}^1T_{2g}$ transitions and also from the two dipole allowed ${}^1A_{1g} \longrightarrow {}^1T_{1u}$ charge transfer transitions. Figure 14 shows the ultraviolet spectrum of $\text{W}(\text{CO})_6$ in cyclohexane and the assigned transitions. As expected the d-d bands, ${}^1A_{1g} \longrightarrow {}^1T_{1g}$ and ${}^1A_{1g} \longrightarrow {}^1T_{2g}$ have low intensity as they are symmetry forbidden. The two intense bands are assigned to the allowed charge transfer transitions ${}^1A_{1g} \longrightarrow {}^1T_{1u}$.

Photolysis of $\text{W}(\text{CO})_6$ in a poly-methylmethacrylate matrix at room temperature was reported to result in the formation of a yellow species, which was assigned as the coordinatively unsaturated $\text{W}(\text{CO})_5$ species.²⁴ Other workers postulated the formation of an $M(\text{CO})_5$ intermediate ($M = \text{Cr}, \text{Mo}, \text{or W}$) in the photochemical preparation of $M(\text{CO})_{6-n}L_n$ complexes from $M(\text{CO})_6$.²⁵ However, in view of more recent results, it is most unlikely that this species is coordinatively unsaturated. Matrix isolation studies of $M(\text{CO})_6$ ($M = \text{Cr}, \text{Mo}, \text{or W}$) revealed that the position of maximum absorption of the $M(\text{CO})_5$ depends on the nature of the isolating matrix.²⁶ Perutz and Turner have suggested that this dependence is the result of an interaction between the pentacarbonyls and the isolating matrix.²⁶ This is surprising considering the inertness of many of the media used, e.g. CF_4 , Argon, SF_6 , etc. Kelly *et al*.²⁷, following the flash photolysis of $M(\text{CO})_6$ ($M = \text{Cr}, \text{Mo}$ or W), reported that the coordinatively unsaturated $M(\text{CO})_5$ produced, is extremely reactive and reacts with a variety of species including cyclohexane, N_2 and CO with rate constants approaching the diffusion controlled limit.

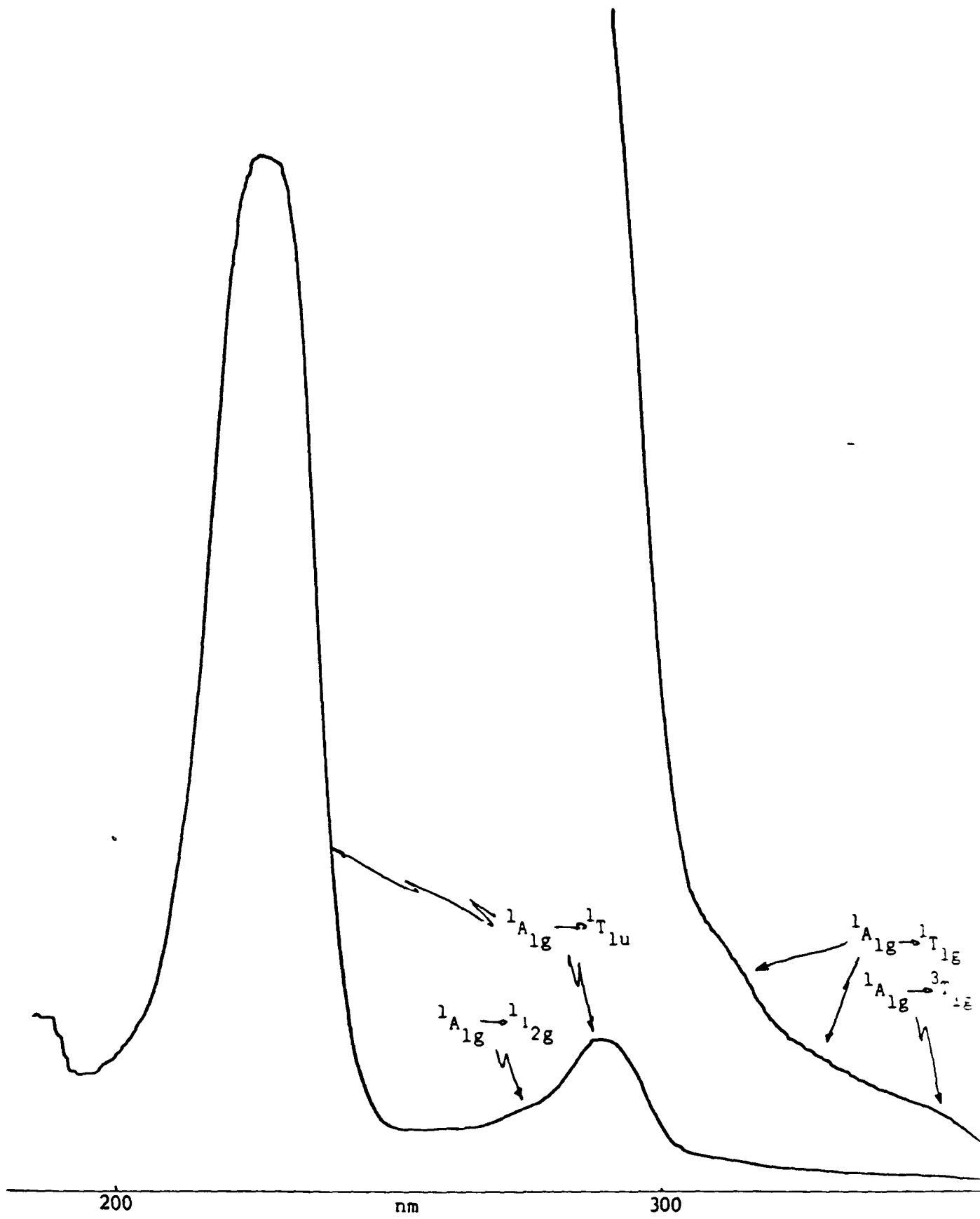
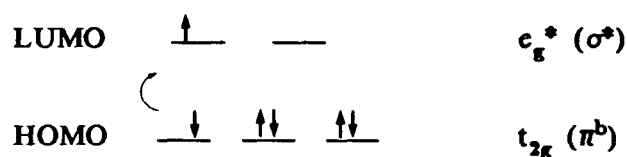


Figure 1.4. The ultraviolet spectrum of $W(CO)_6$ in cyclohexane.

The high quantum efficiency for the loss of carbonyl from $M(CO)_6$ ($M = Cr, Mo$ or, W) can be explained by considering the electronic configuration of both the ground and first excited state of the metal hexacarbonyl.²⁸ On examining the molecular orbital diagram (Figure 12) it can be seen that the highest occupied molecular orbitals (HOMO) are those of t_{2g} symmetry. These orbitals are essentially metallic in character and are involved in π -bonding with the carbonyl ligands. The lowest unoccupied molecular orbitals (LUMO) have e_g symmetry and are principally situated on the metal. These orbitals are σ -antibonding in nature. Irradiation into the low energy bands of the hexacarbonyls removes an electron from the orbitals involved in π -bonding (π^b) to one which is σ antibonding (σ^*), as in Scheme 12.



Scheme 12

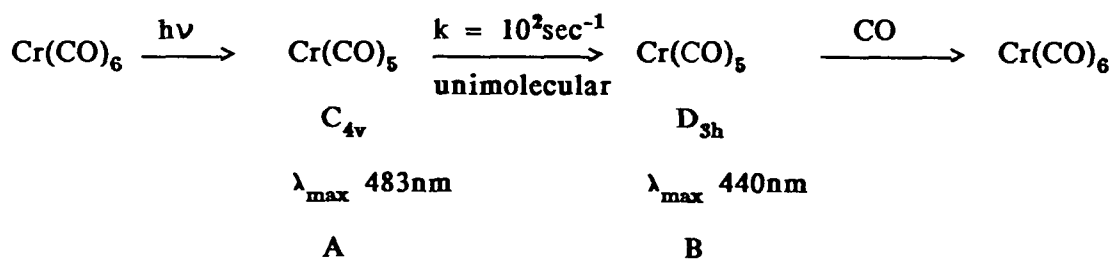
This transition results in an efficient loss of one carbonyl ligand

Dobson and co-workers first obtained infrared characterisation of the $M(CO)_5$ ($M=Cr, Mo, \text{ or } W$) intermediates produced following the photolysis of $M(CO)_6$ in methylcyclohexane glasses at 77K.²⁹ The spectra obtained implied a C_{4v} $M(CO)_5$ intermediate, however, upon thawing, the $M(CO)_5$ displayed evidence of isomerisation from a species of C_{4v} symmetry to one of D_{3h} symmetry. This explanation of the spectroscopic changes observed by Dobson et al, was not fully accepted by later workers.³⁰

Turner et al³¹ provided evidence for $M(CO)_5$ ($M = Cr, Mo, \text{ or } W$) having C_{4v} symmetry by photolyzing $M(CO)_6$ in argon matrices at 20K, by monitoring

infrared and uv-vis spectral changes. They also discovered that nitrogen could be weakly bound to $M(CO)_5$ in matrices of pure nitrogen or mixed argon-nitrogen at 20K.

First flash photolysis of group six metal hexacarbonyls carried out at room temperature in cyclohexane by Nasielski et al.³² provided conflicting results, in that two intermediates were observed, which were assigned as $C_{4v} M(CO)_5$ and $D_{3h} M(CO)_5$. Also claiming that the latter, $D_{3h} M(CO)_5$, was only capable of recombining with CO to give the original $M(CO)_6$ (Scheme 1.3)



Scheme 1.3

Turner and co-workers³³, pointed out that Nasielski's scheme lacks two points, firstly the slow interconversion rate for $C_{4v}M(CO)_5 \longrightarrow D_{3h}M(CO)_5$ and secondly the possibility of CO reacting with $C_{4v} M(CO)_5$. Since $C_{4v} M(CO)_5$ fragments react with excess CO in argon matrices at about 40K³³ Turner et al.³³, suggested a rapid $C_{4v} \longrightarrow D_{3h}$ with equilibrium lying towards C_{4v} .

Brattermann and coworkers^{30(a)} rejected the evidence for the existence of the $D_{3h} M(CO)_5$ for two reasons. Firstly, their work indicates that room temperature dissolved $Cr(CO)_5$ has C_{4v} symmetry and secondly, the new species is formed neither in primary photolysis nor under photoreversal conditions.

More recently, Turner and co-workers³⁴, confirmed C_{4v} symmetry of $M(CO)_5N_2$, obtained by an analysis using a frequency-factored force field of the infrared active C-O stretching modes of the isotopic variants $Mo(^{12}CO)_x(^{13}CO)_{5-x}N_2$ ($0 \leq x \leq 5$). An estimate of $90 \pm 4^\circ$ for the $OC_{ax}-Mo-CO_{eg}$ bond angle was provided from the relative intensities of the bands due to $Mo(^{12}CO)_5N_2$.

Perhaps the most important contribution from Turner and co-workers has come from the experiments carried out with polarized light³⁵. A photochemical mechanism (Figure 1.5) was proposed, which accounted for almost all the experimental data on matrix-isolated $M(CO)_5$ ($M=Cr, Mo, \text{ or } W$), $M(CO)_5N_2$, and $M(CO)_5CS$ ³⁵. The mechanism is based on evidence obtained by polarized photolysis and polarized spectroscopy of C_{4v} $M(CO)_5-L$ ($L = Ar, Xe, Ne, \text{ etc}$) species. Their work suggests a three step mechanism, firstly the loss of a carbonyl group to produce a pentacarbonyl species which is not in its ground state. This excited pentacarbonyl, which is assumed to have C_{4v} symmetry relaxes to the ground state pentacarbonyl (also with C_{4v} symmetry) via a pentacarbonyl with D_{3h} symmetry. This ground state C_{4v} pentacarbonyl can either combine with another ligand or recombine with carbonyl.

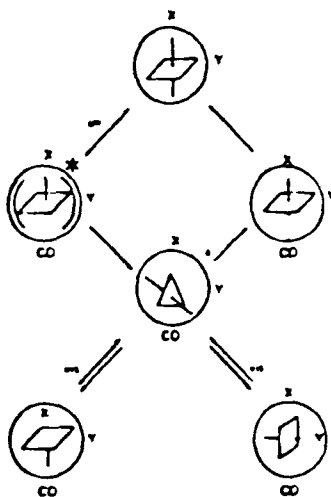
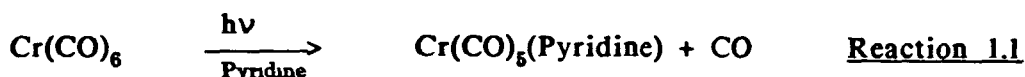


Figure 1.5 The Photochemical Behaviour of $M(CO)_5$ in a Mixed Matrix Containing X and Y (Ref. 35).

Church and co-workers using fast time-resolved infrared spectroscopy showed that gas phase photolysis of Cr(CO)_6 results in predominant formation of Cr(CO)_5 ³⁶ They report the first gas phase IR spectrum of naked Cr(CO)_5 which is consistent with a square pyramidal (C_{4v}) symmetry³⁶

The quantum efficiency of loss of carbonyl from M(CO)_6 ($\text{M} = \text{Cr, Mo, or W}$) originally estimated to be unity,³⁷ is now viewed with some doubt. More recent estimates of the quantum yield of the photosubstitution of CO by pyridine in Reaction 1.1 have suggested a value of 0.67 ± 0.02 for irradiation at 313nm.³⁸



This would suggest that there is a route, other than the loss of carbonyl, for the relaxation of the excited state. The use of benzophenone as a sensitizer for the above (Reaction 1.1) has led the authors to propose that the photoproduative state is the triplet, $^3\text{T}_{1g}$ state³⁸. This proposition was doubted by Rest *et al*³⁹. They assigned the emission from a Cr(CO)_6 /toluene mixture in an argon matrix as $^3\text{T}_{1g} \longrightarrow ^1\text{A}_{1g}$, toluene acting as a triplet sensitizer. Argon matrices containing only Cr(CO)_6 in the absence of toluene, failed to emit. Rest *et al*³⁹, concluded that the quantum efficiency of intersystem crossing from singlet to triplet excited states must be low. Therefore, this would imply that alternative decay routes are available for the singlet excited state. The apparent randomisation of the carbonyl orientation proposed by Turner *et al*³⁵, Figure 1.5, may also explain why the quantum efficiency of loss of carbonyl from the hexacarbonyl is not unity.

1.b.

References

- 1 (a) M. Wrighton, Chem. Rev., 1974, 74, 401
(b) S W Kirtley, "Comprehensive Organometallic Chemistry", Wilkinson, Stone, Abel, 1982
- 2 P Schutzenberger, J Chem Soc, 1871, 1009
- 3 L Mond, C Langer, and F Quinche, J. Chem. Soc., 1890, 749
- 4 (a) L Mond and C Langer, J Chem. Soc., 1891, 1090.
(b) M Berthelot, Compt Rend, 1891, 112, 1343
- 5 L Mond, H Hirtz, and M. D Cowap, J Chem Soc, 1910, 97, 798
- 6 B Owen, J English, H G Cassidy, and C V Condon, Inorg Synth, 1950, 3, 156
- 7 E O Fischer, W Hafner, and K Oefele, Chem Ber., 1959, 3050
- 8 J Donohue and A Caron, Acta Cryst., 1962, 15, 930
- 9 E W Abel and F G Stone, Quart Rev Chem Soc, 1969, 23, 325
- 10 W Rudorff and U Hoffmann, Z Phys Chem (B), 1935, 28, 351
- 11 L O Brockway, R V G Ewen, and M W Lister, Trans Faraday Soc, 1938, 34, 1350
- 12 (a) F A Cotton and C S Kraihansel, J Am Chem Soc, 1962, 84, 4432
(b) C S Kraihansel and F A Cotton, Inorg Chem, 1963, 2, 533
(c) F A Cotton, Inorg Chem, 1964, 3, 702
(d) R N Perutz, J J Turner, Inorg Chem, 1975, 14, 262

- 13 (a) W Hieber, E Romberg, Z. Anorg. Allg. Chem., 1935, 221, 321
(b) B B Owen, J English, H G Cassidy, and C V Dundon, Inorg. Synth., 1950, 3, 156
- 14 H E Podall, H B Prestige, and H Shapiro, J. Am. Chem. Soc., 1961, 83, 2057
- 15 (a) D T Hurd, US Pat 2554194 (1951) (Chem. Abstr., 1951, 45, 7314)
(b) D T Hurd, US Pat 2557744 (1951) (Chem. Abstr., 1951, 45, 8728)
- 16 (a) J B Johnson and W G Klemperer, J. Am. Chem. Soc., 1977, 99, 7132
(b) B E Bursten, D G Freier, and R F Fenske, Inorg. Chem., 1980, 19, 1810
(c) D E Sherwood and M. B Hall, Inorg. Chem., 1980, 19, 1805
(d) S Larsson and M. Graga, Int J Quantum Chem., 1979, 15, 1
- 17 H B Gray and N A Beach, J. Am. Chem. Soc., 1963, 85, 2922
- 18 N A Beach and H B Gray, J. Am. Chem. Soc., 1968, 90, 5713
- 19 (a) J M Smith and L H Jones, J. Mol. Spec., 1966, 20, 248
(b) L H Jones, R S McDowell, and M Goldblatt, Inorg. Chem., 1969, 8, 2349
- 20 J A Timney, Inorg. Chem., 1979, 18, 2505
- 21 W C Trogler, S R Desjardins, and E I Solomon, Inorg. Chem., 1979, 18, 2131
- 22 M. B Hall and D E Sherwood Jr, Inorg. Chem., 1979, 18, 2323
- 23 S K Chastain and W R Mason, Inorg. Chem., 1981, 20, 1395
- 24 L E Orgel, Nature, 1961, 191, 1387

- 25 (a) G R Dobson, M A El Sayed, I W Stolz, and R K Sheline, Inorg Chem, 1962, 1, 526.
- (b) W Strohmeier, Chem. Ber., 1961, 94, 3337
- 26 R N Perutz and J J Turner, J. Am Chem Soc., 1975, 97, 4791
- 27 J M Kelly, C Long, and R Bonneau, J Phys Chem, 1983, 87, 3344
- 28 E A Koerner von Gustorf, L H F Leenders, I Fischler, and R N Perutz, Advances in Inorganic Chemistry and Radiochemistry, 1976, 19, 65
- 29 I W Stolz, E R Dobson, and R K Sheline, J Am Chem Soc., 1963, 85, 1013
- 30 (a) M J Boylan, P S Brattermann, and A Fullerton, J Organomet Chem., 1971, 31, C29
- (b) J J Turner, J K Burdett, R N Perutz, and M Poliakoff, Pure and Appl Chem, 1977, 49, 271
- 31 M A Graham, M Poliakoff, and J J Turner, J Chem Soc., 1971, 2939
- 32 J Nasielski, P Kirsch, and L Wilputte-Steinert, J Organomet Chem., 1971, 29, 269
- 33 M A Graham, R N Perutz, M Poliakoff, and J J Turner, J Organomet Chem., 1972, 34, C34
- 34 J K Burdett, A J Down, G P Gaskill, M A Graham, J J Turner, and R F Turner, Inorg Chem., 1978, 17, 523
- 35 J K Burdett, J M Grzyborski, R N Perutz, M Poliakoff, J J Turner, and R F Turner, Inorg Chem., 1978, 17, 147

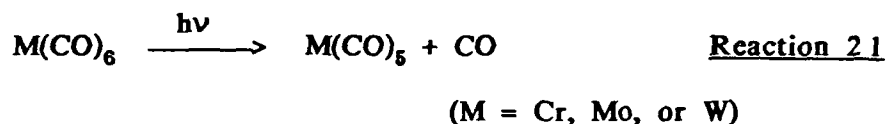
- 36 (a) T. A Seder, S P Church, A J Ouderkink, and E Weitz, J. Am. Chem. Soc., 1985, 107, 1432
(b) T A Seder, S. P Church, and E Weitz, J. Am Chem Soc., 1986, 108, 4721
- 37 W Strohmeier, Angew Chem Int. Ed., 1964, 3, 730
- 38 J Nasielski and A Colas, J. Organomet Chem., 1975, 101, 215
- 39 A J Rest and J R Sodeau, J Chem Soc Faraday Trans II., 1977, 73, 1691

CHAPTER II

KINETIC STUDIES OF TUNGSTEN HEXACARBONYL

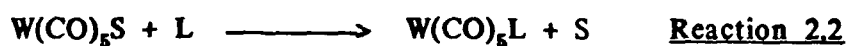
2 a 1. A Laser Flash Photolysis Study of W(CO)₆ in Cyclohexane Containing 2- and 4-picoline

It is now accepted that the primary photoproduct following photo-excitation in condensed phases of the group six hexacarbonyls is the appropriate pentacarbonyl complex (Reaction 2 1)

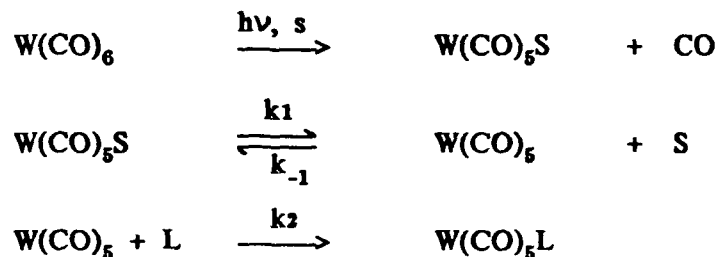


The resulting coordinatively unsaturated 16 valence electron species is extremely reactive and reacts with a variety of species including cyclohexane, N₂ and CO with rate constants approaching the diffusion controlled limit. As a result, the photolysis of M(CO)₆ in cyclohexane solution produces the M(CO)₅ (cyclohexane) species, as the primary product on the nano - to picosecond timescale. Indeed, it has been shown that Cr(CO)₅(cyclohexane) is already formed within 25 picoseconds of excitation of Cr(CO)₆ in cyclohexane³. More recently, subnanosecond flash photolysis excitation at 355nm of W(CO)₆ in perfluoromethylcyclohexane reveals that the solvatopentacarbonyl species is formed with a first order rate constant of 5 x 10¹⁰ s⁻¹ at 20°C². Similar rates were obtained in cyclohexane and a liquid paraffin². Therefore, a study of the reactivity of W(CO)₅(cyclohexane) was undertaken in order to investigate how the nature of the solvent medium can influence the reactivity of coordinatively unsaturated complexes.

In a previous study, the reaction of W(CO)₅S, S donating solvent methylcyclohexane, with the monodentate ligand 4-acetylpyridine (L) exhibited a saturation of the pseudo-first order rate constant with increasing ligand (L) concentration (Reaction 2 2)⁴



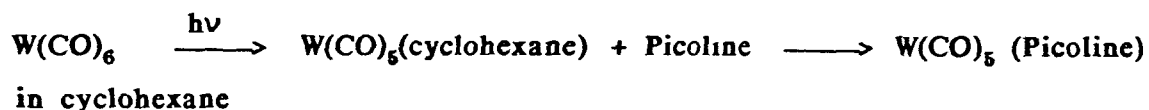
This proposed mechanism is one of reversible dissociation of $\text{W(CO)}_5\text{S}$ to W(CO)_5 and S with rate constants k , and k_{-1} followed by scavenging of the W(CO)_5 by L, with rate constant k_2 (Scheme 2.1)



Scheme 2.1

However, this mechanism would not seem able to explain the results obtained in perfluorosolvents, where evidence for an associative mechanism was obtained for the reaction of $\text{Cr(CO)}_5(\text{cyclohexane})$ with CO^1 Therefore it was decided to investigate the nature of the reaction between $\text{W(CO)}_5(\text{alkane})$ and a variety of substituted pyridines in alkane solvent

Laser pulse photolysis techniques were employed to study the rate of reaction of $\text{W(CO)}_5(\text{cyclohexane})$ with 2- and 4-picolines (Scheme 2.2)



Scheme 2.2

A Xe-Cl excimer laser was employed, producing a line at 308nm with a duration of approximately 10ns. Arrhenius plots of both the 2- and 4-picoline systems yield activation energies for the formation of $W(CO)_5(2\text{-picoline})$ and $W(CO)_5(4\text{-picoline})$ from $W(CO)_5(\text{cyclohexane})$.

2.a.II Results and Discussion

A study of the mechanism for the reactions of $W(CO)_5(\text{cyclohexane})$ with 4-acetylpyridine was impossible, using the equipment available, because of the large extinction coefficient of 4-acetylpyridine at 308nm (approximately $300\text{mol}^{-1}\text{dm}^3\text{cm}^{-1}$). Therefore this investigation was limited to the 2- and 4-picoline systems (Scheme 2.2)

The concentration of $W(CO)_6$ could be determined from its absorbance using its extinction coefficient at 308nm. An acceptable optical density was in the range of 0.6 to 1.6. The solution was degassed by purging with Ar for 10 minutes. The picoline (freshly distilled under reduced pressure), was introduced into the solution from a $10\mu\text{l}$ syringe through a septum cap fitted to the fluorescence cuvette. Temperature was kept constant by circulation of thermostatted water. However, at temperatures greater than 50°C , a decrease in the volume was observed, because of the evaporation of the cyclohexane resulting in changes in the concentration of picoline added.

The absorbance of the solution was monitored at 440nm, and this showed an immediate increase following the laser pulse (Figure 2.1). The rate of change of the optical density was analysed for first order kinetics. All results were obtained as averages over five pulses. Since $W(CO)_5(\text{picoline})$ absorbs to some extent at 440nm, the final optical density was somewhat greater at the end of

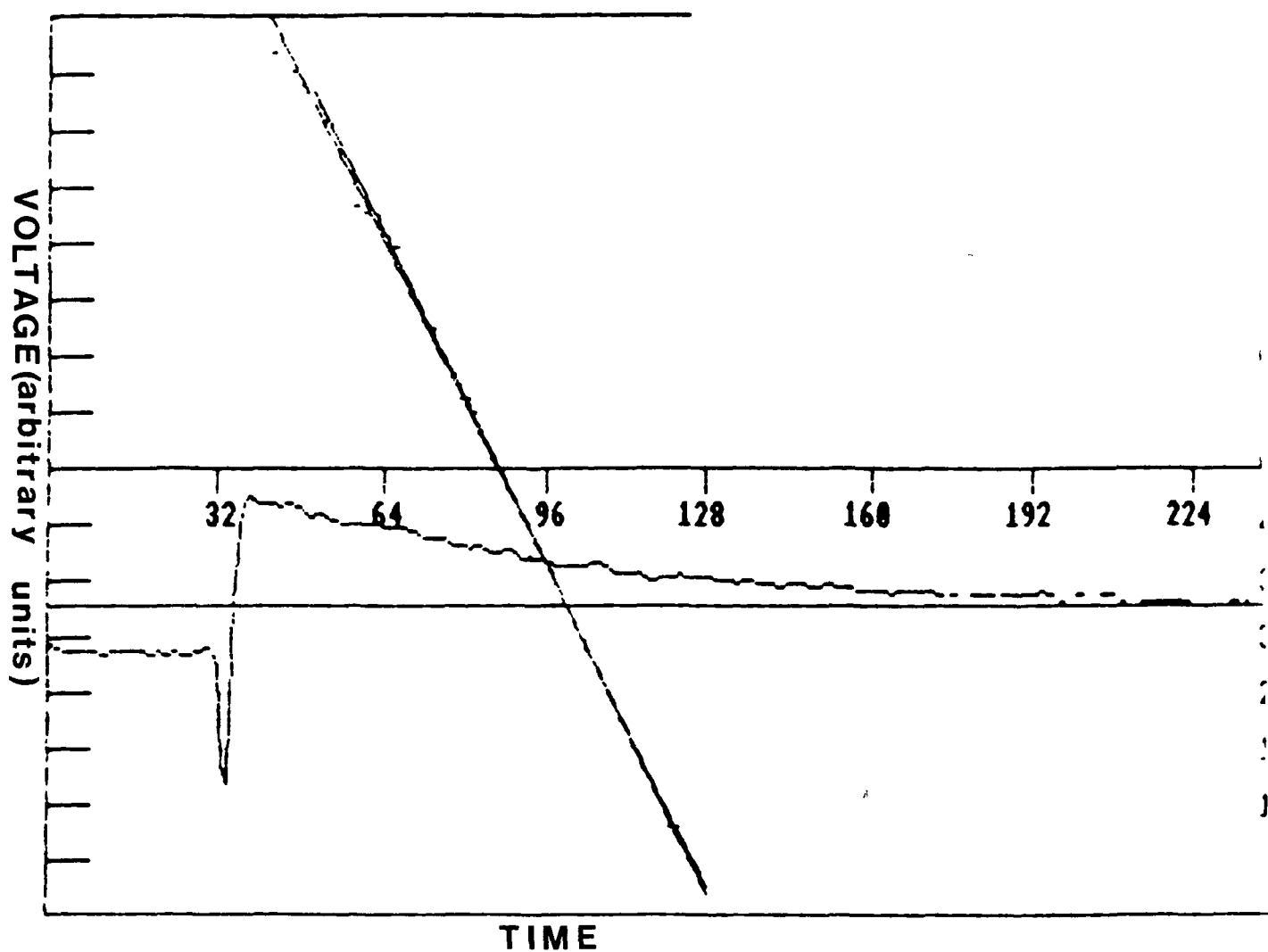


Figure 2.1 A typical transient absorption of $W(CO)_5$ (cyclohexane) in the presence of 1.15×10^{-1} molar 2-picoline.

the reaction than at the beginning (Figure 2.1) Following a series of pulses, a uv-visible spectrum of the solution was identical to the spectrum in the visible region of an authentic sample of the corresponding $W(CO)_6(\text{picoline})$ complex. The analysis for first order kinetics yielded straight lines, of slope k_{obs} (Table 2.1). The concentration of the picoline was varied in the range 0.005 to 0.2 moles dm^{-3} , and the resulting k_{obs} were plotted against the concentration of picoline (Figure 2.2).

The k_{obs} were found to depend linearly on the concentration of picoline within the range of 0.005 to 0.2 moles dm^{-3} (Figure 2.2). The slopes of these straight lines yielded the second order rate constants for both the 2- and 4-picoline systems. These were found to be 1.2×10^7 and $3.6 \times 10^7 \text{ dm}^3 \text{ mol}^{-1} \text{ s}^{-1}$ for the 2- and 4-picoline systems respectively. The variation of these second order rate constants with temperature allowed the calculation of the activation energies (ϵ_{act}) for each system, via an Arrhenius plot (Figure 2.3). A similar Arrhenius plot was obtained for the 2-picoline system. These activation energies were found to be $12 \pm 1 \text{ kJ mol}^{-1}$ and $10 \pm 1 \text{ kJ mol}^{-1}$ for the 2- and 4-picoline systems respectively.

Picoline Concentration (moles dm⁻³)

k_{obs} (S⁻¹)

4-picoline

5.1 x 10 ⁻³	2 x 10 ⁵
1.5 x 10 ⁻²	4.5 x 10 ⁵
2.5 x 10 ⁻²	8.8 x 10 ⁵
3.57 x 10 ⁻²	1.1 x 10 ⁶
4.6 x 10 ⁻²	2.13 x 10 ⁶
5.6 x 10 ⁻²	2.56 x 10 ⁶
6.1 x 10 ⁻²	2.83 x 10 ⁶
6.6 x 10 ⁻²	2.82 x 10 ⁶
7.63 x 10 ⁻²	3.16 x 10 ⁶
8.64 x 10 ⁻²	3.26 x 10 ⁶
9.6 x 10 ⁻²	4.2 x 10 ⁶
1.06 x 10 ⁻¹	3.7 x 10 ⁶
1.16 x 10 ⁻¹	3.96 x 10 ⁶
1.56 x 10 ⁻¹	6.26 x 10 ⁶
1.81 x 10 ⁻¹	6.82 x 10 ⁶
2.3 x 10 ⁻¹	7.98 x 10 ⁶

2-picoline

1.07 x 10 ⁻²	1.3 x 10 ⁵
2.04 x 10 ⁻²	2.4 x 10 ⁵
3.06 x 10 ⁻²	4.2 x 10 ⁵
4.08 x 10 ⁻²	5.5 x 10 ⁵
5.1 x 10 ⁻²	6.2 x 10 ⁵
6.1 x 10 ⁻²	6.9 x 10 ⁵
7.1 x 10 ⁻²	1.01 x 10 ⁶
9.65 x 10 ⁻²	1.04 x 10 ⁶
1.21 x 10 ⁻¹	1.5 x 10 ⁶
1.46 x 10 ⁻¹	1.7 x 10 ⁶

Table 2.1 Kinetic data for the displacement of cyclohexane from W(CO)₅(cyclohexane) by 2- and 4-picoline.

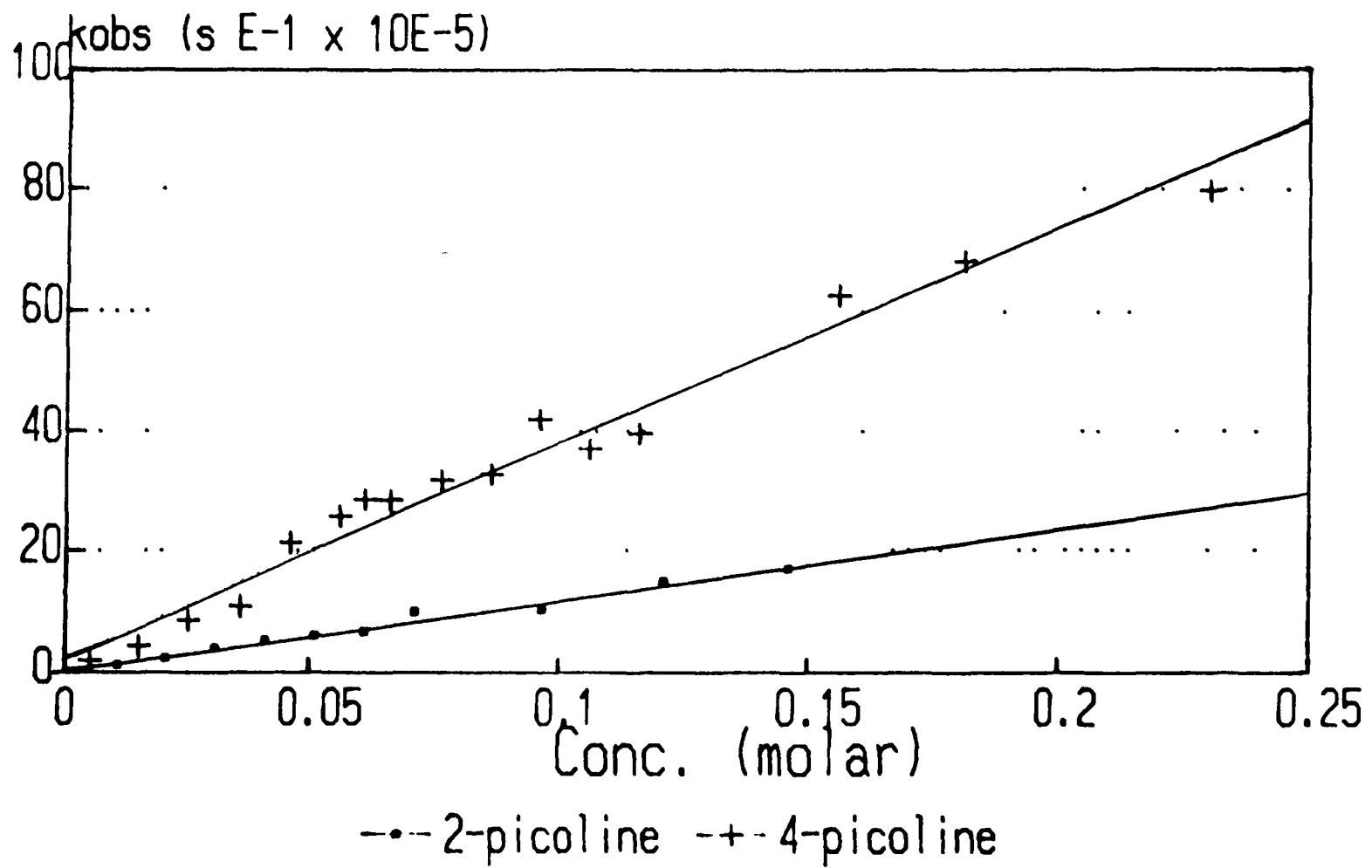


Figure 2.2 Plot of K_{obs} against 2- and 4-picoline concentration

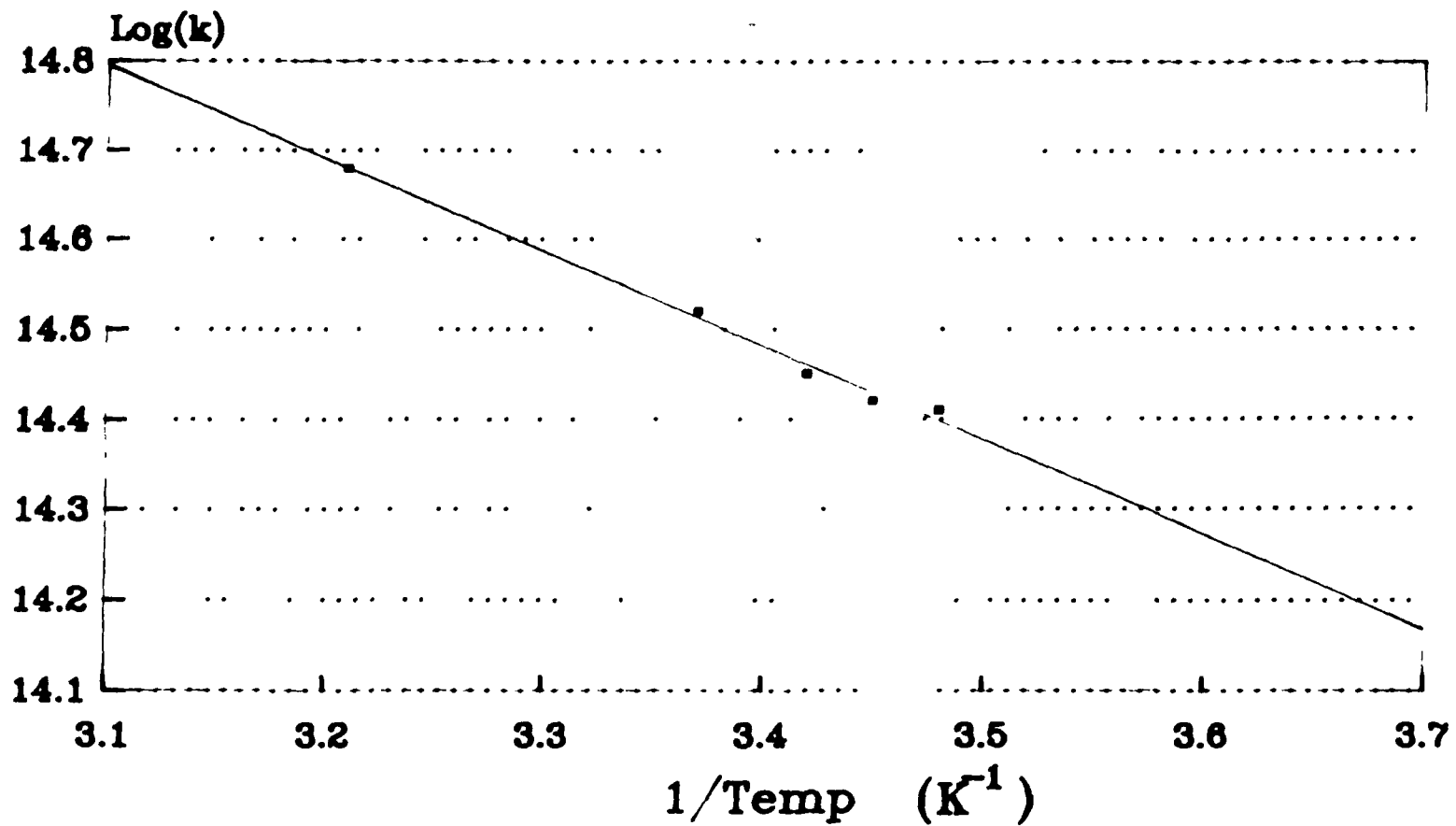
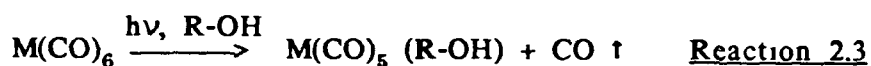


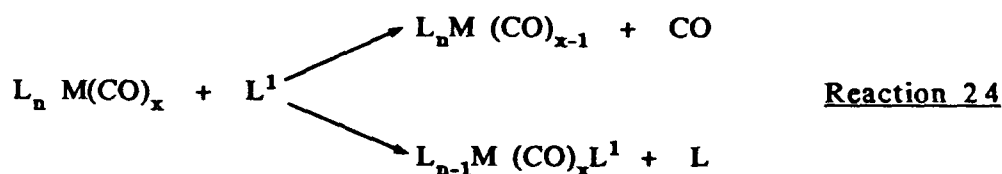
Figure 2.3 Arrhenius plot for the reaction of $W(CO)_5$ (cyclohexane) with 4-picoline.

2.b.I. Kinetic Study of the Solvent Displacement from W(CO)₅(R-OH) (where R = Et or Bu) by 2- and 4-Picoline

The thermal displacement of tetrahydrofuran (thf) from W(CO)₅(thf) by a nitrogen donor ligand is the primary route in the synthesis of the complexes reported in Section 3. An examination of the process involved was thought to be useful, however, it was decided to observe the displacement of alcohol (R-OH) from W(CO)₅(R-OH) (where R = Et or Bu) for two reasons, (a) solubility of group six metal carbonyls in alcohols, (b) stability of W(CO)₅(R-OH). None of the group six hexacarbonyls are particularly soluble in alcohols, however, the photolysis of a suspension of M(CO)₆ (where M = Cr, Mo, or W) in these solvents results in the formation of a clear yellow solution of M(CO)₅(R-OH) (Reaction 2.3). The unphotolysed hexacarbonyl may then be removed by filtration prior to the addition of the ligand. Also a solution of W(CO)₅(R-OH) in R-OH will suffer no decomposition after several days if kept in the dark at ambient temperature.



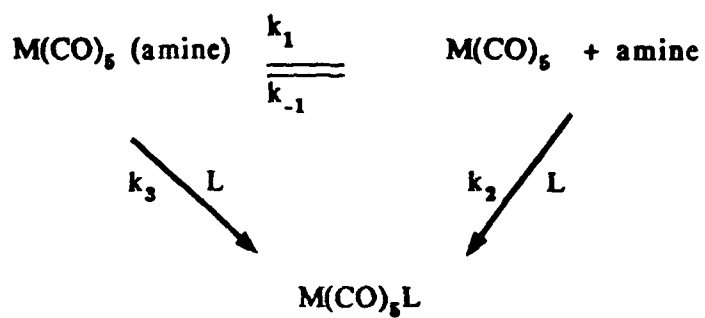
The generalised reaction for ligand substitution entailing derivatives of metal carbonyls may be represented by Reaction 2.4



Basolo has recently published an interesting chronological survey of the mechanisms of carbon monoxide replacement reactions in metal carbonyls⁵ In addition, several reviews on the thermal substitution reactions of metal carbonyls have also been published⁶ Langford and Gray⁷ have classified the three possible intimate mechanisms for ligand substitution processes as (a) dissociative (D), (b) associative (A), and (c) interchange (I) The latter designation may be further subdivided into I_a and I_d depending on the extent to which both the entering and leaving groups participate in the transition state

Work by Graham and Angelici on the $M(CO)_6$ ($M = Cr, Mo, \text{ or } W$) with phosphine and phosphite ligands in decalin solvent found the rate of reaction to be governed by a two term rate law⁸ Dissociative and associative mechanisms are proposed to account for the two terms Also as the size of the metal atom increased from Cr to Mo to W they found the associative mechanism to predominate

Darensbourg showed interest in the thermal stability of metal-amine bonds in $M(CO)_5(\text{amine})$ complexes (where $M = Cr, Mo, \text{ or } W$)^{9,10,11} In the presence of an entering ligand L ($L = \text{triphenylphosphine}$) the displacement of the amine from $M(CO)_5(\text{amine})$ ($M = Mo \text{ or } W$) was found to be a combination of first and second order processes⁹ In the first order process, the rate determining step is the breaking of the metal-amine bond to give an unsaturated $M(CO)_5$ species whereas in the second order process, the rate determining step is the formation of a seven coordinate species At high concentrations of entering ligand, the second order process predominates, while at low concentrations, the first order process is more prominent The proposed mechanism is given in Scheme 2 3



Scheme 2.3

A kinetic study of the displacement of R-OH (where R = Et- or Bu-) from $\text{W(CO)}_5(\text{R-OH})$ by 2- and 4- picoline was undertaken to determine if the schemes developed to explain the thermal displacement of the amine complexes by phosphines, as shown above, could be applied to this system

2.b II Results and Discussion

The rate of decay of $W(CO)_5(R-OH)$ (where $R = Et$ or Bu) was monitored at 415nm following the addition of either 2- or 4- picoline. The maintenance of an isosbestic point throughout the reaction at approximately 397nm would suggest that the reaction proceeds uncomplicated by side or subsequent reactions. The end product of the reaction was the corresponding $W(CO)_5$ (picoline) complex. These were identified by comparison of their respective ultraviolet/visible spectra with the ultraviolet/visible spectra of authentic samples of $W(CO)_5L$ ($L = 2-$ or $4-$ picoline) complexes. The entering ligand concentration was varied in the range 1.66×10^{-2} to 8.32×10^{-2} mol dm^{-3} . The temperature of the solution in the cell was controlled to $\pm 0.1^\circ C$ by circulating thermostatted water.

The reactions were followed using a uv/vis spectrophotometer interfaced with a minicomputer. The rate of change of the absorbance (A) was analysed for first order kinetics using a Guggenheim method or using a least squares method using a plot of $\text{Log } (A_o - A)/(A_t - A)$ against time (t) (where $A_o =$ absorbance at time $t = 0$, $A_t =$ absorbance at time $t = t$, and $A =$ absorbance at time $t = \infty$). The reaction was considered complete when the difference between two successive readings of absorbance was less than 0.0005.

These analyses afforded acceptable straight lines (correlation coefficient greater than 0.999) of slope k_{obs} . The data for both the 2- and 4-picoline with $W(CO)_5$ (Et-OH) systems are listed in Table 2.2. K_{obs} were not listed for the $W(CO)_5$ (Bu-OH) and 4-picoline system, as they were found to be similar to the $W(CO)_5$ (Et-OH) system. As can be seen from Figures 2.4 and 2.5, the observed rate constant K_{obs} displays good linear dependency on the concentration of picoline. This pseudo first order dependence indicates that a second order process predominates in the case of the picoline system.

4-Picoline

<i>Temp (K)</i>	298	303	308	313	318	328
Concentration (Mol dm⁻³)	K_{obs} (s⁻¹) x 10³					
1.66×10^{-2}	0.40	0.58	0.98	1.46	1.95	2.96
3.33×10^{-2}	0.81	1.18	1.94	2.83	3.80	5.48
4.99×10^{-2}	1.17	1.81	2.88	4.15	5.98	8.04
6.67×10^{-2}	1.61	2.37	3.81	5.55	7.92	9.91
8.32×10^{-2}	1.88	2.88	4.56	6.95	9.67	11.96

2-Picoline

3.33×10^{-2}	0.3	0.45	0.67	1.03		
4.99×10^{-2}	0.41	0.61	0.88	1.30	2.25	
6.67×10^{-2}	0.47	0.75	1.05	1.60	2.06	
8.32×10^{-2}	0.51	0.75	1.20	1.90	2.25	

Table 22

**Kinetic data for the displacement of ethanol from
W(CO)₅(Et-OH) by 2- and 4-picoline.**

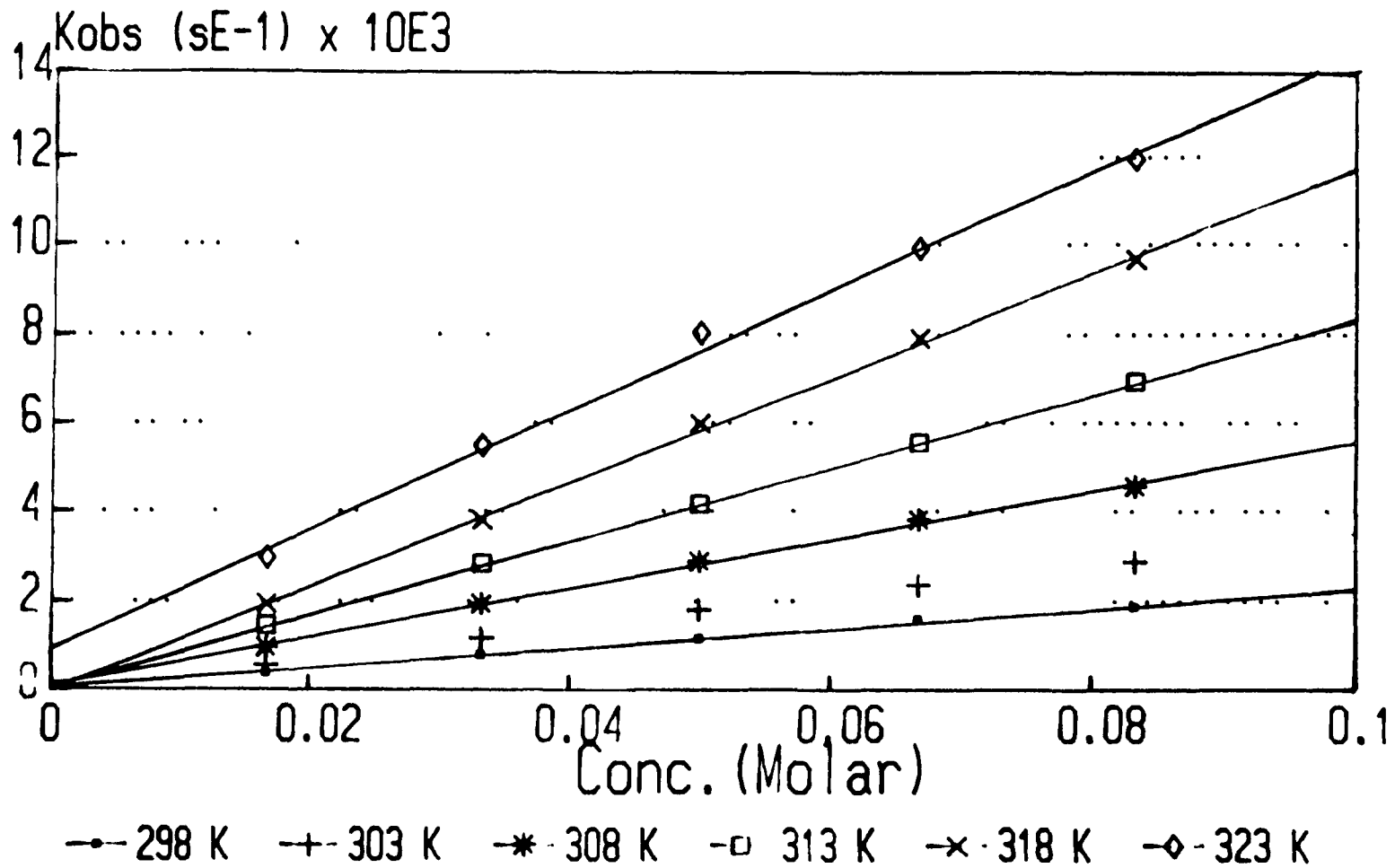


Figure 2.4 Plot of K_{obs} against concentration of 4-picoline at different temperatures

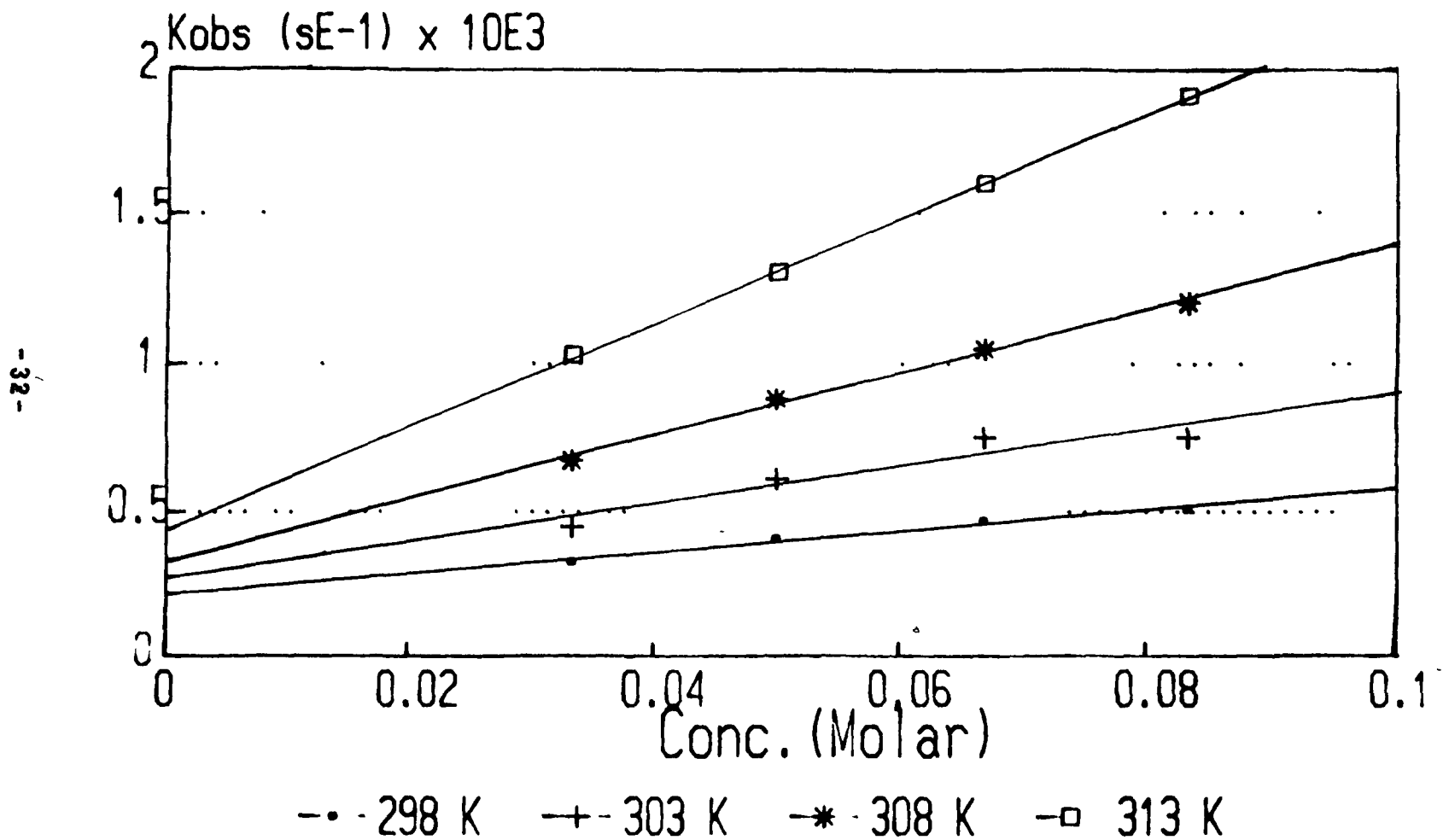
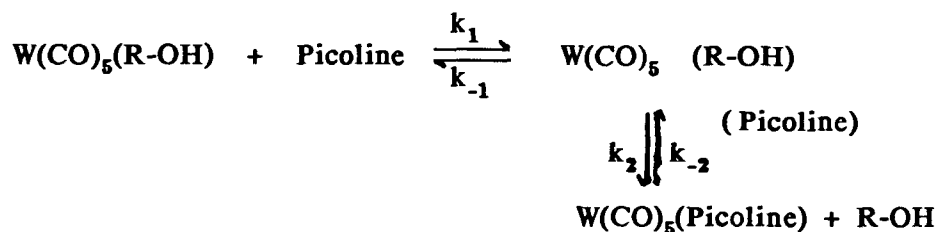


Figure 2.5 Plot of K_{obs} against concentration of 2-picoline at different temperatures

The second order rate constants derived from these pseudo first order plots yield values of $(2.25 \pm 0.1) \times 10^{-2} \text{ dm}^3\text{mol}^{-1}\text{s}^{-1}$ for the 4- picoline and $(4.8 \pm 0.2) \times 10^{-3} \text{ dm}^3\text{mol}^{-1}\text{s}^{-1}$ for the 2- picoline reactions with $\text{W}(\text{CO})_5(\text{Et-OH})$ at a temperature of 25°C . Similarly, a second order rate constant of $(2.21 \pm 0.1) \times 10^{-2} \text{ dm}^3\text{mol}^{-1}\text{s}^{-1}$ was obtained for the $\text{W}(\text{CO})_5(\text{Bu-OH})$ and 4- picoline system. The second order rate constants obtained for the 2- and 4- picoline systems at varying temperatures are listed in Table 2.3.

These results suggest that an associative mechanism occurs, presumably by the formation of a seven coordinate species. The second order rate constant for the 4-picoline system is larger than that for the 2- picoline system. This is not surprising as the presence of a methyl group α to the coordinating nitrogen in 2- picoline would be expected to hinder the formation of a seven coordinate species. The proposed associative mechanism is given in Scheme 2.4.



Scheme 2.4

Second order rate
constants, k
(dm³ mol⁻¹ s⁻¹)

Temperature
Kelvin, K

W(CO)₅(Et-OH) + 4- Picoline

2 25	x 10 ⁻²	298
3 47	x 10 ⁻²	303
5 41	x 10 ⁻²	308
8 20	x 10 ⁻²	313
11 74	x 10 ⁻²	318
13 46	x 10 ⁻²	323

W(CO)₅(Et-OH) + 2- Picoline

4 80	x 10 ⁻³	298
9 14	x 10 ⁻³	303
1 07	x 10 ⁻²	308
1 78	x 10 ⁻²	313
1 44	x 10 ⁻²	318

W(CO)₅(Bu-OH) + 4- Picoline

2 21	x 10 ⁻²	298
3 22	x 10 ⁻²	303
5 04	x 10 ⁻²	308
7 47	x 10 ⁻²	313
10 11	x 10 ⁻²	318
15 17	x 10 ⁻²	323

Table 2.3 Second order rate constants (k) for the 2- and 4-picoline systems at varying temperatures.

By solving the rate equation for this scheme, the observed rate constant is found to equal $k_1[\text{picoline}]$. The slope of the pseudo first order plot is therefore the rate constant k_1 for the formation of the seven coordinate intermediate

The variation of the second order rate constant with temperature allows for the determination of the activation energy (E_{act}), the enthalpy of activation (ΔH^\ddagger), and the entropy of activation (ΔS^\ddagger) for each system. The activation parameters are

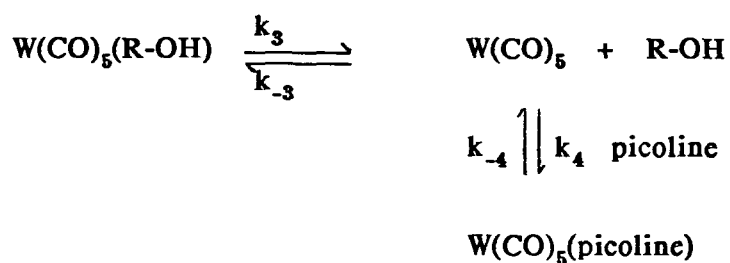
$\text{W(CO)}_5(\text{R-OH})$	Picoline	E_{act} (kJ Mol ⁻¹)	ΔH^\ddagger (kJ Mol ⁻¹)	ΔS^\ddagger J K ⁻¹ Mol ⁻¹
$\text{W(CO)}_5(\text{Et-OH})$	2-picoline	63.0	60.9	-84.3
$\text{W(CO)}_5(\text{Et-OH})$	4-picoline	60.0	57.1	-84.4
$\text{W(CO)}_5(\text{Bu-OH})$	4-picoline	61.0	58.9	-78.7

Table 2.4 Activation Parameters for the $\text{W(CO)}_5(\text{R-OH})$ Reactions with 2- and 4- picoline

listed in Table 2.4. The negative values for the entropy of activation (ΔS^\ddagger) would suggest that an associative mechanism predominates.

As can be seen from Figures 2.4 and 2.5, there exists non-zero intercepts in the pseudo first order plots for both the 2- and 4- picoline systems. This would suggest that a further reaction path is available for the $\text{W(CO)}_5(\text{R-OH})$ and picoline. The values of the non-zero intercepts obtained from a least squares

linear regression was $1.34 \times 10^{-4} \text{ s}^{-1}$ and $4.6 \times 10^{-5} \text{ s}^{-1}$ for 2- and 4-picoline respectively at 25°C. The values of these intercepts were observed to increase with increasing temperature (Figures 2.4 and 2.5). This intercept can be explained by the contribution of a dissociative mechanism to the overall reaction. This dissociative mechanism leads to the formation of a coordinatively unsaturated pentacarbonyl species which then reacts with the free picoline ligand, as in Scheme 2.5.



Scheme 2.5

The rate of this dissociative reaction is independent of the picoline concentration and is determined by the rate constant for the dissociation of the $\text{W(CO)}_5(\text{R-OH})$ solvated species into the coordinatively unsaturated species, W(CO)_5 .

Further evidence for this was obtained by continual scanning over the ultraviolet-visible spectral range from 500nm to 300nm of a solution of $\text{W(CO)}_5(\text{Et-OH})$ in the absence of picoline, every twenty minutes at 50°C (Figure 2.6). A decrease in the absorption band at 415nm, which is characteristic of the $\text{W(CO)}_5(\text{Et-OH})$ complex, was observed. Similarly, this was observed for the $\text{W(CO)}_5(\text{Bu-OH})$ complex. This would suggest that the solvated pentacarbonyl, $\text{W(CO)}_5(\text{R-OH})$, is thermally unstable. This thermal instability, presumably results in the formation of W(CO)_6 and other products with the coordinatively unsaturated pentacarbonyl species, W(CO)_5 , being initially produced and very short-lived. However, this was not verified.

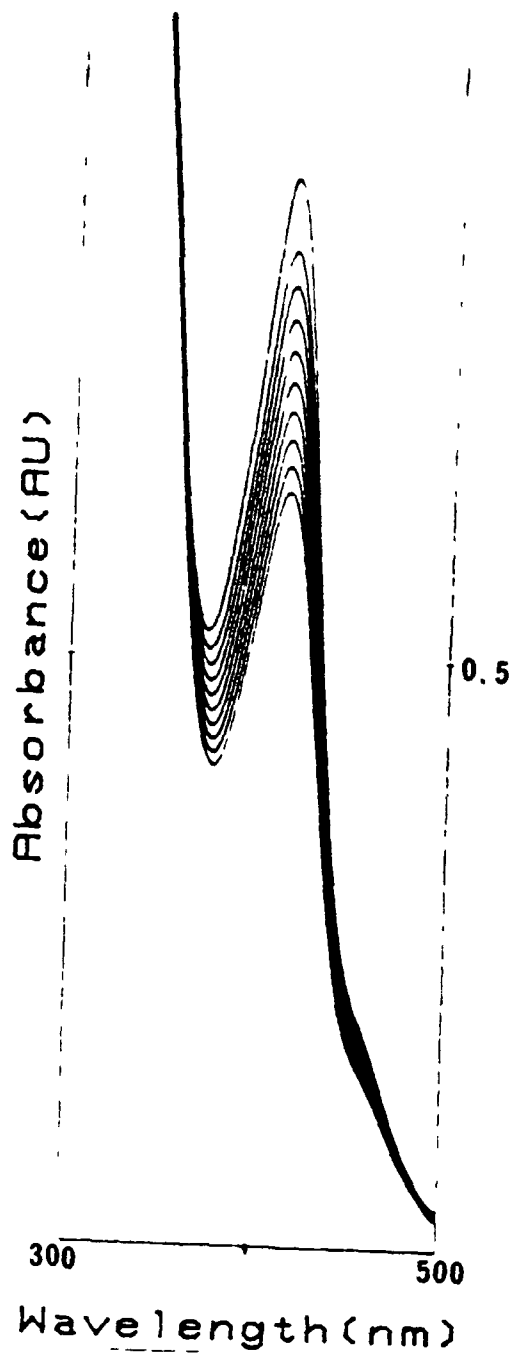
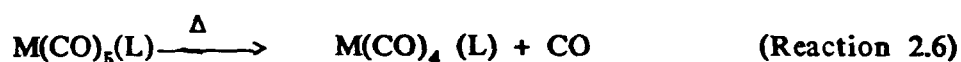
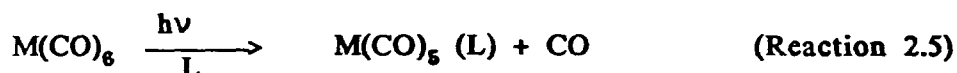


Figure 26

Absorption spectral sequence of a solution of $W(CO)_5(R-OH)$ at $50^\circ C$ at 20 minute intervals

2.c.1 Kinetic Study of the Formation of $W(CO)_4(L)$ (where L = Bipyridine or 3,6-bis(2-pyridyl)1,4-dihydro-1,2,4,5-tetrazene from $W(CO)_5(Toluene)$)

The photochemical formation of $M(CO)_4(L)$ complexes (where M = Cr, Mo, or W and L is a bidentate ligand), is thought to proceed according to reactions 2.5 and 2.6



Evidence for the monodentate intermediate $M(CO)_5(L)$ was reported by Staal *et al.* for M = Cr or Mo and L = 1,4-diphenyl-1,4-diazabutadiene, who observed a green transient during the substitution reaction of the corresponding $M(CO)_5$ (Tetrahydrofuran) complex with L at $-60^\circ C$ ¹³ This intermediate was observed to react rapidly at room temperature to form $M(CO)_4(L)$ product. However, direct spectral evidence for the $M(CO)_5(L)$ transient and quantitative reactivity measurements were not reported in this work. Recently, Wrighton and coworkers have provided spectral evidence for the formation of $M(CO)_5(L)$, where M is Cr or W and L is 4,4'-dialkyl-2,2'-bipyridine ligand, using rapid-scanning Fourier-transform infrared spectroscopy¹⁴ Furthermore, Connor *et al.* have isolated monodentate $M(CO)_5(L)$ complexes, where M = Mo or W and L is a bidentate phosphorous arsenic donor ligand, and determined the rate of their chelation reactions with the use of infrared spectroscopy¹⁵

More recently, the photolysis of $M(CO)_6$ (where M = Cr, Mo, or W) solutions containing diimine ligands (1,10 phenanthroline, 2,2'-bipyridine, 1,4-diazabutadiene, or their derivatives) were followed with the use of a microprocessor-controlled diode-array uv-visible spectrophotometer.¹⁶

The time-dependent spectra illustrate rapid formation of a reaction intermediate that is assigned to be $M(\text{CO})_5(\text{L})$, where L is a diimine ligand coordinated in a monodentate fashion. The monodentate $M(\text{CO})_5(\text{L})$ subsequently extrudes CO thermally via a first-order kinetic process to form the stable $M(\text{CO})_4(\text{L})$ species. Also the marked dependence of reaction rate on diimine and resulting negative activation entropy values suggested that the chelation mechanism proceeds with a substantial associative component.

In Section 3, the monodentate $\text{W}(\text{CO})_5(\text{L})$ complex, where L is 2,2'-dipyridylamine, a bidentate ligand was isolated. This pentacarbonyl complex was found to be stable unless exposed to light or heat. The application of heat resulted in the formation of the $\text{W}(\text{CO})_4(2,2'\text{-dipyridylamine})$ complex. Attempts to monitor this chelation reaction spectrophotometrically proved difficult because there was no suitable solvent for both the pentacarbonyl species, $\text{W}(\text{CO})_5(2,2'\text{-dipyridylamine})$, and the tetracarbonyl species, $\text{W}(\text{CO})_4(2,2'\text{-dipyridylamine})$, was not found. However, as will be seen later in Section 3, it was monitored using a thermogravimetric analyser.

Also in Section 3, tetracarbonyl complexes, $M(\text{CO})_4(3,6\text{-Bis}(2\text{-pyridyl})\text{-}1,4\text{-dihydro-}1,2,4,5\text{-tetrazene})$ ($M = \text{Cr}, \text{Mo}, \text{or W}$) were isolated. Therefore, a kinetic study of the photolysis of $\text{W}(\text{CO})_6$ solution containing 3,6-Bis(2-pyridyl)-1,4-dihydro-1,2,4,5-tetrazene, (SL), was undertaken to determine if the SL system would behave as the 2,2'-bipyridine system, already reported by Lees and coworkers¹⁶. It was also decided that a kinetic study of the photolysis of $\text{W}(\text{CO})_6$ solution containing 2,2'-bipyridine might also be useful. A microprocessor-controlled diode-array ultraviolet-visible spectrophotometer was used to monitor the formation of $\text{W}(\text{CO})_4(\text{L})$ (where $\text{L} = 2,2'\text{-bipyridine}$ or 3,6-bis, (2-pyridyl)-1,4-dihydro-1,2,4,5-tetrazene) after the photolysis of a $\text{W}(\text{CO})_6$ solution containing either of the bidentate ligands.

2.c.11 Results and Discussion

A typical experiment consisted of approximately 2 seconds ultraviolet excitation of a solution of toluene (3ml) which was 5×10^{-4} mol $W(CO)_6$ and 1×10^{-3} mol of the concerned ligand. All solutions were degassed by the freeze-pump thaw method prior to photolysis. No attempt was made to determine the amount of $W(CO)_6$ which was photodissociated after photolysis, however it would appear that approximately 1×10^{-4} mol of $W(CO)_6$ was photodissociated. This value was estimated from the known quantum yield of $M(CO)_6$,¹⁷ $M = Cr, Mo$ or W , and from the amount of tetracarbonyl formed.

The spectral sequence obtained following ~ 2 s ultraviolet photolysis of a deoxygenated toluene solution at $20^\circ C$ containing 5×10^{-4} mol $W(CO)_6$ and 1×10^{-3} mol 2,2'-bipyridine is shown in Figure 27. In this experiment, the initial spectrum was recorded approximately 2 seconds after excitation. Subsequent to photolysis, the diode-array ultraviolet spectrophotometer was referenced by a solution containing 5×10^{-4} mol $W(CO)_6$ and 1×10^{-3} mol 2,2'-bipyridine. The formation of $W(CO)_4(2,2'\text{-bipyridine})$ as a product was characteristic by the growth of its intense metal-ligand charge-transfer (MLCT) transition at 514nm. The final spectrum obtained was similar to a spectrum of an authentic sample of $W(CO)_4(2,2'\text{-bipyridine})$ in the visible region. The existence of two isosbestic points at 398nm and 498nm would suggest that the reaction proceeds uncomplicated by side or subsequent reactions.

Lees et al.,¹⁶ proposed the following reactions 27, 28, and 29 to account for the overall reaction for the formation of $W(CO)_4(2,2'\text{-bipyridine})$ from the photolysis of $W(CO)_6$ solution containing 2,2'-bipyridine

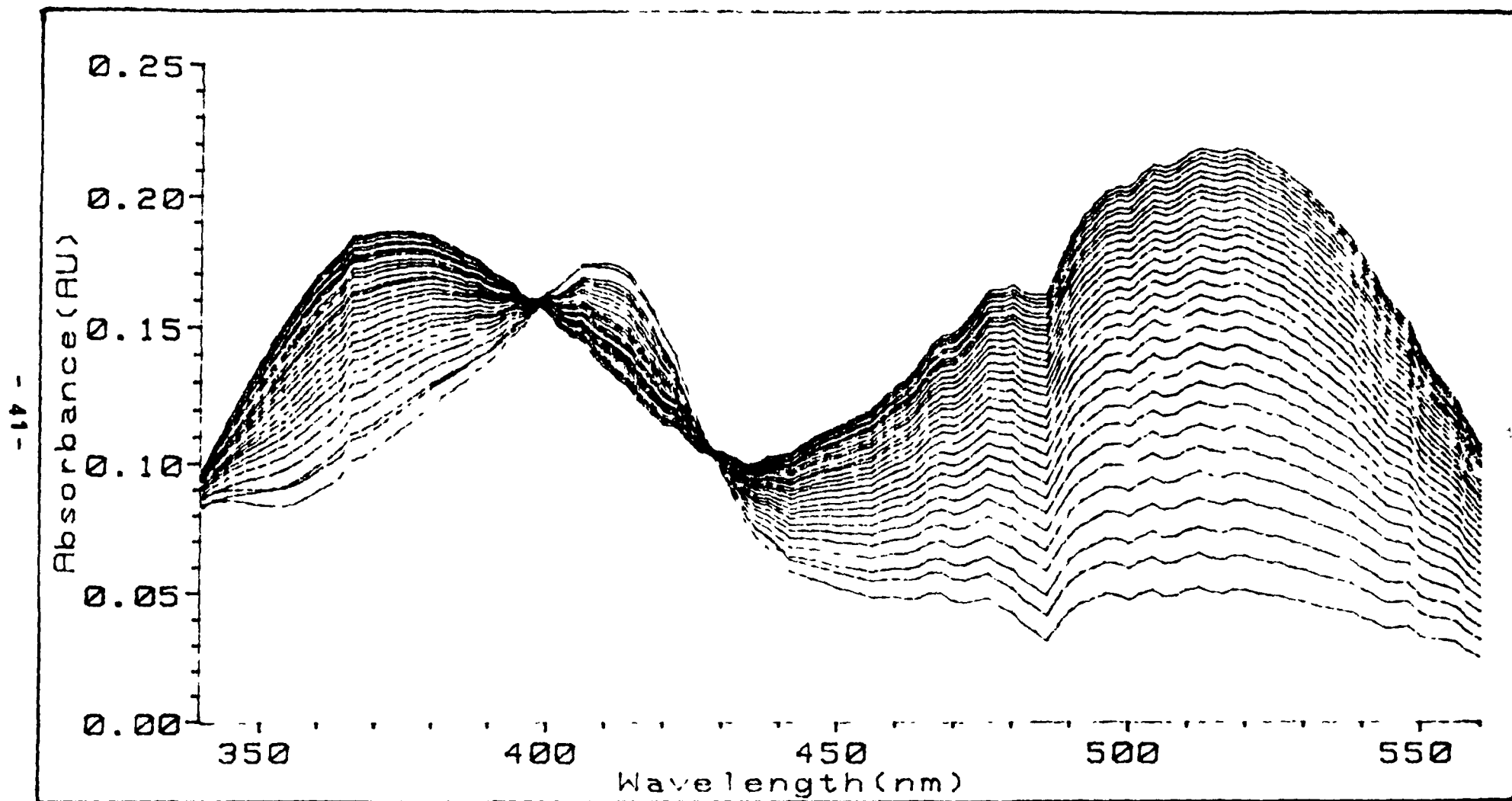


Figure 2.7 Absorption spectral sequence recorded following approx. 2-s u.v. irradiation of a solution of 5×10^{-4} $W(CO)_6$ in toluene containing 3×10^{-3} M 2,2'-bipyridine at 20°C

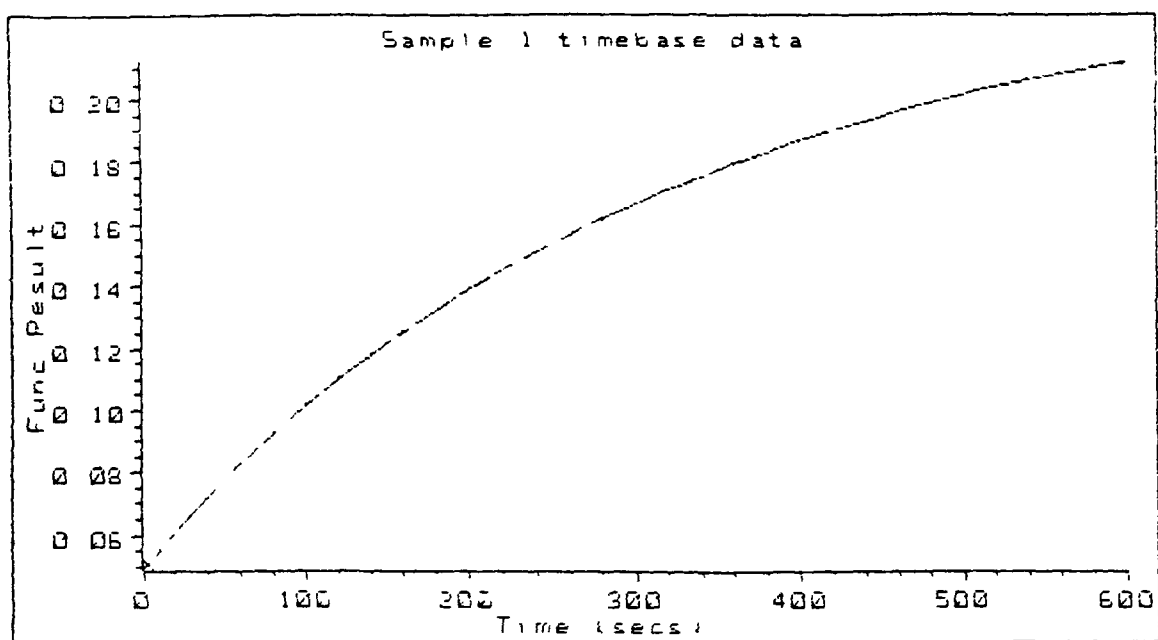
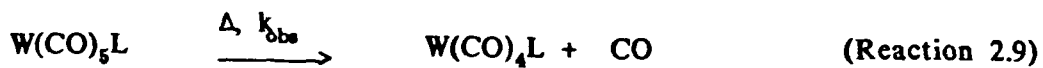
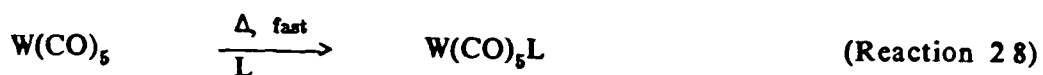
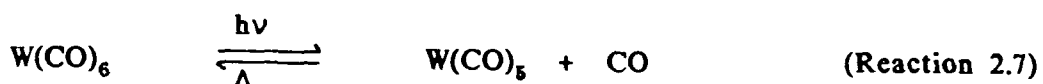


Figure 2.8 First order plot for the rate of formation of $W(CO)_4$ (2,2'-bipyridine)



L = 2,2'bipyridine

Kinetic measurements have been carried out for the reaction in which $W(CO)_5(2,2'\text{-bipyridine})$ extrudes CO to form $W(CO)_4(2,2'\text{-bipyridine})$, (Reaction 2.9). In each case, the rate of this reaction was determined by monitoring the growth of the long-wavelength MLCT absorption band of $W(CO)_4(2,2'\text{-bipyridine})$ product.

The growth of $W(CO)_4(2,2'\text{-bipyridine})$ was found in all cases to fit a first order analysis (as seen in Figure 28) The first order rate constants are listed in Table 25 The rate of formation of $W(CO)_4(2,2'\text{-bipyridine})$ was found to be 0.2 s^{-1} at 20°C Moreover, these rate constants were found to be independent of ligand concentration for the range 10^{-3} and $3 \times 10^{-3}\text{M}$, within experimental error

Lee's et al,¹⁶ suggested that the absorbance at approximately 410nm was due to the $W(CO)_5(2,2'\text{-bipyridine})$ complex which is formed initially after the photolysis of $W(CO)_6$ This intermediate then slowly forms the $W(CO)_4(2,2'\text{-bipyridine})$ end-product

The spectral sequence obtained following $\sim 2\text{s}$ photolysis of a solution containing $5 \times 10^{-4}\text{M}$ $W(CO)_6$ in absence of added ligand is shown in Figure 29 This absorbance at 410nm is thought to be due to the solvated pentacarbonyl

Ligand (L)	Concentration of Ligand (M dm^{-3})	K_{obs} (s^{-1})
2,2'Bipyridine	1×10^{-3}	0.20
	3×10^{-3}	0.21
3,6-bis(2-pyridyl) 1,4 dihydro 1,2,4,5 tetrazene	1×10^{-3}	6.0×10^{-3}
	4×10^{-3}	5.5×10^{-3}

Table 25: First order rate constants obtained from the reaction of $W(CO)_5L$ to form $W(CO)_4L$ and CO.

$W(CO)_5(\text{toluene})$, which is formed from the highly reactive uncoordinated pentacarbonyl $W(CO)_5$ and toluene As seen in Figure 29, the $W(CO)_5(\text{toluene})$ is -

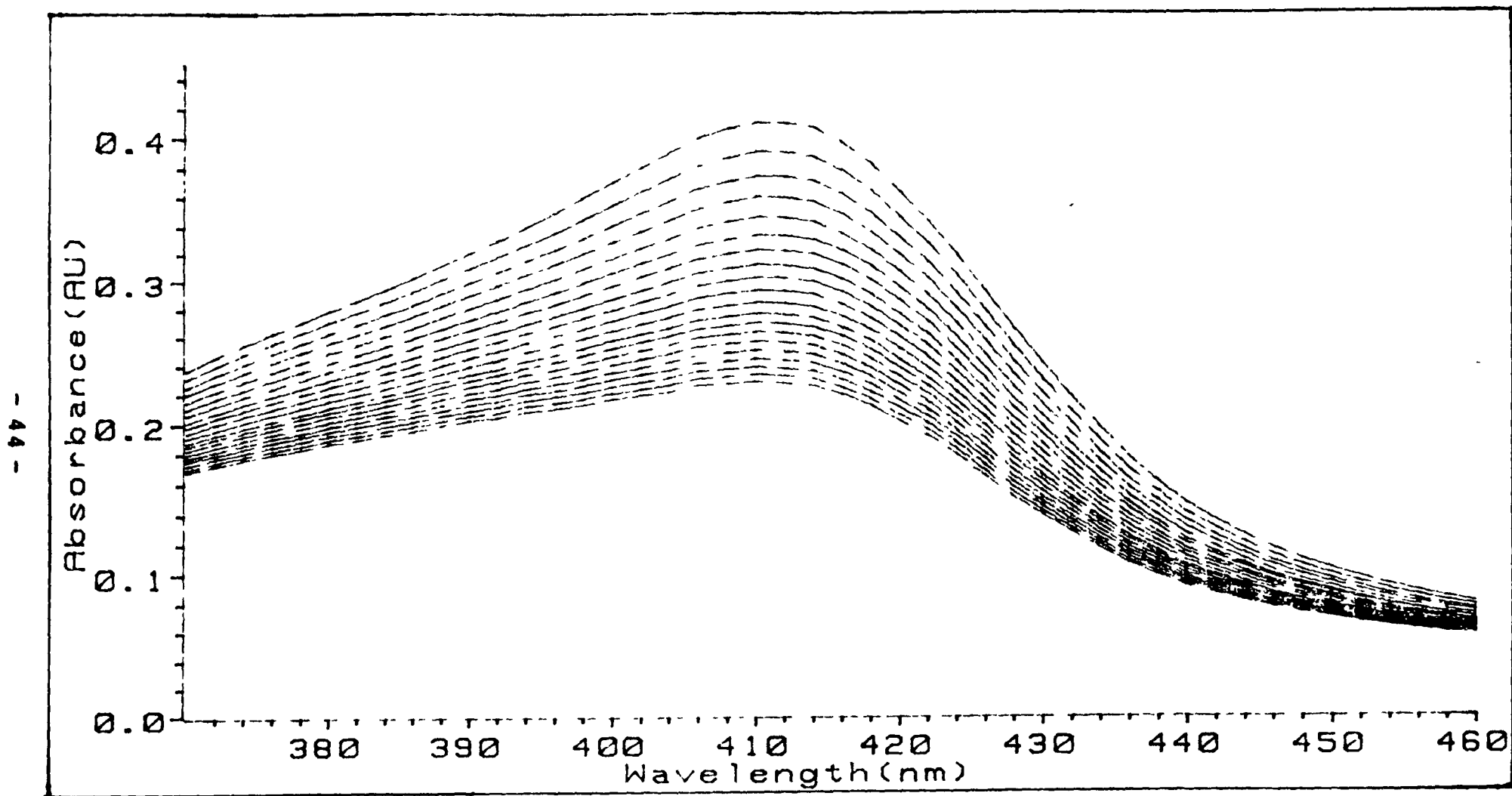
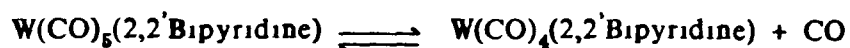
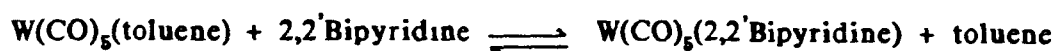
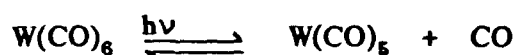


Figure 2.9 Absorption spectral sequence recorded following approx. 2-s u.v. irradiation of a solution of 5×10^{-4} mol. $W(CO)_6$ in toluene at $20^\circ C$ with 3 minute intervals

not stable, and presumably decomposes to form $W(CO)_6$ and side products. The rate of this decomposition was also found to be first order with a rate constant of 0.02 s^{-1} . Therefore, since toluene is present in excess of ligand and $W(CO)_6$, it would seem possible to suggest that $W(CO)_5(\text{toluene})$ is formed initially and this intermediate be assigned the transition at 410nm in the spectral sequence following photolysis of $W(CO)_6$ solution containing 2,2'-bipyridine, as in Figure 27

The following set of reactions in Scheme 26 are suggested to account for the overall reaction of the photolysis of $W(CO)_6$ in toluene containing the bidentate ligand, 2,2'-bipyridine



Scheme 26

Since both $W(CO)_5(\text{toluene})$ and $W(CO)_4(2,2'\text{-bipyridine})$ absorb in the 350 to 420nm region of the spectrum, isolation of the transition of the $W(CO)_5(2,2'\text{-bipyridine})$ would seem difficult. Also, as seen in Section 3, uv-visible spectra of $W(CO)_5(2\text{-phenylpyridine})$, $W(CO)_5(2,2'\text{-dipyridylamine})$ and $W(CO)_5(\text{pyridyl - pyrimidine})$ in toluene, all exhibited transitions in the 370 to 390nm range. Therefore, identification of the $W(CO)_5(2,2'\text{-dipyridine})$ intermediate would seem difficult.

In the case where the ligand is 3,6-bis(2-pyridyl)1,4-dihydro-1,2,4,5-tetrazene (SL), a different spectral sequence was observed, as in Figure 2.10. The same method was adopted for the SL system as in the 2,2'-bipyridine system, only that the spectra were recorded every 3 minutes instead of 20 seconds. The rate of formation of $W(CO)_4SL$ was much slower than the rate of formation of $W(CO)_4(2,2'\text{-bipyridine})$. As before, the rate of the reaction was monitored by the increase in the MLCT absorption band of the $W(CO)_4(SL)$ at 538nm. The final spectrum obtained was similar to that of a uv/visible spectrum of an authentic sample of $W(CO)_4(SL)$ in the visible region. The absence of any isosbestic points would suggest that the reaction is more complicated than the 2,2'-bipyridine system.

As before with the 2,2'-bipyridine system, the growth of the $W(CO)_4(SL)$ was found to fit a first order plot. The first order rate constants are listed in Table 2.4. The rate of formation of $W(CO)_4(SL)$ was found to be $6.0 \times 10^{-3} \text{ s}^{-1}$ at 20°C. The rate constants were also found to be independent of ligand concentration for the range 10^{-3} and $4 \times 10^{-3} \text{ M}$, within experimental error.

The characteristic peak for the $W(CO)_5(\text{toluene})$ intermediate at 410nm is short lived, as seen in Figure 2.10. Within approximately 3 minutes of photolysis, the observed peak at 410nm had disappeared and an absorption maxima at 398nm was observed. The spectral sequence recorded at 20 second time intervals following ~2 sec photolysis of a toluene solution containing $5 \times 10^{-4} \text{ M } W(CO)_6$ and $4 \times 10^{-3} \text{ M SL}$ is shown in Figure 2.11. A depletion in the absorption band of the $W(CO)_5(\text{toluene})$ intermediate at 410nm was initially observed, followed by a shift of the transition band towards 390nm. This would suggest that the $W(CO)_5(SL)$ species is longer lived than the $W(CO)_5(2,2'\text{-bipyridine})$ and as expected, absorbs in the 390 to 400nm region. There also exists the possibility of

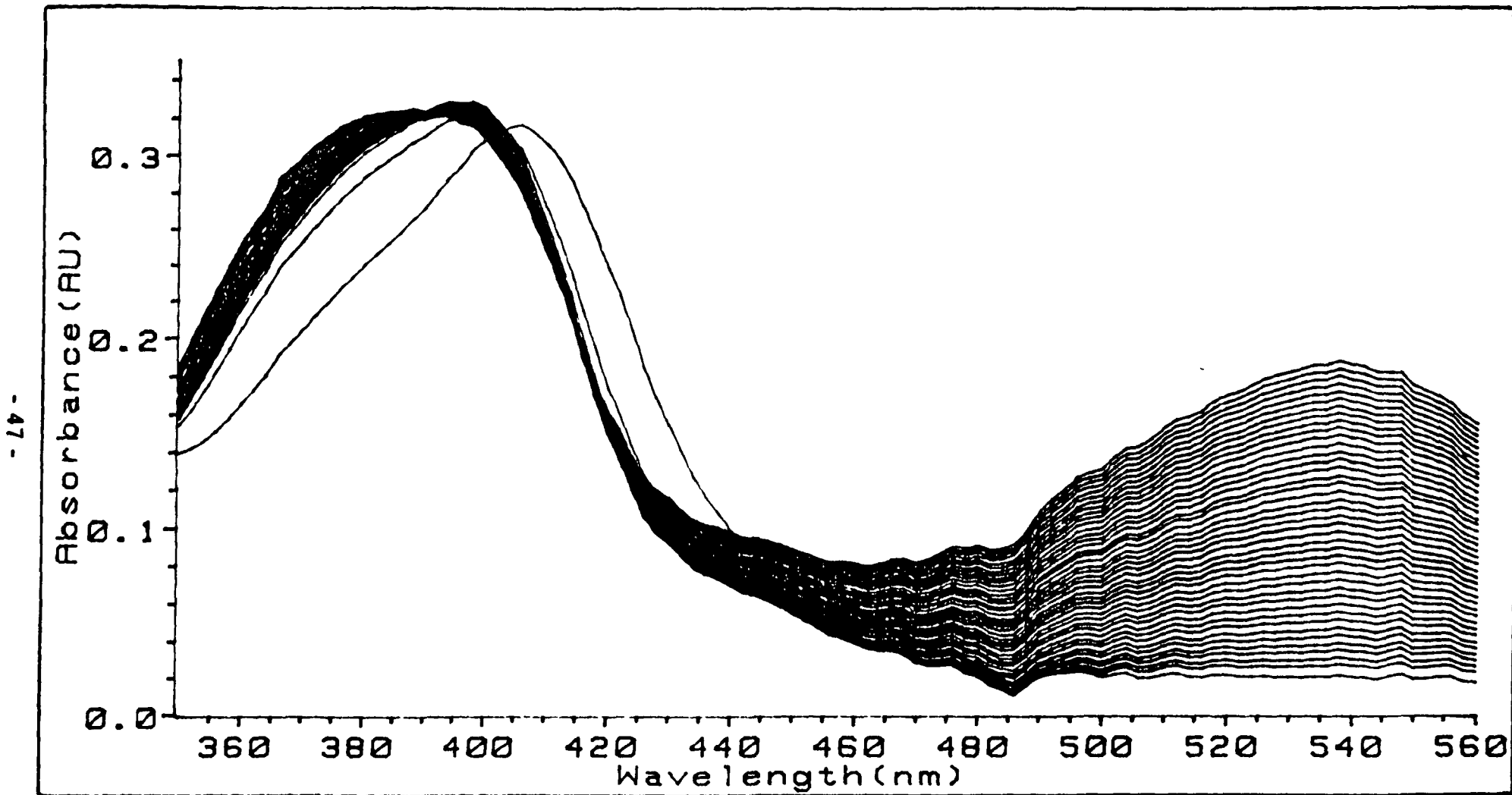


Figure 2.10 Absorption spectral sequence recorded following approx. 2-s u.v. irradiation of a solution of $5 \times 10^{-4} \text{ M W(CO)}_6$ in toluene containing $4 \times 10^{-3} \text{ M SL}$ at 20°C with 3 minute intervals

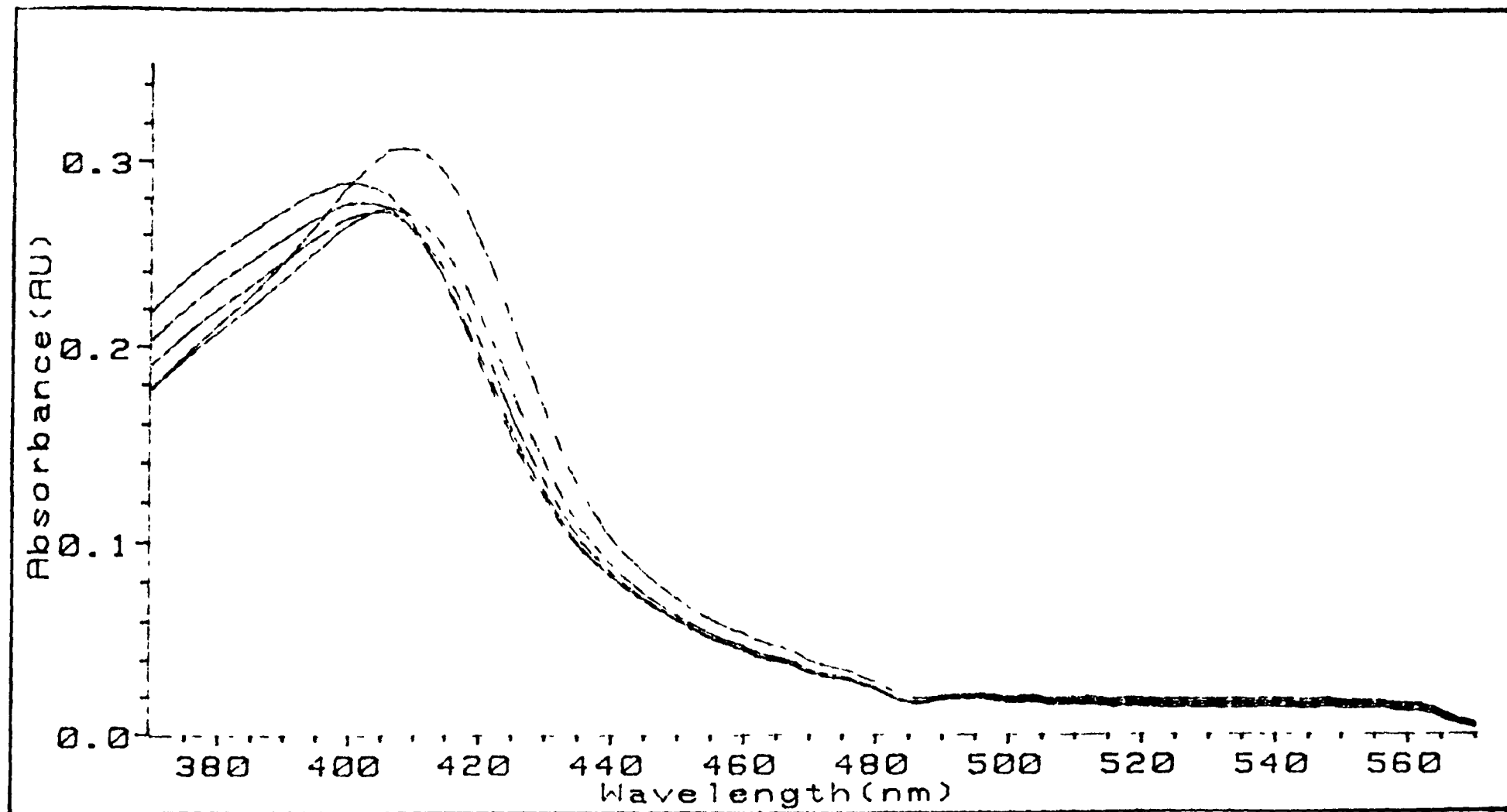


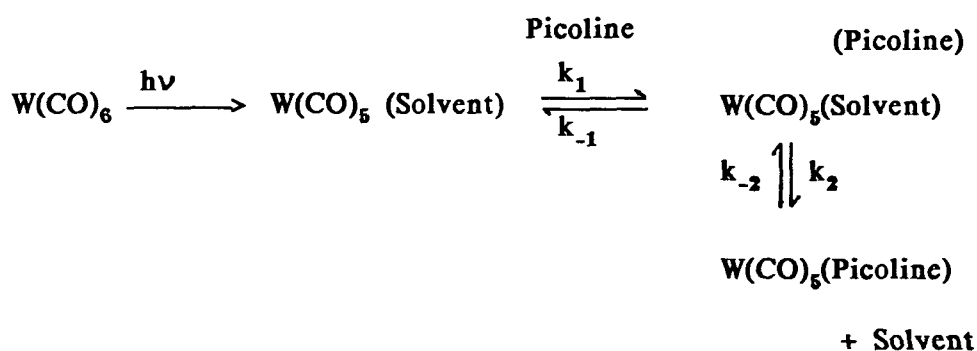
Figure 2.11 Absorption spectral sequence recorded following approx. 2-s u.v. irradiation of a solution of $5 \times 10^{-4} \text{ M } W(CO)_6$ in toluene containing $4 \times 10^{-3} \text{ M SL}$ at 20°C with 20 second intervals

the ligand-bridged species, $W(CO)_4(SL)W(CO)_4$, being formed. However, in the presence of excess ligand, the probability of $W(CO)_4(SL)W(CO)_4$ being formed is small.

2 d. CONCLUSION

The linear dependence of K_{obs} on picoline concentration would seem to suggest that the dissociative mechanism proposed for the 4-acetyl-pyridine system⁴, is not required to explain the behaviour of the picoline system. It would appear that the $W(CO)_5(\text{cyclohexane})$ and picoline systems follow simple second order kinetics. The exact mechanism of the reaction remains unclear however, an associative mechanism involving the formation of a coordinatively expanded species is a possibility (Scheme 2.7)

The second order rate constants for these systems were determined to be 1.2×10^7 and $3.6 \times 10^7 \text{ dm}^3\text{mol}^{-1}\text{s}^{-1}$ for



Scheme 2.7

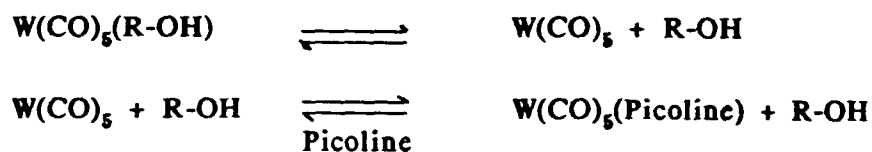
2- and 4-picoline respectively. The rate constant for the formation of the intermediate species is smaller for 2-picoline than for 4-picoline. This is not surprising as the presence of a methyl group α to the coordinating nitrogen in 2-picoline would be expected to hinder the formation of a seven coordinate species, assuming an associative mechanism.

Further evidence for an associative mechanism was obtained from the study of the reaction of $W(CO)_5(R-OH)$, (where $R = \text{Et}$ or Bu), with 2- and 4-picoline

The mechanism for the displacement of alcohol from $W(CO)_5(R-OH)$ by 2- and 4-picoline has been shown to involve two pathways. The principal pathway would appear to be an associative mechanism involving the formation of a seven coordinate intermediate or transition state (Scheme 27), in a rate determining step

The second order rate constants for this process were determined to be $480 \times 10^{-3} \text{ dm}^3\text{mol}^{-1}\text{s}^{-1}$ and $225 \times 10^{-2} \text{ dm}^3\text{mol}^{-1}\text{s}^{-1}$ for the 2- and 4-picoline systems respectively, at 25°C . The negative values for the entropy of activation would further support an associative mechanism

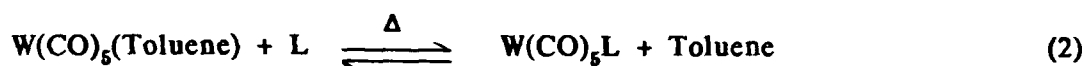
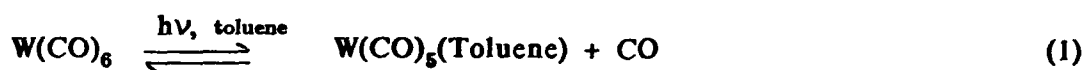
The existence of non-zero intercepts in the pseudo first order plots provided evidence for a dissociative mechanism (Scheme 28). The contribution



Scheme 28

of which is greater for the 2- picoline system than for the 4- picoline. This would be as expected since an α -substituent on the pyridine ring would greatly hinder the formation of a seven-coordinate intermediate. Further evidence for the existence of an equilibrium between $W(CO)_5(R-OH)$ and the uncoordinated pentacarbonyl $W(CO)_5$, is supported by the fact that $W(CO)_5(R-OH)$ was found to be thermally unstable

The set of reactions in Scheme 2.9 are suggested to account for the overall reaction following the photolysis of a solution containing $W(CO)_6$ and L, where L is a bidentate ligand. The rate of formation of $W(CO)_4(L)$ from $W(CO)_5(L)$ was found to obey first order kinetics with rate constants of 0.2 s^{-1} and $6.0 \times 10^{-3} \text{ s}^{-1}$ at 20°C when L is 2,2'-bipyridine and 3,6-Bis(2-pyridyl)-1,4-dihydro-1,2,4,5-tetrazene respectively. The intermediate observed approximately



Scheme 2.9

2 seconds after photolysis was assigned to the solvated pentacarbonyl, $W(CO)_5(\text{toluene})$, which in the absence of free ligand decomposed with a first order rate constant of 0.02 s^{-1} .

2.e Experimental

2.e.I Apparatus

The laser flash photolysis apparatus consisted of a Xe-Cl excimer laser, producing a line at 308nm with a duration of approximately 10ns. The monitoring beam was at right angles to the excitation beam (Figure 2.12) and was generated by a Xe arc lamp fitted with a pulsing unit. After passing through the sample, the monitoring beam was passed through a radiance grating monochromator and detected by an IP28 photomultiplier. The signal was stored and digitised on a Philips 3311 oscilloscope and analysed using a BBC B+ computer. A more detailed description of the laser flash photolysis apparatus is given in Figure 2.12.

The kinetics of the thermal displacement of R-OH from $W(CO)_5(R-OH)$ by 2- or 4-picoline was monitored by a Shimadzu (UV-240) ultraviolet-visible spectrophotometer. The spectrophotometer was interfaced (via a Shimadzu option program/interface (OPI-1)) to a Commodore 8032-SV minicomputer, a CMM 8050 discdrive and a 4022S printer. Rate constants were calculated using a Guggenheim method or a least squares method using a plot of $\text{Log}(A_0 - A)/(A_t - A)$ versus time, t , where

A_0 = Absorbance at time, $t = 0$

A_t = Absorbance at time, $t = t$

A = Absorbance at time, $t = \infty$

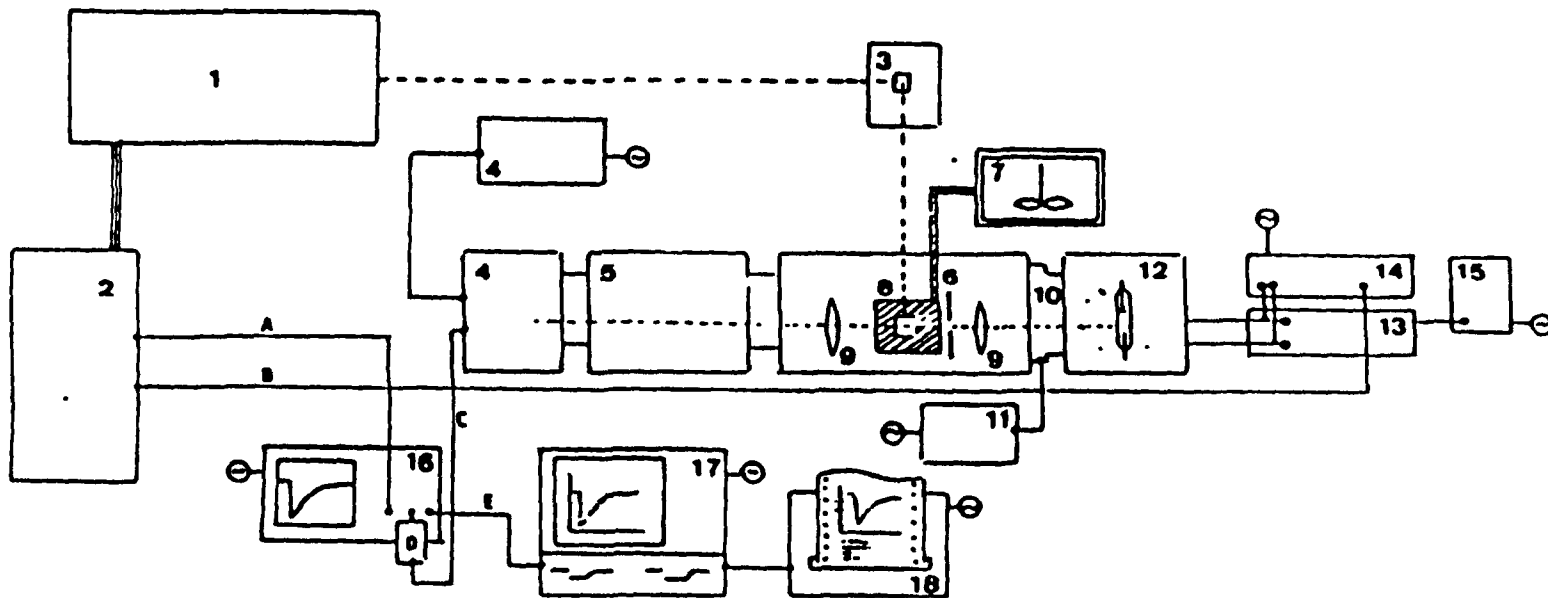
The reactions of a photolysed solution containing $W(CO)_6$ and a bidentate ligand were followed using a Hewlett-Packard 84252A Diode Array spectrophotometer.

2.c.II Materials

The tungsten hexacarbonyl was obtained from Strem Chemicals Ltd and was used without further purification

The cyclohexane used was of spectroscopic grade, obtained from BDH Ltd, and was used without further purification. All other solvents were reagent grade and were fractionally distilled (twice) prior to use.

2- and 4-picoline were obtained from Riedel-de-Haen and were distilled under reduced pressure prior to use. 2,2'-bipyridine was also obtained from Riedel-de-Haen and used without further purification. 3,6-bis(2-pyridyl)1,4-dihydro-1,2,4,5-tetrazene was received as a present from the University of Leiden and used without further purification.



- | | | |
|--|--|--|
| <p>1 Lambda Physik EMG 50 excimer laser.
 2 Laser power supply.
 3 Dye Laser (Coumarin 1)
 4 Photomultiplier (Hamamatsu R928) housing and power supply.
 5 F/3.4 monochromator (Applied Photophysics (AR)).
 6 Iris.
 7 Waterbath.
 8 Thermostatted cell holder and housing (AR)</p> | <p>9 $f = 125$ quartz lens.
 10 Electronic shutter.
 11 Shutter control and triggerbox (AR).
 12 25W Xenon synchronised monitoring lamp and housing (AR).
 13 Xenon lamp power supply (AR).
 14 Arc lamp pulsing unit (AR).
 15 Interlock unit with temperature sensor (AR).
 16 Phillips PM3311C storage oscilloscope.
 17 BBC microcomputer.
 18 Printer.</p> | <p>A Oscilloscope trigger
 B Laser trigger delayed a preset amount w.r.t. lamp pulse trigger.
 C Signal output to lead resistor
 D Lead resistor (RC-time = 17ns at 50 Hz-time = 23ns at 100 Hz).
 E IEEE bus.</p> |
|--|--|--|

Figure 2.12 The laser flash photolysis apparatus

2f REFERENCES

- 1 J M Kelly, C Long, and R Bonneau, J Phys Chem, 1983, 87, 3344
- 2 C H Langford, C Moralejo, and D K Sharma, Inorg Chim Acta, 1987, L11
- 3 J A Walsh, S K Peters, and V J Vaida, J Phys Chem, 1982, 86, 1941
- 4 A J Lees and R W Adamson, Inorg Chem, 1981, 20, 4381.
- 5 F Basolo, Inorg Chim Acta, 1981, 50, 65
- 6 (a) R J Angelici, Organomet Chem Rev, 1988, 3, 173
(b) D A Brown, Inorg Chim Acta Rev, 1967, 1, 35
(c) H Werner, Angew Chem Int Ed Engl, 1968, 7, 930
(d) G R Dobson, Acc Chem Res, 1978, 9, 300
(e) D J Darensbourg, Adv Organomet Chem, 1982, 21, 113
- 7 C H Langford and H B Gray, "Ligand Substitution Processes", Benjamin, New York, 1965
- 8 J R Graham and R J Angelici, Inorg Chem, 1967, 6, 2082
- 9 D J Darensbourg and T L Brown, Inorg Chem, 1968, 7, 1679
- 10 D J Darensbourg, M Y Darensbourg, and R J Dennenbourg, J Am Chem Soc, 1971, 93, 2807
- 11 R J Dennenbourg and D J Darensbourg, Inorg Chem, 1972, 11, 72
- 12 W von Niessen, G H F Diercksen, and L S Cederbaum, Chem Phys, 1975, 10, 354
- 13 L H Staal, D J Stufkins, and A Oskam, Inorg Chim Acta, 1978, 26, 255
- 14 R J Kazlauskas and M S Wrighton, J Am Chem Soc, 1982, 104, 5784

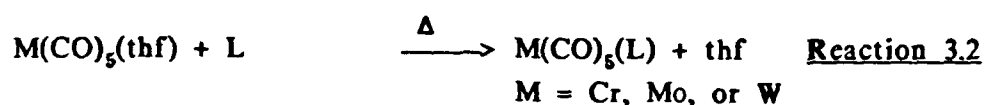
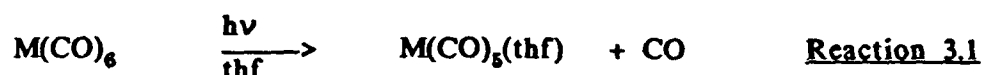
- 15 (a) J A Connor, J. P Day, E M. Jones, and G K McEwan, J. Chem. Soc Dalton Trans., 1973, 347
- (b) J A Connor and G A Hudson, J. Organomet Chem., 1974, 73, 351
- (c) J A Connor and P J Riley, J. Organomet Chem., 1975, 94, 55
- 16 (a) M. J Schadt, N J Gresalfi, and A J Lees, J. Chem Soc Chem. Comm., 1984, 506
- (b) M. J Schadt, N J Gresalfi, and A J Lees, Inorg Chem., 1985, 24 2942
- (c) M. J Schadt and A J Lees, Inorg Chem., 1986, 25, 673
- (d) D E Marx and A J Lees, Inorg Chem., 1987, 26, 620
- 17 J Nasielski and A Colas, J. Organomet Chem., 1975, 101, 215

CHAPTER III

SYNTHESIS OF GROUP SIX METAL HEXACARBONYL COMPLEXES WITH N-DONOR LIGANDS

3.a INTRODUCTION

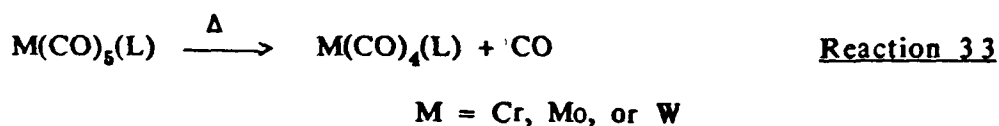
The synthesis and characterisation of substituted derivatives of Group 6 hexacarbonyls was undertaken as a preliminary study to the investigation of the metal carbonyls containing nitrogen donor (N-donor) ligands. The synthesis of such complexes involve the initial photolysis of the parent hexacarbonyl in solution, followed by the addition of the appropriate ligand in the same solvent (Reactions 3.1 and 3.2).



Tetrahydrofuran (thf), the most commonly used solvent was adopted in this case. This is because both the group 6 metal hexacarbonyls and most of the ligands (L) used in this study are soluble in thf.

Photolysis of the group 6 hexacarbonyls in this solvent results in the formation of a clear yellow solution of $\text{M(CO)}_5(\text{thf})$ complex (Reaction 3.1). Addition of the ligand leads to the thermal displacement of the solvent from the solvent adduct and the formation of the desired product (Reaction 3.2).

In the case where the incoming ligand (L) is a bidentate ligand, such as 3,6-bis(2-pyridyl)-1,4-dihydro-1,2,4,5-tetrazene, chelated complexes of the form $\text{M(CO)}_4(\text{L})$ were synthesised using the above synthetic route. This results in a further decarbonylation (Reaction 3.3).



The stable $M(CO)_4(L)$ product synthesised would appear to have been formed via a thermal ring closure process with the elimination of one CO (Reaction 3.3). The kinetics and mechanism of reactions of both penta- and tetra-carbonyl complexes as synthesised using the above route, are discussed in Section 2.

The nature of the lowest energy absorption band in $M(CO)_5(L)$ complexes (where $M = Cr, Mo, \text{ or } W$ and $L = \text{pyridine or substituted pyridine}$) has been investigated by a number of techniques such as luminescence¹, photoelectron² and ultra-violet/ visible^{1,3} spectroscopy. It is agreed that this band has considerable ligand field character, which is generally observed at approximately the same wavelength, approx 400nm. Theoretical calculations⁴ showed that both the e_g and t_{2g} metallic orbital degeneracy was removed due to the loss of one carbonyl ligand from the original metal hexacarbonyl. The filled d-orbitals which are involved in back-bonding to the carbonyls are affected by the loss of one π -acceptor group on the unique Z-axis. Of the two unfilled d-orbitals, only the d_{z^2} is influenced by the presence of a σ -donor ligand on this axis. The overall d-orbital energy diagram for $M(CO)_5(L)$ complexes is given in Figure 3.1.

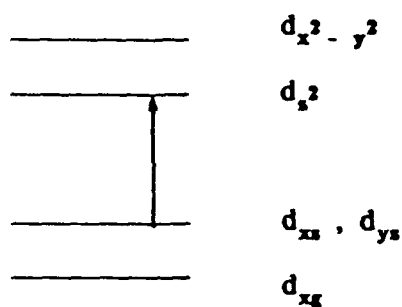
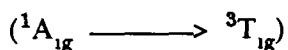


Figure 3.1 d-orbital energy diagram for $M(CO)_5(L)$ complexes.

Wrighton³ has suggested that the splitting pattern of the d-orbitals is more influenced by the π -acceptor ability of the carbonyl ligands than the σ -donor qualities of the unique ligand. Owing to the larger spin-orbital coupling in the heavier metal, tungsten complexes have a weak band on the low energy side of the lowest energy maximum³. This is assigned to the singlet triplet transition



Infrared spectroscopy has been used extensively for the characterisation of both metal carbonyl⁵ and pyridine⁶ containing complexes. Usually the carbonyl stretching bands of metal carbonyl complexes occur at lower energy than that of free carbon monoxide (2155cm^{-1}). This has been explained by proposing that the metal can "back donate" electron density into the π^* -orbitals on the carbonyl ligands. The work reported in this study is concerned only with the infrared carbonyl stretching region. Assuming that $\text{W}(\text{CO})_5(\text{L})$ (where L = pyridine or substituted pyridine) has a C_{4v} structure, the expected CO stretching frequencies would be due to two A_1 , one B_1 and one E mode. The B_1 mode being Raman active and not infrared active will not be observed in the infrared CO stretching region, resulting with three expected CO stretching frequencies.

3.b.1 Ultraviolet/visible spectroscopy of $W(CO)_5L$ (L = pyridine and substituted pyridine) complexes

The lowest energy absorption maxima for pyridine and substituted pyridine complexes prepared in this work are given in Table 3.1 along with their probable assignments

Compound	λ_{max} (nm) ${}^1A_{1g} \rightarrow {}^1T_{1g}$	ϵ ($\text{mol}^{-1}\text{dm}^3\text{cm}^{-1}$)	Solvent
$W(CO)_5(\text{pyridine})$	382	7.7×10^3	Cyclohexane
	380	-	thf
$W(CO)_5(2\text{-phenylpyridine})$	382	6.4×10^3	Cyclohexane
	416	2.9×10^3	thf
$W(CO)_5(4\text{-phenylpyridine})$	394	7.7×10^3	Cyclohexane
	377	6.9×10^3	thf
$W(CO)_5(2,2'\text{-dipyridylamine})$	378	3.9×10^3	Cyclohexane
	384	-	thf

Peak positions accurate to $\pm 2\text{nm}$

Extinction coefficients (ϵ) accurate to 10%

Table 3.1 Ultraviolet/visible spectral data for the $M(CO)_5(L)$ complexes

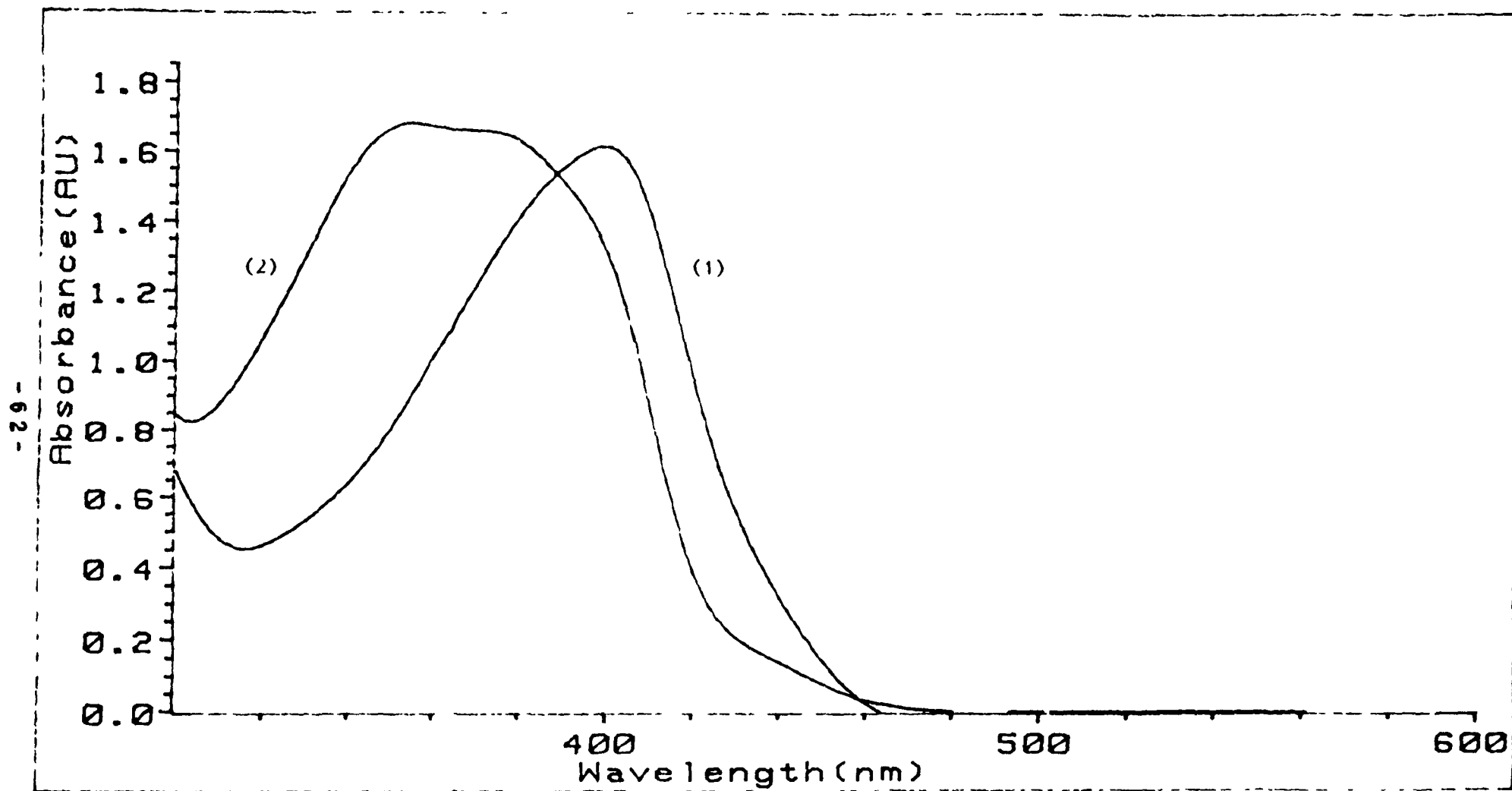


Figure 3.2 Ultraviolet/visible spectrum of the $\text{W}(\text{CO})_5(4\text{-phenylpyridine})$ complex recorded in CCl_4 (1) and thf (2)

The lowest energy absorption of these complexes show considerable solvent dependence, as can be seen from Figure 3.2. This suggests the existence of a charge transfer band at an energy close to that of the ligand field band. A charge transfer band was found for all the $W(CO)_5(L)$ ($L =$ pyridine and substituted pyridine) complexes and its position has been shown to be dependent on the nature of the pyridine ring substituent and also the polarity of the solvent.³ Electron withdrawing groups on the pyridine ring lower the energy of the charge transfer band, while the band is shifted towards higher energy in more polar solvents. This solvent and substituent dependency will be discussed in greater detail later on in this chapter.

3.11 Infrared Spectroscopy of $W(CO)_5(L)$ ($L =$ pyridine and substituted pyridine) complexes

As stated earlier, infrared spectroscopy has been used extensively for the characterisation of both metal carbonyls⁵ and metal carbonyl pyridine containing complexes⁶. The CO stretching frequencies for $W(CO)_5(L)$ ($L =$ pyridine and substituted pyridine) complexes prepared in this work are listed in Table 3.2, along with their assignments. Infrared spectra were obtained in a variety of solvents and also KBr.

Compound	$\nu_{\text{co}} \text{ (cm}^{-1}\text{)}$			Medium	
	$A_1^{(2)}$	E	$A_1^{(1)}$		
$\text{W(CO)}_5(\text{Pyridine})$	2071(w)	1932(s)	1919(s)	n-Hexane	
$\text{W(CO)}_5(4\text{-Phenylpyridine})$	2070(w)	1982(w)	1932(s)	1917(m)	n-Hexane
	2068(m)	1973(w)		1924(s)	p-Xylene
	2067(s)	1969(s)		1905(s)	KBr
$\text{W(CO)}_5(2\text{-Phenylpyridine})$	2069(w)	1982(s)	1930(s)	1911(m)	n-Hexane
	2068(w)	1976(m)	1924(s)	1898(m)	p-Xylene
	2070(w)	1972(s)	1929(s)	1883(m)	Nitromethane
	2067(s)	1969(s)		1905(s)	KBr
$\text{W(CO)}_5(2,2'\text{-dipyridylamine})$	2073(w)	1977(w)	1935(s)	1919(s)	n-Hexane
	2072(w)	1978(w)	1931(s)	1920(s)	p-Xylene
	2073(s)	1980(s)		1886(s)	KBr

w = weak, m = medium and s = strong

ν_{co} accurate to 3cm^{-1}

Table 32 The carbonyl stretching absorptions of $\text{W(CO)}_5(\text{pyridine and substituted pyridine})$ complexes

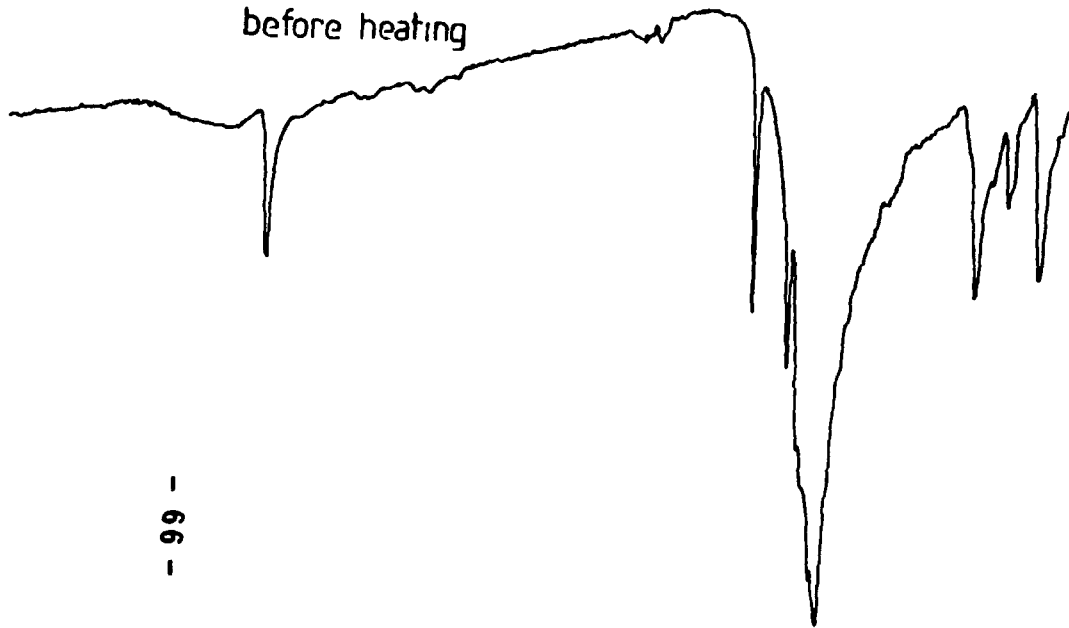
All the $\text{W(CO)}_5(\text{L})$ complexes prepared in this work have the characteristic peak of all group 6 metal pentacarbonyls at approximately 2070cm^{-1} ⁹. The infrared spectra obtained for $\text{W(CO)}_5(\text{substituted pyridine})$ compares well with the spectra obtained earlier by Sheline *et al*⁸. According to Bratterman⁷, n-hexane was found to be the most useful solvent for examining these absorptions because more polar

solvents tend to broaden bands owing to solvent-solute interactions. This might also be able to explain the shift in the absorption band at approx 1919cm^{-1} . Nitromethane being more polar, we observe this $A_1^{(1)}$ band at approx 1885cm^{-1} . Infrared spectra obtained using KBr resulted in both the E and $A_1^{(1)}$ band, both in the low 1900cm^{-1} region, being unresolved.

The presence of an absorption band at 1977cm^{-1} for the $\text{W}(\text{CO})_5(2,2'\text{-dipyridylamine})$ complex is not characteristic of a pure C_{4v} structure. Microanalysis (see experimental) of this complex rules out the cause due to any residual $\text{W}(\text{CO})_6$ which would absorb at approximately 1980cm^{-1} . Therefore, it would seem possible to suggest that this was due to a reduced symmetry caused by the pyridylamine side chain. Thus making the B_1 mode of the carbonyl stretching frequencies, thought only to be Raman active, somewhat infrared active. This would also explain the existence of a similar band in the spectra of the $\text{W}(\text{CO})_5(2\text{-phenylpyridine})$ complex. However, this would not explain the existence of a similar band in the spectra of the $\text{W}(\text{CO})_5(4\text{-phenylpyridine})$ complex.

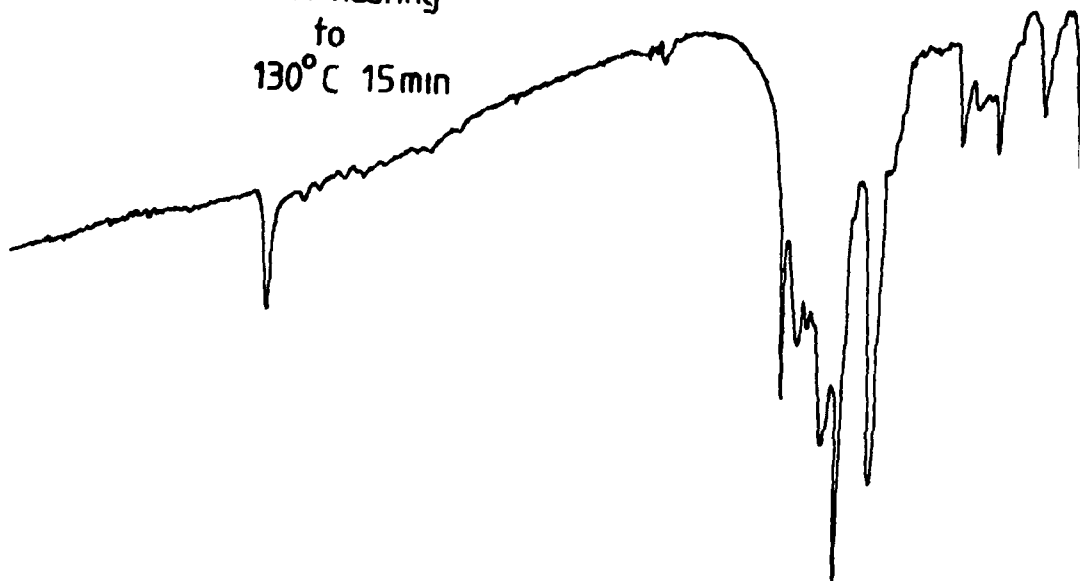
Earlier, spectra of $\text{M}(\text{CO})_5(4\text{-vinylpyridine})$ and $\text{M}(\text{CO})_5(2\text{-vinylpyridine})$ (where $M = \text{Cr}$ or W) obtained by Kelly *et al*¹⁰ exhibited no absorption band in the 1980cm^{-1} region. Also the relative instability of the $\text{W}(\text{CO})_5(2\text{-vinylpyridine})$ complex as compared with the 4 vinylpyridine analogue, was not experienced with the $\text{W}(\text{CO})_5(\text{L})$ (where $L = 2\text{-}$ and 4-phenylpyridine). Both 2- and 4-phenylpyridine tungsten pentacarbonyl complexes were air stable, however, they exhibited photosensitivity.

$W(CO)_5$ -dipym
before heating



- 99 -

after heating
to
 $130^{\circ}C$ 15 min



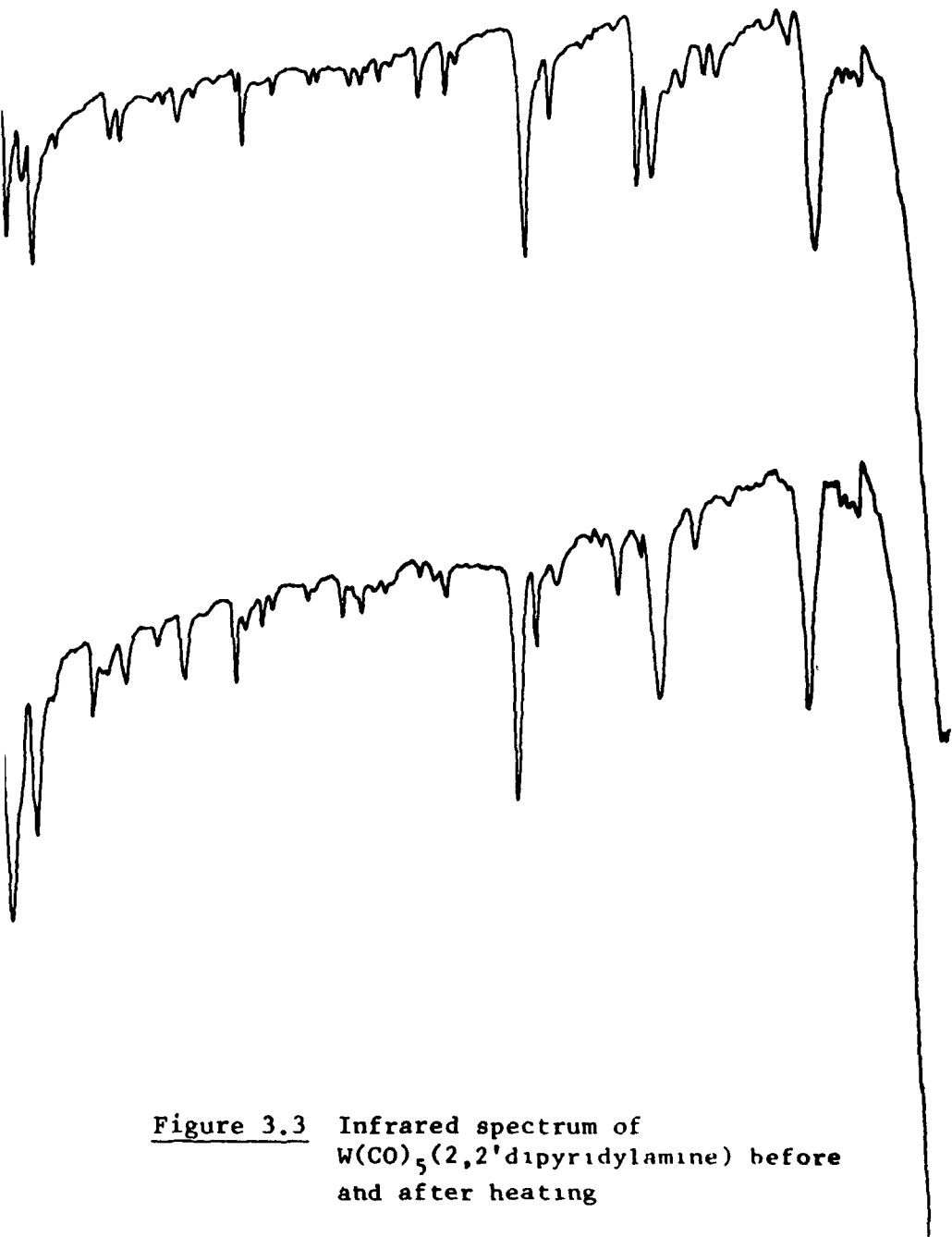


Figure 3.3 Infrared spectrum of $W(CO)_5(2,2'\text{-dipyridylamine})$ before and after heating

As can be seen from Figure 33, heating the $W(CO)_5(2,2'$ -dipyridylamine) complex results with the thermal displacement of one carbonyl ligand and the formation of $W(CO)_4(2,2'$ -dipyridylamine) as evidenced by the formation of the characteristic carbonyl stretching pattern. An absorption peak at approximately 2000cm^{-1} is characteristic of a group 6 metal tetracarbonyl complex, e.g. $W(CO)_4(\text{pyridine})_2$ has an absorption band at 2012cm^{-1} and $W(CO)_4(2,2'$ -dipyridyl) at 2010cm^{-1} .⁹ The depletion of the band at 2073cm^{-1} and the growth of the band at 2000cm^{-1} with time, is shown in Table 33.

ν_{co} (cm^{-1})				Time @ 110°C (min)
2073	1980	1886		0
2073	2003	1896	1857	15
	2005	1960	1904	90
	2005	1901	1857	450
	2005	1900	1857	1440

All spectra recorded using KBr.

ν_{co} accurate to $\pm 3 \text{ cm}^{-1}$

Table 33 The carbonyl stretching absorptions of $W(CO)_5(2,2'$ -dipyridylamine) recorded at different time intervals after being heated to 110°C .

Attempts to monitor the formation of $W(CO)_4(2,2'$ -dipyridylamine) complex from $W(CO)_5(2,2'$ -dipyridyl(amine)) complex spectrophotometrically proved difficult due to the fact that a suitable solvent for both complexes could not be found. However, the reaction was monitored using a thermogravimetric analyser, and this shall be discussed in Section 3 d

3 b III Proton Nuclear Magnetic Resonance Spectroscopy of $W(CO)_5(L)$ (L = Substituted Pyridine) Complexes

Proton nuclear magnetic resonance spectra (1H nmr) of $W(CO)_5(L)$ (where L = 2 or 4-phenylpyridine, or 2,2'-dipyridylamine) were obtained. Comparison of spectra from the pentacarbonyl complexes synthesised with the free ligands were made in order to determine the effect of binding pyridine like ligands to a metal pentacarbonyl moiety. 4-Substituted pyridines are most suited to this study as the substituent reduces ring proton coupling, and greatly simplifies the 1H nmr spectrum.

The 1H nmr spectra of the $W(CO)_5(4$ -phenylpyridine) is shown in Figure 3 4. The resonances in the 1H nmr of 4-phenylpyridine and $W(CO)_5(4$ -phenylpyridine) are listed in Table 3 4, and assignment of those resonances is straightforward using the numbering system given in Figure 3 5. The effect of the coordination of 4-phenylpyridine is a downfield shift of the α and β protons on the pyridine ring.

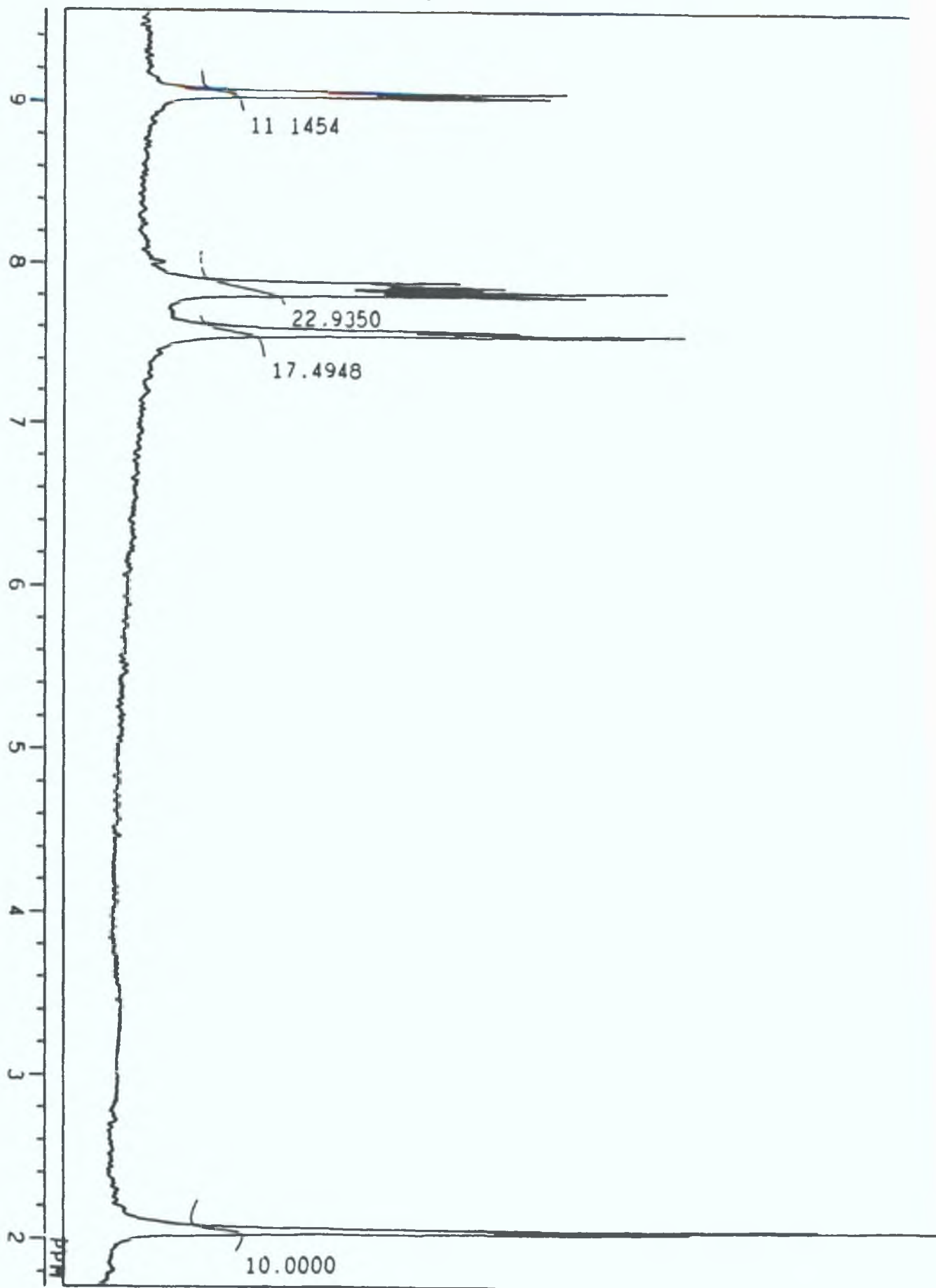


Figure 3.4 The ^1H nmr spectra of the $\text{W}(\text{CO})_5(4\text{-phenylpyridine})$ complex

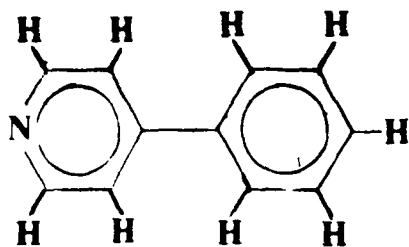


Figure 3.5 The molecular structure of 4-phenylpyridine

Compound	ppm		
4 Phenyl Pyridine	8.7, 2H,m	7.5, 7H,m	
W(CO) ₅ 4 Phenyl Pyridine	9.04, 2H,m	7.8, 4H,m	7.6, 3H,m

Table 3.4 The chemical shift of protons in W(CO)₅(4-phenyl pyridine) and free 4 phenyl pyridine.

Assignment of the peaks in the spectra of the W(CO)₅(2-phenylpyridine) and W(CO)₅(2,2'-dipyridylamine) complexes proved difficult, due to the complicated ring coupling. However, in both cases, a downfield shift of the protons α to the coordinated nitrogen was observed.

3.c The crystal and molecular structure of $W(CO)_5(2,2'$ -dipyridylamine)

The crystal structure of $W(CO)_5(2,2'$ -dipyridylamine) was determined by R A Howie¹¹ Crystals suitable for analysis were grown in nitromethane solution under nitrogen in the dark $W(CO)_5(2,2'$ -dipyridylamine) in crystalline form is air stable for some months, provided it is not exposed to heat or light

The crystallographic methods and the parameters used in the calculation of this structure will be discussed elsewhere¹¹ and only the derived structural information is referred to in this work

The crystal structure of $W(CO)_5(2,2'$ -dipyridylamine) is given in Figure 3.6 The ligands are arranged about the metal in a distorted octahedral configuration Of the four equatorial carbonyl ligands, two carbonyl ($C_{30}O_{30}$ and $C_{31}O_{31}$) ligands bend away from the unique ligand, and two ($C_{32}O_{32}$ and $C_{33}O_{33}$) bend towards it The two carbonyl groups which bend away from the unique ligand are those which are cis- to the pyridylamine side chain, while those carbonyl ligands trans-bend towards the unique ligand The angles for these and all the other bonds are listed in Table 3.5

Also as can be seen from Table 3.5, is the variation in bond lengths between the metal and carbonyl ligands All metal to carbon bond lengths differ, varying from 1.77Å to 2.12Å This can be compared to the metal to carbon bond length in $W(CO)_6$ of 2.059Å¹²

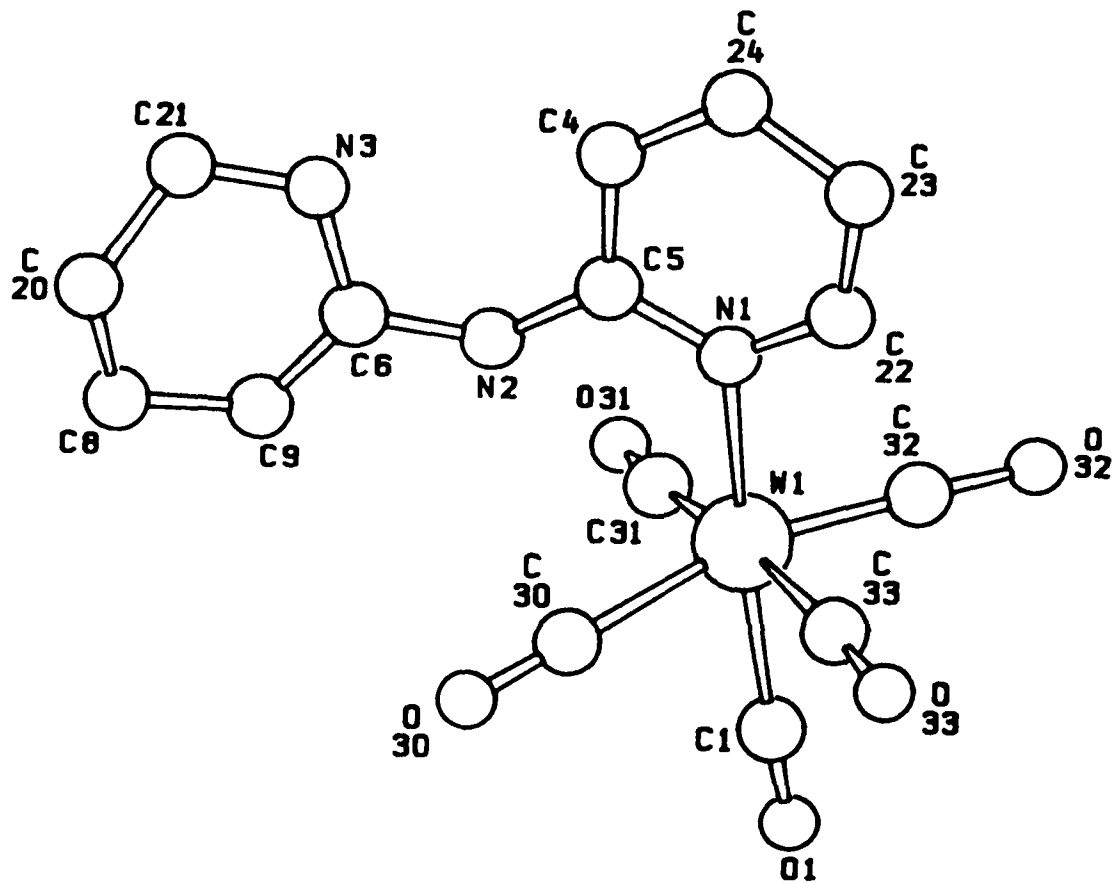


Figure 3.6 The crystal structure of $W(CO)_5(2,2'$ -dipyridylamine)

The metal to nitrogen bond distance is 2.38 Å. This bond length is in the range expected for metal-amine bonds and compares to a similar metal-nitrogen bond in $W(CO)_5(4\text{-vinylpyridine})$ of 2.323 Å¹⁰. The slightly longer metal bond length is a consequence of the steric hindrance of the pyridylamine side chain in the α position to the nitrogen.

The bond lengths and angles are given in Table 3.5. Assignment of the bond lengths and angles is straightforward using the numbering system in Figure 3.6.

BOND	LENGTH(Å)	BOND ANGLE	ANGLE(°)
W-N	2.38	C ₃₀ -W-N ₁	97
W-C ₃₀	2.10	C ₃₁ -W-N ₁	101
W-C ₃₁	1.77	C ₃₂ -W-N ₁	87
W-C ₃₂	1.81	C ₃₃ -W-N ₁	84
W-C ₃₃	2.12	C ₁ -W-N ₁	167
W-C ₁	2.05	C ₃₀ -W-C ₃₁	93
C ₃₀ -O ₃₀	1.18	C ₃₀ -W-C ₃₃	82
C ₃₁ -O ₃₁	1.18	C ₃₀ -W-C ₁	80
C ₃₂ -O ₃₂	1.26	C ₃₀ -W-C ₃₂	162
C ₃₃ -O ₃₃	1.16	C ₃₁ -W-C ₁	92
C ₁ -O ₁	1.10	C ₃₁ -W-C ₃₂	103
N ₁ -C ₂₂	1.29	C ₃₁ -W-C ₃₃	174
N ₁ -C ₅	1.37	C ₃₂ -W-C ₁	92
C ₂₂ -C ₂₃	1.43	C ₃₂ -W-C ₃₃	81
C ₂₃ -C ₂₄	1.59	C ₃₃ -W-C ₁	83
C ₂₄ -C ₄	1.38	W-N ₁ -C ₅	121
C ₄ -C ₅	1.45	W-N ₁ -C ₂₂	117
C ₅ -N ₂	1.38		
N ₂ -C ₆	1.37		
C ₆ -N ₃	1.39		
N ₃ -C ₂₁	1.37		
C ₂₁ -C ₂₀	1.55		
C ₂₀ -C ₈	1.39		
C ₈ -C ₉	1.48		
C ₉ -C ₆	1.38		

Table 35

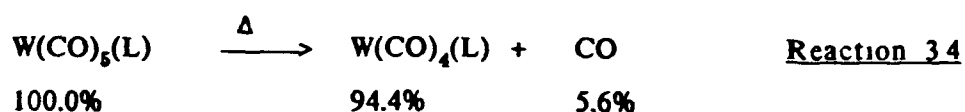
Table of bond lengths and angles of the
W(CO)₅(2,2' dipyridylamine) complex

3.d Thermogravimetric Analysis of W(CO)₅(2,2'-dipyridylamine)

Evidence was obtained from the infrared spectroscopy for the conversion of W(CO)₅(L) to W(CO)₄(L) where L is 2,2'-dipyridylamine (see Section 3 b II). Attempts to monitor this thermal displacement of CO using general spectrophotometric methods proved difficult due to the fact that no solvent could be found for both the pentacarbonyl and tetracarbonyl complexes. Therefore an attempt was made to monitor this chelation reaction using a thermogravimetric analyser.

The thermogravimetric analysis of W(CO)₅(2,2'-dipyridylamine) is shown in Figure 3.7. The percentage weight loss was monitored under nitrogen atmosphere over the temperature range of 20°C to 130°C against time. The resulting weight loss was obtained to be approximately 35%.

If the chelation reaction taking place was uncomplicated and resulted in complete conversion of the pentacarbonyl to the tetracarbonyl complex (Reaction 3.4), the expected weight loss would be approximately 5.6%. Therefore,



it is possible to suggest that another reaction other than the thermal displacement of a carbonyl ligand is taking place. Reaction 3.5 is proposed to account for the thermogravimetric analysis of W(CO)₅(2,2'-dipyridylamine) as in Figure 3.7. The observed weight loss of

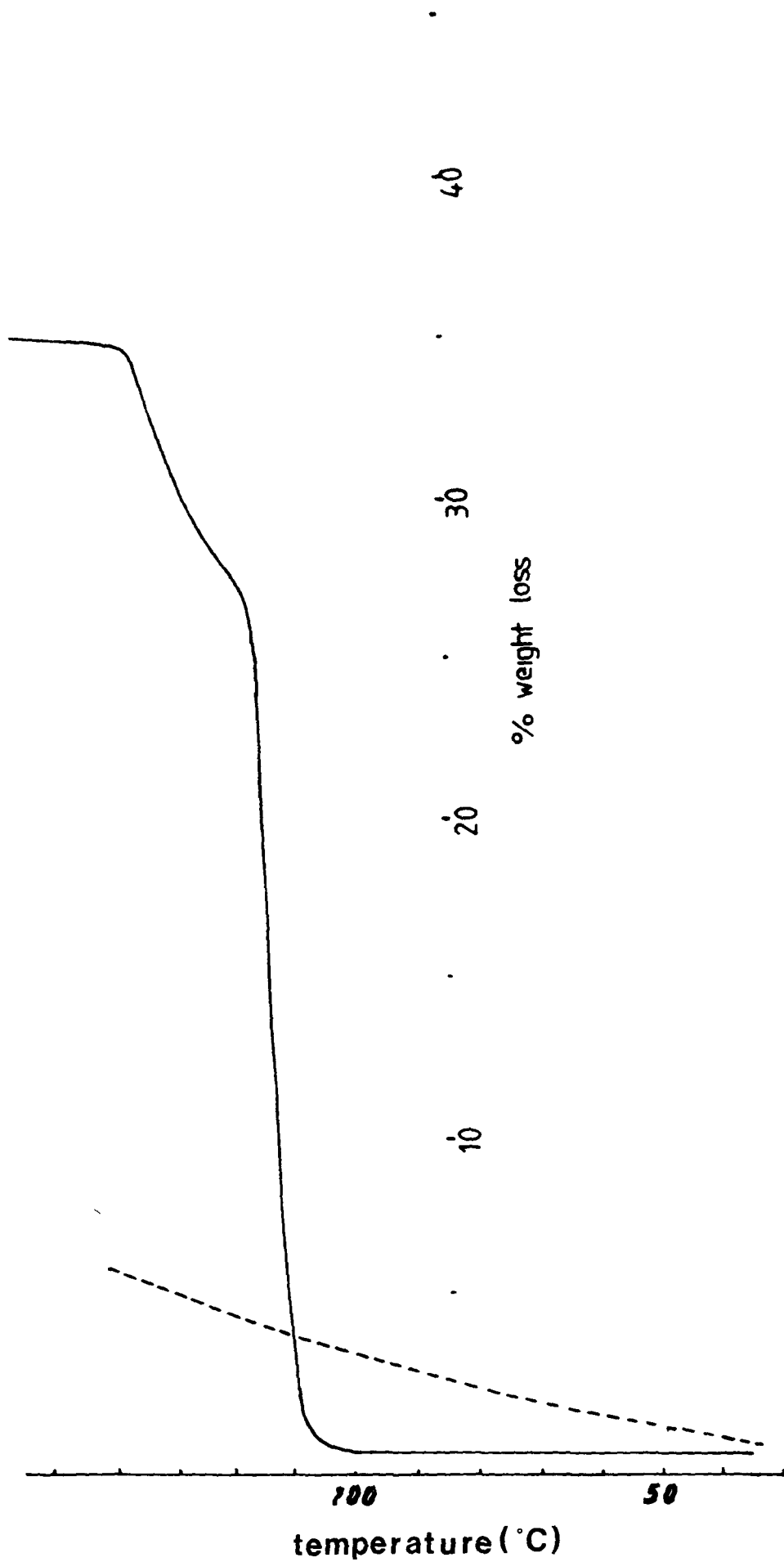
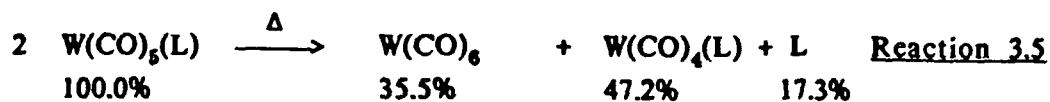


Figure 3.7 The thermogravimetric analysis of the $W(CO)_5(2,2'$ dipyridylamine) complex



35.0% could be attributed to the sublimation of the W(CO)_6 formed during the reaction. These results indicate that the formation of $\text{W(CO)}_4(\text{L})$ from $\text{W(CO)}_5(\text{L})$ is not a simple unimolecular process.

3.e.1 The Preparation of M(CO)_4 (3,6-bis(2-pyridyl)1,4-dihydro-1,2,4,5-tetrazene (M = Cr, Mo, and W) Complexes

3,6-bis(2-pyridyl)-1,4-dihydro-1,2,4,5-tetrazene (SL) derivatives of M(CO)_6 (M = Cr, Mo or, W) can be synthesised by the addition of the ligand to a solution of $\text{M(CO)}_5(\text{L})$ (L = donor solvent). The same synthetic procedure that was used in the preparation of W(CO)_5 (Pyridine and substituted pyridine) complexes was applied to the SL derivatives of the group 6 hexacarbonyls. The displacement of a further carbonyl group from the pentacarbonyl proceeds at room temperature. The ease of the formation of $\text{M(CO)}_4(\text{SL})$ from $\text{M(CO)}_5(\text{thf})$ is a consequence of the chelating ability of the SL ligand. The molecular structure for the SL tetrazene ligand is given in Figure 3.8.

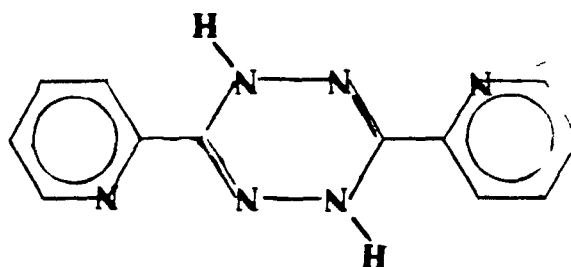


Figure 3.8 The molecular of 3,6-bis(2-pyridyl)1,4-dihydro-1,2,4,5-tetrazene (SL)

One mole equivalent of the ligand was added to a solution of $M(\text{CO})_5(\text{thf})$ ($M = \text{Cr, Mo, or W}$) During the addition, the colour of the solution changed from yellow to dark blue The solvent was then removed under reduced pressure at room temperature and the remaining dark crude product was recrystallized from acetonitrile An attempt was also made to isolate the bridging bis chelate ligand, $\text{Mo}(\text{CO})_4(\text{SL})\text{Mo}(\text{CO})_4$, by adding one half of the molar equivalent of the ligand However, characterisation of this bridging bis chelate complex proved difficult

The kinetics of the solvent adduct displacement and formation of the tetracarbonyl complex with the bidentate ligand SL, was monitored using a diode-array UV/vis spectrophotometer, and is discussed in Section 2 The crystal structure of $\text{W}(\text{CO})_4(\text{SL})$ was also obtained, and is discussed later in this section

2 c II Ultraviolet/visible spectroscopy of $M(\text{CO})_4(3,6\text{-bis}(2\text{-pyridyl})\text{-1,4-dihydro-1,2,4,5-tetrazene})$

The lowest energy absorption band in $M(\text{CO})_4(\text{SL})$ (where $\text{SL} = 3,6\text{-bis}(2\text{-pyridyl})\text{-1,4-dihydro-1,2,4,5-tetrazene}$ and $M = \text{Cr, Mo, or W}$) has been assigned as a metal-to-ligand charge transfer (MLCT) transition There has been a strong interest in complexes with low energy MLCT transitions in recent years, because many of these complexes are photostable in solution and have long lived MLCT excited states from which luminescence¹⁴ and electron-transfer¹⁵ reactions can occur

The lowest energy absorption maxima of these tetracarbonyl complexes are listed in Table 3.6. Previous studies¹⁶ on other diimine tetracarbonyl metal complexes have shown that this long wavelength

Compound	λ_{MAX} (nm)	ϵ ($\text{mol}^{-1}\text{dm}^3\text{cm}^{-1}$)
$\text{Cr}(\text{CO})_4(\text{SL})$	650	1.28×10^4
$\text{Mo}(\text{CO})_4(\text{SL})$	493	3.5×10^3
$\text{W}(\text{CO})_4(\text{SL})$	512	5.7×10^3
$\text{Mo}(\text{CO})_4(\text{SL})\text{Mo}(\text{CO})_4$	493	5.3×10^3

Peak positions accurate to $\pm 2\text{nm}$

Extinction coefficients accurate to 10%

All spectra obtained in THF

SL = 3,6-bis(2-pyridyl)-1,4-dihydro-1,2,4,5-tetrazene

Table 3.6 Ultraviolet/visible spectral data for the $\text{M}(\text{CO})_4(\text{SL})$ ($\text{M} = \text{Cr}, \text{Mo}, \text{or W}$) complexes.

MLCT absorption band can comprise of several transitions from filled d levels to the unoccupied lowest π^* orbital of the ligand. The most important transition being symmetry-allowed $d_{yz} \rightarrow \pi^*$. As can be seen from Table 3.6, the chromium complex has the lowest energy MLCT transition at 650nm, while the molybdenum complex has the highest energy MLCT transition at 493nm. This is possibly due to the fact that the metal-centred highest occupied molecular orbital is most destabilized in chromium tetracarbonyl compounds¹⁷. Both molybdenum complexes exhibit a MLCT absorption band at 493nm but with different molar extinction coefficients.

The significant difference in the molar extinction coefficients for these complexes is the only spectroscopic evidence for the existence of the ligand-bridged compound $\text{Mo}(\text{CO})_4(\text{SL})\text{Mo}(\text{CO})_4$, as the infrared and uv/visible band positions for this complex and $\text{Mo}(\text{CO})_4(\text{SL})$ are identical

3.e.III Infrared spectroscopy of $M(\text{CO})_6$, 3,6-bis(2-pyridyl)-1,4-dihydro-1,2,4,5-tetrazene (M= Cr, Mo or W) Complexes

Four carbonyl stretching bands are expected in the infrared spectra of cis-tetracarbonyl metal complexes. An absorption peak at 2000cm^{-1} approximately, is characteristic of a tetracarbonyl metal complex. The carbonyl stretching absorptions for all the 3,6-bis(2-pyridyl)-1,4-dihydro-1,2,4,5-tetrazene (SL) derivatives of $M(\text{CO})_6$ (M = Cr, Mo, or W) are given in Table 3.7. All the complexes prepared contain the characteristic peak at approximately 2000cm^{-1} . Of the four expected CO stretching bands, the two central bands are not always resolved.

As already seen before in Section 3.e.II, there exist similarities in the ultraviolet/visible spectra of the $\text{Mo}(\text{CO})_4(\text{SL})$ and $\text{Mo}(\text{CO})_4(\text{SL})\text{Mo}(\text{CO})_4$ complexes. Similarities are again observed in the carbonyl stretching region of the infrared spectra of both complexes (Table 3.7). Previous synthesis of $\text{Mo}(\text{CO})_4(\text{bptz})$ and $\text{Mo}(\text{CO})_4(\text{bptz})\text{Mo}(\text{CO})_4$ (where bptz = 3,6-bis(2-pyridyl)-1,2,4,5-tetrazene), complexes by Kaim and Kohlmann¹³ reported the following CO absorption bands in the carbonyl stretching region, $2005(\text{m})$, $1928(\text{br,vs})$, and $1877(\text{s})\text{ cm}^{-1}$ for $\text{Mo}(\text{CO})_4(\text{bptz})$ and $1995(\text{vs})$, $1940(\text{br,s})$ and $1875(\text{s})\text{ cm}^{-1}$ for $\text{Mo}(\text{CO})_4(\text{bptz})\text{Mo}(\text{CO})_4$.

Compound	ν_{CO} (cm ⁻¹)					Medium
Cr(CO) ₄ SL	2015	1979	1934	1870	1834	Acetonitrile
	2011		1930	1879		THF
	2029 2016		1938	1885		KBr
Mo(CO) ₄ SL	2018		1907	1880	1835	Acetonitrile
	2013	1965	1902	1885	1846	THF
	2007		1901		1860	KBr
W(CO) ₄ SL	2010		1894	1873	1834	Acetonitrile
	2005		1889		1842	THF
	1999		1891		1857	KBr
Mo(CO) ₄ SL	2018	1979	1907	1880	1835	Acetonitrile
	2013	1975	1902	1886	1846	THF
	2007	1903	1861		1800	KBr

SL = 3,6 bis(2-pyridyl)-1,4-dihydro-1,2,4,5-tetrazene

Table 37 The carbonyl stretching absorptions of M(CO)₄(SL)
(M = Cr, Mo, or W) complexes.

Kaim¹³ also found that with the bptz ligand, the formation of binuclear complexes proceeds very rapidly and special care is necessary to form the mononuclear complex. They also found that the mononuclear complex was quite unstable, and tended to form the binuclear complex on standing¹³

Further evidence for the existence of two complexes was obtained with the SL derivative of chromium. The infrared spectra of $\text{Cr}(\text{CO})_4(\text{SL})$ displays two distinct absorptions at 2029cm^{-1} and 2016cm^{-1} in KBr (Table 3.7). However, in solution, there exists only one distinct carbonyl absorption band at 2011cm^{-1} approximately. This could be due to the rapid formation of the binuclear complex in solution.

3.e.IV Proton Nuclear Magnetic Resonance Spectroscopy of the
3,6-Bis(2-pyridyl)-1,4-dihydro-1,2,4,5-tetrazene derivatives of $\text{M}(\text{CO})_6$
(M = Cr, Mo, or W)

Proton nuclear magnetic resonance (^1H nmr) spectra were obtained for all the metal carbonyl derivatives of 3,6-bis(2-pyridyl)-1,4-dihydro-1,2,4,5-tetrazene. Assignment of protons proved difficult, due to ring coupling. However, as expected, a downfield shift of the pyridine protons was observed. Again this is probably due to the effect of coordination in the electron density at the ligand. The deshielding of the protons is the result of an electron drain through the metal to the nitrogen α bond.

3.f The Crystal and Molecular Structure of $W(CO)_4(3,6\text{-bis}(2\text{-pyridyl)})\text{-1,4-dihydro-1,2,4,5-tetrazene}$

The crystal structure of $W(CO)_4(SL)$ (where SL is 3,6-bis(2-pyridyl)1,4-dihydro 1,2,4,5-tetrazene) was determined by Long et al¹⁸ Crystals suitable for analysis were grown in acetonitrile under nitrogen in the dark $W(CO)_4(SL)$ in crystalline form is air stable for some months, provided it is not exposed to light or heat

The derived structural information is discussed in this section, while the crystallographic methods and the parameters used in the calculations are discussed elsewhere¹⁸ The crystal structure for $W(CO)_4(SL)$ is given in Figure 3.9 The tungsten atom has an octahedral coordination

The W-CO distances of the carbonyl ligands trans to the SL coordinating nitrogen atoms are about 0.1 Å longer than the W-CO distances of the cis-carbonyls perpendicular to the SL ligand (Table 3.8) This is due to the influence of the SL ligand, which has different σ -donor properties compared to the CO ligands The bond lengths for these and all other bonds are listed in Table 3.8

The SL ligand is non-planar, which of course is the result of the partly saturated character of the central six membered ring Two hydrogen atoms bound to N(123) and N(126) of SL One of the shortest intermolecular distances of 2.77 Å is between H₁₂₆ and O(12) This suggests that intermolecular hydrogen bonding might be present in this structure

The bond lengths and angles for all bonds are listed in Table 3.8, and assignment of these lengths and angles is straightforward using the numbering system in Figure 3.10

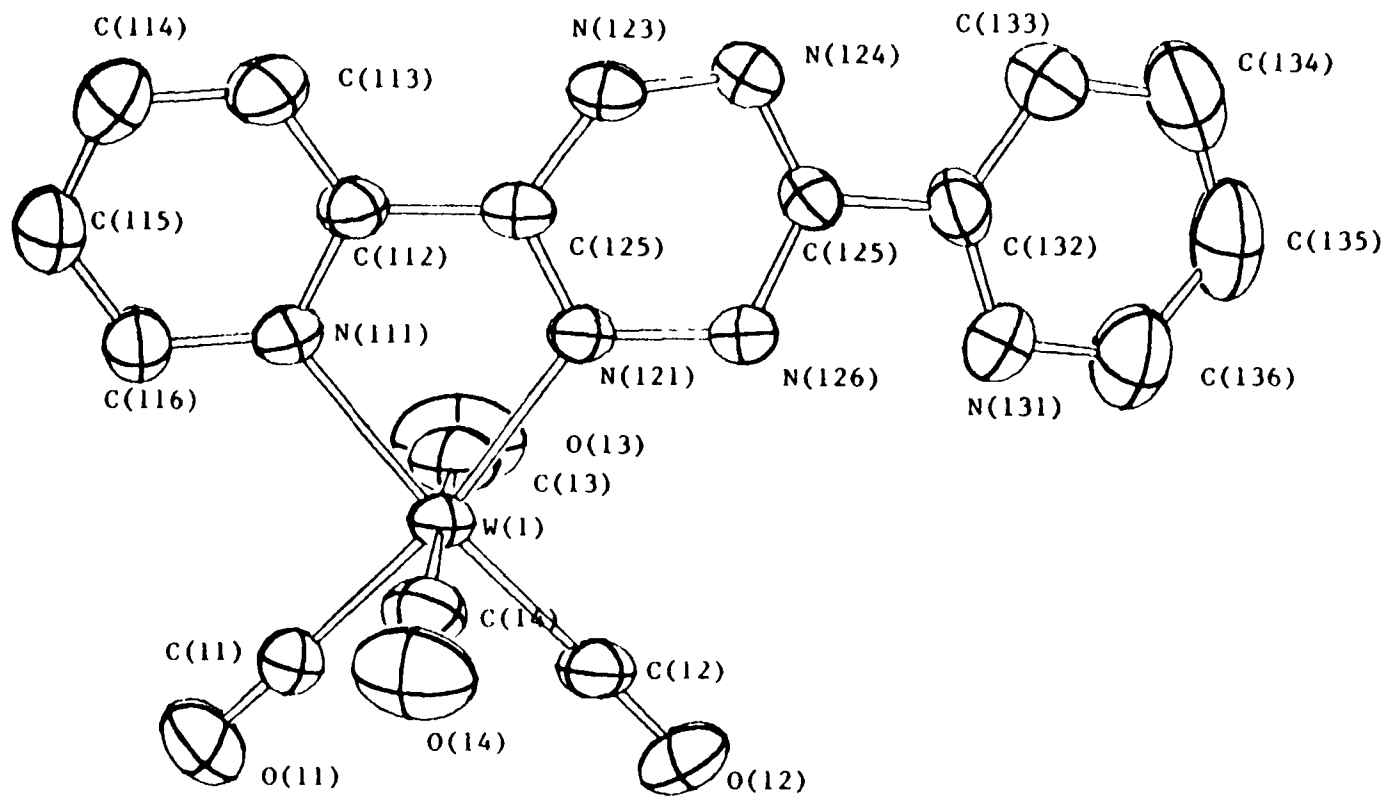


Figure 3.9 The crystal structure of $W(CO)_4(SL)$

BOND	LENGTH(Å)	BOND ANGLE	ANGLE(°)
W ₁ -C ₁₁	1 95	C ₁₁ -W-C ₁₂	87
W ₁ -C ₁₂	1 95	C ₁₁ -W-C ₁₃	85
W ₁ -C ₁₃	2 03	C ₁₁ -W-C ₁₄	88
W ₁ -C ₁₄	2 05	C ₁₁ -W-N ₁₁₁	110
W ₁ -N ₁₁₁	2 25	C ₁₁ -W-N ₁₂₁	171
W ₁ -N ₁₂₁	2 21		
		C ₁₂ -W-C ₁₃	88
C ₁₁ -O ₁₁	1 16	C ₁₂ -W-C ₁₄	86
C ₁₂ -O ₁₂	1 16	C ₁₂ -W-N ₁₁₁	172
C ₁₃ -O ₁₃	1 14	C ₁₂ -W-N ₁₂₁	102
C ₁₄ -O ₁₄	1 13		
		C ₁₃ -W-C ₁₄	172
N ₁₁₁ -C ₁₁₂	1 36	C ₁₃ -W-N ₁₁₁	95
N ₁₁₁ -C ₁₁₆	1 34	C ₁₃ -W-N ₁₂₁	94
C ₁₁₂ -C ₁₁₃	1 37	C ₁₄ -W-N ₁₁₁	91
C ₁₁₄ -C ₁₁₅	1 36	C ₁₄ -W-N ₁₂₁	94
		N ₁₁₁ -W-N ₁₂₁	71
N ₁₂₁ -C ₁₂₂	1 29		
N ₁₂₁ -N ₁₂₆	1 42		
C ₁₂₂ -N ₁₂₃	1 38		
N ₁₂₃ -N ₁₂₄	1 43		
N ₁₂₄ -C ₁₂₅	1 27		
C ₁₂₅ -N ₁₂₆	1 40		
C ₁₂₅ -C ₁₃₂	1 47		

Table 3.8

Table of bond lengths and angles of the W(CO)₄(SL) complex.

3.g The Preparation of $W(CO)_5(2\text{-aminomethylpyridine})$ and $W(CO)_5(\text{Bispicoylamine})$

As previously indicated, $W(CO)_5(2\text{-aminomethylpyridine})$ and $W(CO)_5(\text{bispicoylamine})$ were prepared by adding the same molar equivalents of the ligand to the solvated tungsten pentacarbonyl. Thermal displacement of the solvent resulted with the formation of the desired product. The molecular structure of bispicoylamine is shown in Figure 3.10. Synthesis of both complexes did not prove successful. Both tetra- and penta-carbonyl complexes of both 2-aminomethyl pyridine and bispicoylamine were detected by infrared spectroscopy. Isolation and purification of any of these products proved difficult.

Both tungsten pentacarbonyl forms of 2-aminomethylpyridine and bispicoylamine appeared to be oils, and thermally unstable resulting, with the formation of a tetracarbonyl species. Further evidence of this was obtained in the carbonyl stretching region of the infrared spectrum. Application of heat to the $W(CO)_5(2\text{-aminomethylpyridine})$, resulted with an increase in the absorption band at 2004cm^{-1} and a depletion in the absorption band at 2070cm^{-1} . The bands at 2070cm^{-1} and at 2004cm^{-1} are characteristic of a pentacarbonyl and tetracarbonyl species respectively.

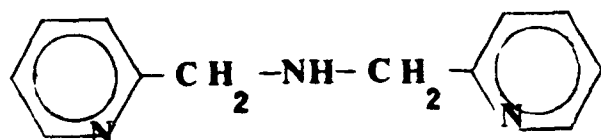


Figure 3.10 The molecular structure of bispicoylamine

3 h I The Solvatochromic Behaviour of Some Group Six Metal Carbonyl Complexes with N-Donor Ligands

Solvent effects on the absorption spectra of transition-metal complexes have been recognised for a number of octahedral and square planar systems. The solvatochromic properties are generally a result of shifts in the energy of transitions that are predominately charge-transfer in character. The strong solvent effects on the metal to diimine charge-transfer transition ($M \rightarrow \pi^*$) for *cis*- $M(CN)_2L_2$ ($M=Fe$ or Ru)¹⁹ and $M(CO)_4(L)$ ($M = Cr, Mo, \text{ or } W$)²⁰ complexes, where $L = 2,2'$ -bipyridine, 1,10 phenanthroline, 1,4-diazabutadiene have been noted by several investigators. Many of these complexes possess low-lying d-d and metal-to-ligand charge-transfer (MLCT) excited states. The MLCT transition is generally observed to be very solvent sensitive. These compounds are particularly suited for studies of solvent phenomena²¹ because they are zerovalent and thus soluble in a wide range of organic media.

For complexes of the general formula $M(CO)_4(\text{diimine})$ ($M = Cr, Mo, \text{ or } W$) the variation in energy of the MLCT state is one of the largest known among inorganic or organometallic species²². These tetracarbonyl complexes exhibit negative solvatochromism, that is, the MLCT absorption blue shifts in progressively more polar solvent media. Negative solvatochromism for metal carbonyl and other coordination complexes has been interpreted in terms of a reduced excited-state electric dipole²³. This is a consequence of the Franck-Condon principle, and implies that there is a substantial electric dipole moment associated with the ground-state solute molecule, which is reduced, reversed, or realigned

with the MLCT transition. As a result of this, a polar medium can be considered to stabilise the ground-state species to a greater extent than the excited molecule

Recent investigations by Lees et al²⁴, with $W(CO)_4(2,2'$ -bipyridine) and $W(CO)(pyrazine)W(CO)_5$ found good correlations between the solvent parameters and the energy of the MLCT transitions (E_{MLCT} , kJ mol⁻¹). The solvent parameters consisted of the Kosower's Z parameter²⁵, the Reichardt and Dimroth's E_T solvent polarity scale²⁶, and the Kamlet and Taft's π^* solvent polarity parameter^{21(b),27}. They also found good correlations with the bulk dielectric constant (ϵ_b),²⁸ the optical dielectric constant (ϵ_{op}),²⁹ the dipole moment values (μ),³⁰ the solvent polarizability values (α), and the optical polarizability values (α_{op})²⁹

Kaim and Kohlmann³¹ proposed a few rules for estimating the degree of solvatochromism. Strong solvent sensitivity can be expected if (a) the number of allowed metal-to-ligand transitions in one molecule at one energy is large, (i.e. polynuclear (ligand-bridged) complexes and species containing ligands with π^* orbital degeneracy should exhibit particularly strong solvatochromism), (b) the σ donation exerted by the ligand is high in the ground state, and the σ donation capability increases relatively little in the excited state, as may be inferred from π MO calculations or from electron spin resonance data of reduced systems, (c) the π back-donation is sufficiently large, and (d) the metal fragment is electron poor, as may be estimated from electrochemical oxidation potentials

3.h.II Solvatochromism of $W(CO)_5$ (Pyridine and Substituted Pyridine) Complexes

The ultraviolet/visible spectra of the following $W(CO)_5(L)$ complexes where L is pyridine, 2-phenylpyridine, 4-phenylpyridine, 2,2'-dipyridylamine, 4-vinylpyridine, pyridylpyrimidine, and 1(2-pyridine)-triazole were recorded in a wide range of solvents. The uv/vis spectra of $W(CO)_5(4\text{-phenylpyridine})$ recorded in a number of solvents is shown in Figure 3.11. The metal-to-ligand charge transfer (MLCT) absorption maxima (nm) for each complex is listed in Table 3.9. The corresponding energy (E_{MLCT}) for these absorptions is listed in Table 3.10.

Complications can be expected with the protic and chlorinated solvents. The former through hydrogen bonding and the latter because the highly polarizable chlorine centres are known to lead to ill-behaved solvent correlations²².

As can be seen from both Table 3.9 and 3.10, all the tungsten pentacarbonyl complexes exhibit varying degrees of solvatochromism. However, the MLCT absorption for $W(CO)_5(\text{pyridine})$ and $W(CO)_5(\text{pyridylpyrimidine})$ showed very little solvent dependencies.

If the MLCT absorptions (as in Table 3.9) obtained in the protic and chlorinated solvents are ignored, then $W(CO)_5(4\text{-phenyl-pyridine})$ and $W(CO)_5(4\text{-vinyl-pyridine})$ are found to exhibit negative solvatochromism. Likewise $W(CO)_5(1(2\text{-pyridyl})\text{-triazole})$ is found to exhibit positive solvatochromism. Both $W(CO)_5(2\text{-phenyl pyridine})$ and $W(CO)_5(2,2'\text{-dipyridylamine})$ show very little solvent dependencies in this case.

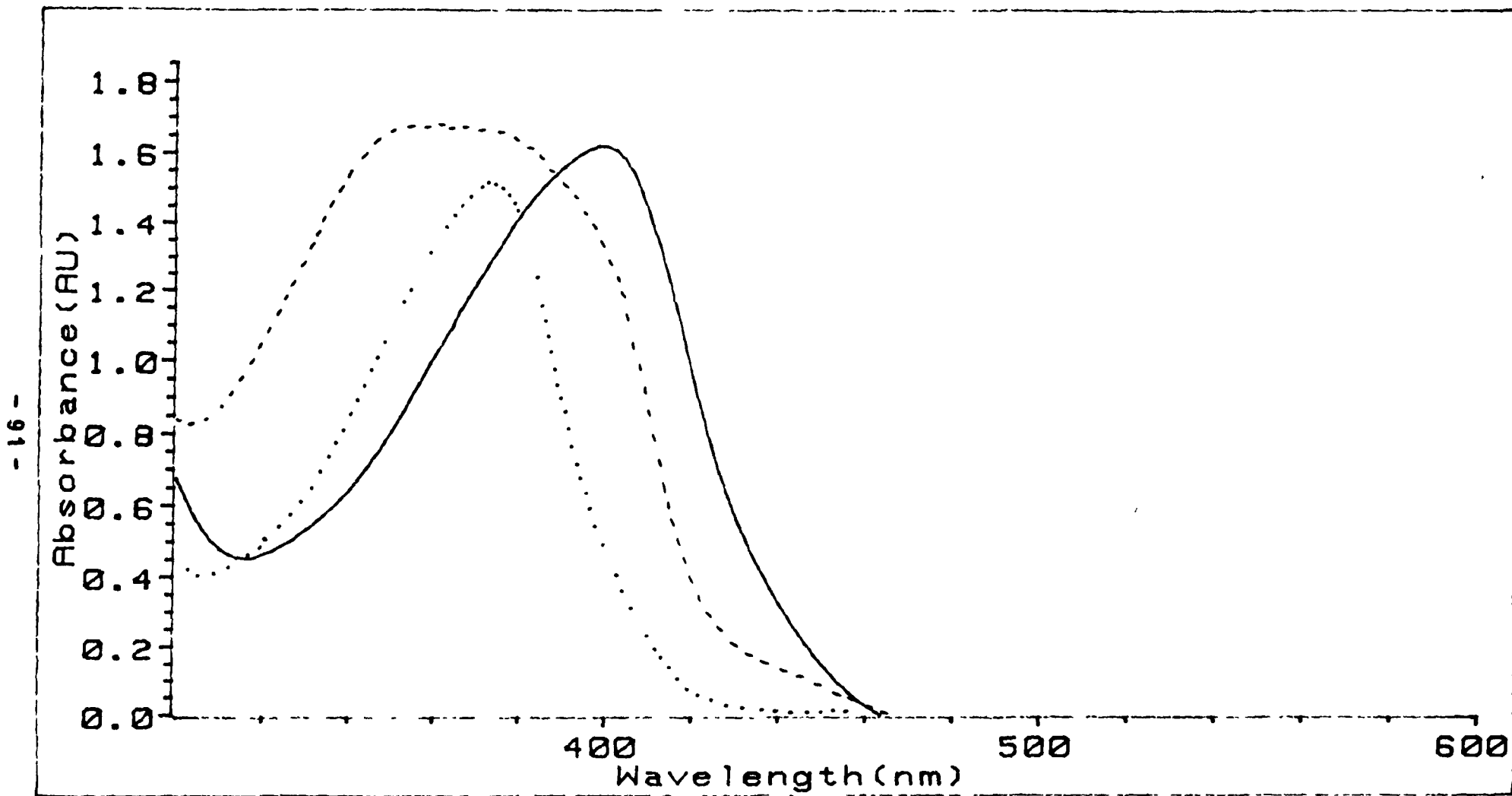


Figure 3.11 The uv/vis spectrum of $W(CO)_5(4\text{-phenylpyridine})$ recorded in (a) CCl_4 (—), (b) cyclohexane (...), and (c) thf (---)

L	Pyridine	4 phenyl pyridine	2 phenyl pyridine	4 vinyl* pyridine	2,2' dipyrid- ylamine	Pyridyl* pyrimidine	1(2-pyr- idyl) triazole*
Solvent							
Carbon tetra-chloride	382	398	382		376		
Toluene	378	384	374	394	382	398	374
Ether	378	376	370	384	382	398	378
Dichloro- Methane	376	374	368	382	378	396	376
Butanol	378	376	392	382	384	396	376
Tetrahydro- furan	380	354	378	380	384	396	392
Chloroform	376	382	370	392	378	396	372
Acetone	380	344	378	374	380	394	390
Acetonitrile	378	344	374	350	376	392	386
Methanol	380	348	390	374	394	394	392

Peak absorptions accurate \pm 2nm

Table 39 The MLCT absorption maxima (nm) for $W(CO)_5(L)$ complexes.

* received from C. Long (Dublin City University) -
used without further purification.

L	Pyridine	4 phenyl pyridine	2 phenyl pyridine	4 vinyl pyridine	2,2' dipyrid- ylamine	Pyridyl pyrimidine	1(2-pyr- idyl)- triazole
Solvent							
Carbon tetra-chloride	313 1	300 5	313 1		318 1		
Toluene	316 4	311 5	319 8	303 6	313 1	300 5	319 5
Ether	316 4	318 1	323 2	311 5	313 1	300 5	316 4
Dichloro- methane	318 1	319 8	325.0	313 1	316 4	302 0	318 1
Butanol	316 4	318 1	305 1	313 1	311 5	302 0	318 1
Tetrahydro- furan	314 7	337 9	316 4	314 7	311 5	302 0	305 1
Chloroform	318 1	313 1	323 2	305 1	316 4	302 0	321 5
Acetone	314 7	347 7	316 4	319 8	314 7	303 6	306 7
Acetonitrile	316 4	347 7	319 8	341 7	318 1	305 1	309 8
Methanol	314 7	343 7	306 7	319 8	303 6	303 6	305 1

E_{MLCT} accurate \pm 1.7 kJmol⁻¹

Table 3 10 Energy positions (E_{MLCT} (kJMol⁻¹)) of the MLCT Absorption Maxima for W(CO)₅L complexes.

As stated earlier, Lees et al.,²⁴ found good correlations between the energy positions of the MLCT absorption maxima (E_{MLCT}) of $W(CO)_4(2,2'$ -bipyridine) and $W(CO)_5(\text{Pyrazine})W(CO)_5$ complexes with the solvent parameters. These parameters are directly obtainable from literature data, or can be derived from such, and are listed in Table 3.11.

The E_{MLCT} data (Table 3.10) for the $W(CO)_5(L)$ complexes were correlated with the empirical solvents parameter (S), from 3.11, according to equation 3.1, where m is the slope of the regression line

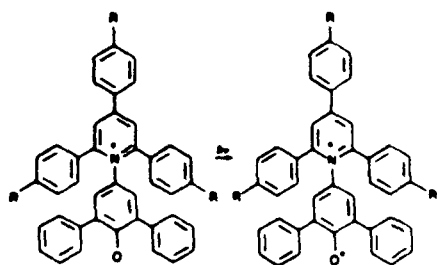
$$E_{MLCT} = mS + C \quad \text{Equation 3.1}$$

Of the ten solvents adopted in this study, it was attempted to obtain correlations from the following groups of solvents: (a) the combined ten solvents, (b) the combined minus the chlorinated solvents, (c) the combined minus both the chlorinated and protic solvents, and (d) the chlorinated solvents.

	ϵ_T	n_D	ϵ_b	ϵ_{op}	μ	α	α_{op}
Carbon tetra-chloride	136.0	0.29	2.24	2.13	0	6.80	6.56
Toluene	141.8	0.54	2.38	2.24	0.37	7.59	6.98
Ether	144.8	0.27	4.34	1.83	1.23	12.50	5.17
Dichloro-methane	172.0	0.83	9.08	2.03	1.90	17.40	6.08
Butanol	210.0	0.46	17.10	1.96	2.96	20.10	
Tetrahydro furan	156.5	0.58	7.39	1.97	1.69	16.3	5.85
Chloroform	163.6	0.58	4.81	2.09	1.11	12.1	6.38
Acetone	176.6	0.71	20.7	1.85	3.11	20.7	5.2
Acetonitrile	192.5	0.85	37.5	1.81	3.39	22.0	5.06
Methanol	232.2	0.60	32.7	1.77	2.97	21.8	4.85

Table 3.11 Relevant Solvent Parameters

The Reichardt's ϵ_T solvent polarity parameter²⁶ is based on the transition energy of an intramolecular charge transfer transition (Scheme 3 1) for a pyridinium N-phenol betaine molecule (4-(2,4,6-triphenylpyridine)-2,6-diphenylphenoxide). The charge transfer in this betaine molecule is highly solvent sensitive, with the dipole moment of the ground state greater than that of the excited state, and thus exhibits negative solvatochromism.



Scheme 3 1

The ϵ_T parameters were found to correlate poorly with the E_{MLCT} values of the $W(CO)_5(L)$ complexes. A correlation was considered to be poor when the correlation coefficient obtained was less than 0.80. However, good correlation (correlation coefficients greater than 0.98) were obtained for all $W(CO)_5(L)$ complexes when the ϵ_{MLCT} values were correlated with the ϵ_T parameters of the chlorinated solvents.

The Kamlet and Taft's π^* solvent parameter is based on the solvatochromism of the $\pi \rightarrow \pi^*$ transition in seven nitrobenzene and benzophenone derivatives²⁷. The averaging of the absorption energies has minimised some of the solvation problems encountered in the single model compound parameter, e.g. betaine for the ϵ_T parameter. The π^* scale is dimensionless as the values have been normalized from 0(cyclohexane) to 10(dimethylsulphoxide) according to equation 3.2.

$$\pi^* = (\text{XYZ} - \text{XYZ}_0)/s; \quad s = \text{XYZ}_1 - \text{XYZ}_0 \quad \text{Equation 3.2}$$

- XYZ = the average electronic absorption energy in a given solvent,
 XYZ_0 = the average electronic absorption energy in cyclohexane,
 XYZ_1 = the average electronic absorption energy in dimethylsulphoxide,
 S = solvatochromic coefficient, and
 π^* = solvent polarity or solvatochromic parameter

As with the ϵ_T parameters, the π^* solvent parameters correlated poorly with the E_{MLCT} values of the $\text{W}(\text{CO})_5(\text{L})$ complexes, however correlation coefficients greater than 0.9 were obtained for the chlorinated solvents

Although the ϵ_T and π^* parameters are helpful in predicting solvent effects on a wide range of organic transformations²⁷ and can yield good fits with metal carbonyl MLCT energies, they are statistically based (on the mean transition energies of a number of model compounds) and offer little to an understanding of solvent phenomena on the molecular level

Neither the bulk dielectric constant (ϵ_b)²⁸ or the optical dielectric constant (ϵ_{op})²⁹ parameters showed good correlation with the ϵ_{MLCT} values of the $\text{W}(\text{CO})_5(\text{L})$ complexes. However, the E_{MLCT} values of $\text{W}(\text{CO})_5(2\text{-vinylpyridine})$ and $\text{W}(\text{CO})_5(\text{pyridylpyrimidine})$ complexes showed good correlation (correlation coefficients greater than 0.90) with the bulk dielectric constant (ϵ_b), in all solvent groups

The E_{MLCT} values of the $W(CO)_5(L)$ ($L = 4\text{-phenylpyridine, 4-vinylpyridine or pyridylpyrimidine}$) complexes displayed good correlation with the solvent dipole moment (μ) parameters in all solvent groups

The solvent polarizability (α and α_{op}) parameters²⁹ displayed poor correlation with the E_{MLCT} values of the $M(CO)_5(L)$ complexes. However, the E_{MLCT} values of $W(CO)_5(L)$ ($L = 4\text{-phenylpyridine or pyridylpyrimidine}$) complexes correlated well (correlation coefficients greater than 0.80) with the solvent polarizability (α) parameters in all solvent groups

In summary, the E_{MLCT} values of the $W(CO)_5(L)$ complexes were not found to correlate to the relevant solvent parameters as well as for the $W(CO)_5(\text{pyrazine})$ - $W(CO)_5$ and $W(CO)_4(2,2'\text{-bipyridine})$ complexes, as obtained by Lees *et al*²⁴. However, this could be as a result of the broader range of solvents adopted by Lees and coworkers²⁴.

3 h III Solvatochromism of the $M(CO)_4(3,6\text{-bis}(2\text{-pyridyl})1,4\text{-dihydro-1,2,4,5-tetrazene}$ ($M = \text{Cr, Mo, or W}$) and $W(CO)_4(6\text{-styryl-2,2'}\text{bipyridine})$ complexes

The ultraviolet/visible spectra of the $M(CO)_4(SL)$, where $M = \text{Cr, Mo, or W}$ and $SL = 3,6\text{-bis}(2\text{-pyridyl})1,4\text{-dihydro-1,2,4,5-tetrazene}$, and $W(CO)_4(L)$, ($L = 6\text{-styryl-2,2'}\text{bipyridine}$) complexes were recorded in the same range of solvents as in Section 3 h II. Figure 3.12 shows the spectra of $W(CO)_4(SL)$ recorded in a number of solvents. The metal-to-ligand charge transfer (MLCT) absorption maxima (nm) for each complex are listed in Table 3.12. The corresponding energy (E_{MLCT}) for these MLCT absorptions are listed in Table 3.13.

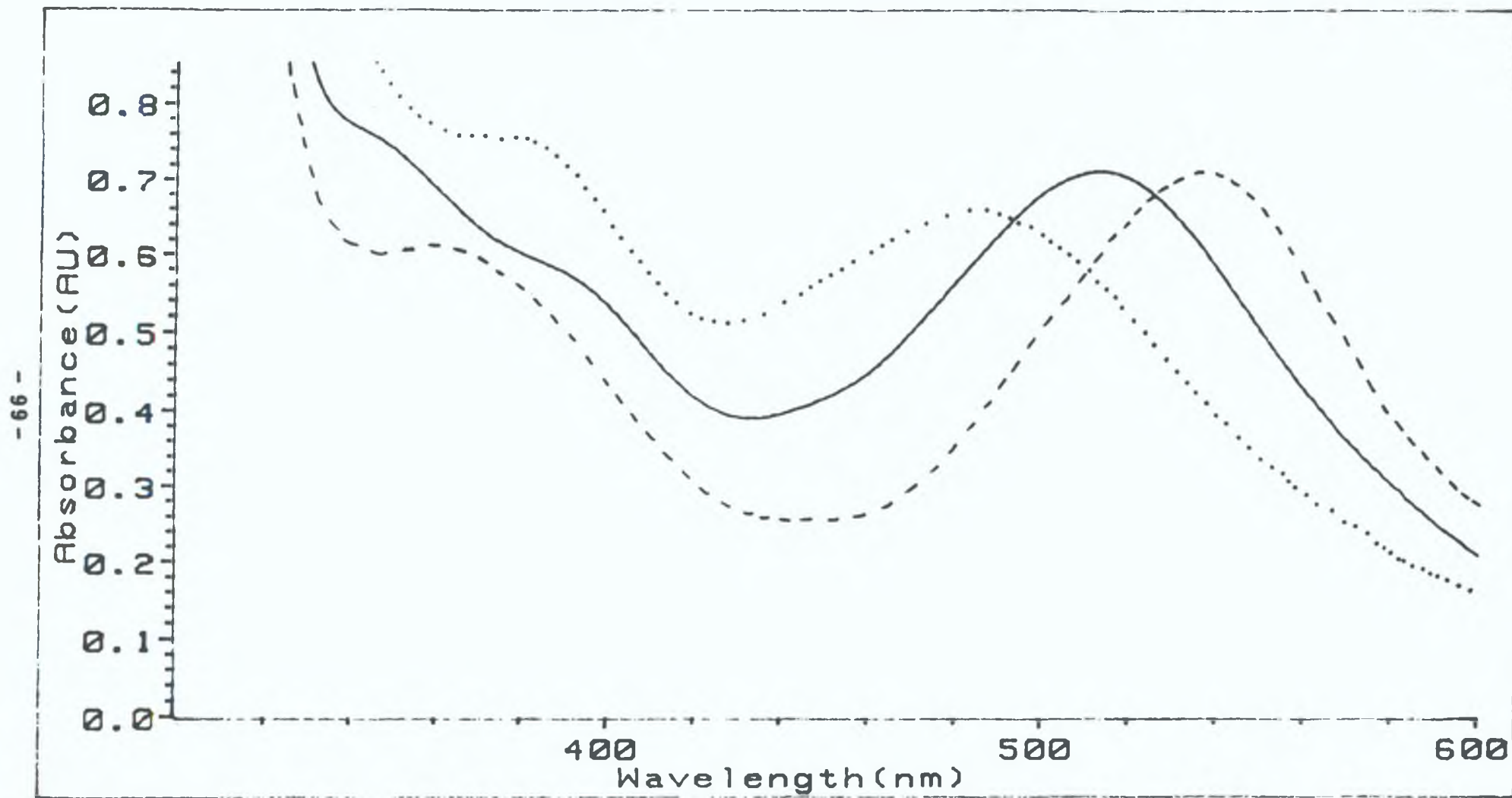


Figure 3.12 The uv/vis spectrum of $W(CO)_4(SL)$ recorded in (a) toluene (---), (b) thf (—), and (c) acetonitrile (...)

If as before in Section 3 h II, the results obtained in protic and chlorinated solvents are ignored, all of the above tetracarbonyl species exhibit negative

Solvent	Cr(CO) ₄ SL	W(CO) ₄ SL	Mo(CO) ₄ SL	W(CO) ₄ (6 styryl 2,2' bipyrid- ine)
Carbon tetrachloride	660	512	550	
Toluene	664	538	520	526
Ether	660	532	514	524
Dichloro- methane	664	518	500	492
Butan-2-ol	658	518	502	498
Tetrahydro- furan	650	514	494	498
Chloroform	666	538	516	512
Acetone	650	494	478	472
Acetonitrile	654	484	470	456
Methanol	658	488	488	

Peak absorptions accurate to ± 2 nm

SL = 3,6-bis(2-pyridyl)-1,4-dihydro-1,2,4,5-tetrazene

Table 3 12 The MLCT absorption maxima (nm) for the group 6 metal-tetracarbonyl complexes.

Solvent	Cr(CO) ₄ SL	W(CO) ₄ SL	Mo(CO) ₄ SL	W(CO) ₄ 6 styryl 2,2' bipyrid- ine
Carbon tetrachloride	181.2	233.6	217.5	
Toluene	180.1	222.3	230.0	227.4
Ether	181.2	233.6	232.7	228.2
Dichloro methane	180.1	230.9	239.2	243.1
Butan-2-ol	181.8	230.9	238.2	240.2
Tetrahydro furan	184.0	232.7	242.1	240.2
Chloroform	179.6	230.9	231.8	233.6
Acetone	184.0	242.1	250.2	253.4
Acetonitrile	182.9	247.1	254.5	262.3
Methanol	181.8	245.1	245.1	

SL = 3,6-bis(2-pyridyl)-1,4-dihydro-1,2,4,5-tetrazene

E_{MLCT} accurate to ± 1.9 kJmol⁻¹

Table 3.13 Energy positions (E_{MLCT} (kJmol⁻¹)) of the MLCT absorption maxima for the group 6 metal tetra-carbonyl complexes.

solvatochromism The greater magnitude of solvatochromism displayed by $W(CO)_4(6\text{-styryl-}2,2'\text{-bipyridine})$ would not appear to be affected by the styryl group, as Lees *et al*²⁴ reported a similar magnitude of solvatochromism for the $W(CO)_4(2,2'\text{-bipyridine})$ complex

As in Section 3 h II, the E_{MLCT} values (Table 3 13) of the group six metal tetracarbonyl complexes were correlated with the relevant solvent parameters (Table 3 11) according to equation 3 1 As with the $W(CO)_5(L)$ complexes, the $M(CO)_4(SL)$ ($M = Cr, Mo, \text{ or } W$) and $W(CO)_4(L)$ complexes correlated poorly with the relevant parameters of the solvents adopted in this study

Infrared spectroscopy has been shown to be a very useful tool for determining the degree of substitution of the group six metal hexacarbonyls

$W(CO)_5(L)$ (where $L = 2\text{-aminomethylpyridine}$ or bispicoylamine) complexes were shown to be thermally unstable and isolation of these complexes proved difficult. Both the penta and tetra-carbonyl species of each ligand were observed by infrared spectroscopy.

The formation of $W(CO)_4(L)$, ($L = 2,2\text{-dipyridylamine}$), from $W(CO)_5(L)$ would appear to be more complicated than just a simple unimolecular process, as determined from thermogravimetric analysis. An observed weight loss of approximately 35% suggested that $W(CO)_6$ was formed during the decarbonylation reaction.

All the group six metal hexacarbonyl derivatives of the nitrogen donor ligands adopted in this study displayed varying degrees of solvatochromism. Poor correlations between the energy of the metal-ligand charge-transfer transition and the relevant solvent parameters were obtained, but these parameters are based on the transition energy of model compounds and do not provide a further understanding of solvent interaction at the molecular level.

3.i EXPERIMENTAL

3.i.1 Photochemical Reactor

Photochemical reactions were carried out in a cylindrical vessel approximately 300mm x 80mm in diameter, fitted with a water cooled quartz immersion well containing a 400W media pressure mercury lamp. The reactant solution was continually stirred and purged with nitrogen gas.

3.i.2 The preparation of $W(CO)_5(L)$ complexes (L = pyridine or substituted pyridine)

0.5g ($\sim 1.5 \times 10^{-3}$ moles) of $W(CO)_6$ was suspended in approximately 200cm³ of tetrahydrofuran (thf) in the photochemical reactor. The mixture was then flushed with nitrogen gas for 15 minutes prior to photolysis. After 4 hours, the lamp was extinguished and the resulting yellow clear solution filtered to remove any unphotolysed $W(CO)_6$. One mole equivalent of the required ligand (dissolved in the minimum volume of thf) was then added to the photolysed solution. The solvent was then removed under reduced pressure at temperatures below 30°C.

The $W(CO)_5(L)$ (where L = pyridine, 2- or 4-phenylpyridine, or 2,2'-dipyridyl amine) were purified by recrystallisation from either methanol or nitromethane. All complexes were treated as air and light sensitive, and were handled under a nitrogen atmosphere. The elemental analysis of the $W(CO)_5(L)$ complexes were satisfactory and are listed in Table 3.14. Yields greater than 60% were obtained.

Compound	Calculated			%	Found		
	C	H	N		C	H	N
$W(CO)_5(2 \text{ phpyr})$	40.10	1.89	2.92	39.68	1.71	2.98	
$W(CO)_5(4 \text{ phpyr})$	40.10	1.89	2.92	40.39	1.83	2.79	
$W(CO)_5(2,2'\text{-dipyridylamine})$	36.38	1.83	8.49	35.92	1.61	8.36	

Table 3.14 Elemental analysis of the $W(CO)_5(L)$ complexes prepared

3.i.III The preparation of $W(CO)_5(L)$ complexes (L = 2-aminomethylpyridine or bispicoylamine)

The same method of preparation of $W(CO)_5(L)$ complexes (Section 3.i.II) was adopted for the preparation of the 2-aminomethylpyridine and bispicoylamine derivatives of $W(CO)_6$. Attempts to recrystallize either of the complexes in a range of solvents failed, resulting with a oily substance. Slow evaporation of the solvent resulted with the formation of a brown solid.

From infrared spectroscopy (Section 3.g), both penta- and tetra-carbonyl complexes of both ligands, 2-aminomethylpyridine and bispicoylamine, were present.

3.i.IV The preparation of $M(CO)_4(SL)$ complexes (M = Cr, Mo or W; SL = 3,6 bis(2-pyridyl)1,4 dihydro 1,2,4,5 tetrazene)

$M(CO)_4(SL)$ complexes (M = Cr, Mo, or W, SL = 3,6bis(2-pyridyl)-1,4-dihydro-1,2,4,5-tetrazene) were prepared by using the same method of preparation as for the $W(CO)_5(L)$ complexes (Section 3 j II) However, in the case of the bridged-ligand complex, $Mo(CO)_4(SL)Mo(CO)_4$, 0.5 mole equivalents of the SL ligand was added to the photolysed solution of $Mo(CO)_6$. All the above complexes were purified by recrystallisation from acetonitrile under nitrogen. The elemental analysis for these complexes are listed in Table 3.15. Yields greater than 60% were obtained.

Compound	Calculated			%	Found		
	C	H	N		C	H	N
$Cr(CO)_4(SL)$	47.78	2.51	20.89	47.81	2.27	20.59	
$Mo(CO)_4(SL)$	43.06	2.26	18.83	44.68	2.37	20.75	
$W(CO)_4(SL)$	35.97	1.89	15.73	37.95	2.13	17.11	
$Mo(CO)_4(SL)Mo(CO)_4$	36.72	1.54	12.85	40.02	2.01	16.67	

SL = 3,6-bis(2-pyridyl)1,4 dihydro-1,2,4,5-tetrazene

Table 3.15 Elemental analysis of the $M(CO)_4(SL)$ complexes

3.i.V Materials

The group six metal hexacarbonyls were obtained from BDH Ltd and Strem Chemicals Ltd, and were used without further purification. 2- and 4-phenyl pyridine and all other nitrogen donor ligands were obtained from Riedel-de-Haen, except 3,6-bis(2-pyridyl)-1,4-dihydro-1,2,4,5-tetrazene (received from University of Leiden), and were used without further purification.

Purification of tetrahydrofuran was obtained by removing the peroxides by shaking with iron(II) sulphate, drying over calcium sulphate, and finally refluxed over lithium aluminium hydride before being fractionally distilled. All other solvents were obtained from Riedel-de-Haen and were fractionally distilled prior to use.

3.i.VI Apparatus

Ultraviolet/visible spectrums were obtained from either a Shimadzu (UV-240) ultraviolet/visible recording spectrophotometer or a Hewlett-Packard (8452A) diode array spectrophotometer. All infrared spectrums were obtained from a Perkin Elmer (983G) infrared spectrophotometer.

Elemental analysis of the complexes prepared in this work were carried out by the Microanalytical Laboratory, University College Dublin. ^1H nmr spectrums were obtained from a 270MHz nmr spectrometer, University College Galway.

References

- 1 (a) M. Wrighton, G S Hammond, and H B Gray, Mol. Photochem, 1973, 5, 179
- (b) H B Abrahamson and M. Wrighton, Inorg. Chem., 1978, 17, 3385
- (c) M. Wrighton, G S Hammond, and H B Gray, Inorg. Chem., 1972, 11, 3122
- 2 H Daamen and A Oskam, Inorg. Chim. Acta, 1978, 26, 81
- 3 (a) M. Wrighton, Inorg. Chem., 1974, 13, 905
- (b) M. Wrighton, H B Abrahamson, and D L Morse, J. Am. Chem. Soc., 1976, 98, 4105
- 4 F A Cotton, W T Edwards, F C Rauch, M. A Graham, R N Perutz, and J J Turner, J. Coord. Chem., 1973, 2, 247
- 5 L H Jones, R S McDowell, and M. Goldblatt, Inorg. Chem., 1969, 11, 2349
- 6 R D Gillard and G Wilkinson, J. Chem. Soc., 1964, 1224
- 7 P S Bratterman "Metal Carbonyl Spectra", Academic Press, 1975
- 8 I W Stolz, H Haas, and R K Sheline, J. Am. Chem. Soc., 87, 4, 1965, 716
- 9 C S Kraihansel and F A Cotton, Inorg. Chem., 1963, 2, 3, 533

- 10 J M Kelly and C Long, J. Organomet. Chem., 1982, 235, 315.
- 11 R A Howie (University of Aberdeen), not yet published
- 12 L O Brockway, R V G Ewens, and M W Lister, Trans Faraday Soc., 1938, 34, 1350
- 13 W Kaim and S Kohlmann, Inorg. Chem., 1987, 26, 1, 68
- 14 (a) G L Geoffrey and Wrighton M S, Organo Photo Chem., Academic, New York 1979
- (b) M S Wrighton and D L Morse, J Am Chem Soc., 1974, 96, 998
- (c) P J Giordano, S M Fredricks, M S Wrighton, and D L Morse, J Am Chem Soc., 1978, 100, 2257
- (d) P J Giordano and M S Wrighton, J Am Chem Soc., 1979, 101, 2888
- (e) A J Lees, J Am Chem Soc., 1982, 104, 2038
- (f) M Manuta and A J Lees, Inorg. Chem., 1983, 22, 572
- 15 (a) M S Wrighton and J Markham, J Phys Chem., 1973, 77, 3042
- (b) N Damas, D Diemente, and E Harris, J Am Chem Soc., 1973 95, 6864
- (c) N Damas, E Harris, and P P McBride, J Am Chem Soc., 1977, 99, 3547
- (d) J C Luong, L Nadjo, and M S Wrighton, J Am Chem Soc., 1978, 100, 5790
- 16 (a) L H Staal, D J Stufkins, and A Oskam, Inorg Chim Acta., 1978, 26 255
- (b) R W Balk, D J Stufkins, and A Oskam, Inorg Chim Acta., 1978, 28, 133
- 17 H tom Diech, and E Z Kuhl, Naturforsch, B Anorg Chem, Org. Chem., 1982, 37B, 324
- 18 Not yet published

- 19 (a) J Bjerrum, A Adamson, and O Bostrup, Acta. Chem. Scand., 1956, 10, 329
- (b) J Burgess, Spectrochim Acta Part A, 1970, 26A, 1369 and 1957
- (c) J N Damass, T F Turner, and G A Crosby, Inorg Chem., 1969, 8, 674
- 20 (a) H Bock, and H tom Diek, Angew Chem Int Ed, Engl 1966, 5, 520
- (b) D Walther, Anorg Allg Chem, 1973, 396, 46
- (c) H Saito, F Fujita, and K Saito, Bull Chem Soc Jpn, 1968, 41, 863
- (d) J Burgess, J Organomet. Chem, 1969, 19, 218
- (e) M S Wrighton and D L Morse, J Organomet Chem, 1975, 97, 405
- (f) J Burgess, J G Chambers, and R I Haines, Transition Met Chem, (Weinheim Ger) 1981, 6, 145
- (g) J A Connor, C Overton, and N J El Murr, J Organomet Chem, 1984, 277, 277
- 21 (a) C Reichardt, Solvents Effects in Organic Chemistry, Verlag Chemie, Weinheim, W Germany and New York 1979
- (b) J M Kamlet, J L M. Abboud, and R W Taft, Prog Phys Org Chem, 1981, 13, 385
- (c) A B P Lever, Inorganic Electronic Spectroscopy, 2nd Ed, Elsevier, Amsterdam 1984, pp 208-212
- 22 D M. Manuta and A J Lees, Inorg Chem, 1983, 22, 3825
- 23 (a) I G Dance and T R Miller, J Chem. Soc Chem Comm, 1973, 433
- (b) T R Miller and I G Dance, J. Am Chem Soc, 1973, 95, 6970
- (c) I W Renk and H Dieck, Chem Ber, 1972, 105, 1403
- 24 D M. Manuta and A J Lees, Inorg Chem, 1986, 25, 3212
- 25 (a) Kosower E M, An Introduction to Physical Organic Chemistry, Wiley, New York, 1968, p293
- (b) E M. Kosower, J Am Chem Soc, 1958, 80, 3253

- 26 (a) C Reichardt, Angew. Chem. Int. Ed. Engl., 1965, 4, 29
(b) C Reichardt, Angew. Chem. Int. Ed. Engl., 1979, 18, 98
- 27 Taft R W and Kamlet M. J., Inorg. Chem., 1983, 22, 250
- 28 I A Koppel and V A Palm, Advances in Linear Free Energy Relationships, Chapman N B Shorter, J Eds, Plenum London 1972, p254
- 29 R D Weast, Ed Handbook of Chemistry and Physics, 62nd ed CRC Press, Boca Raton, FL 1982, pC65
- 30 A L McLellan, Table of Exptl Dipole Moments, W H Freeman Co San Francisco, CA, 1963
- 31 W Kaim and S Kohlmann, Inorg. Chem., 1986, 25, 3306